SYNTHESIS AND PHOTOPOLYMERIZATIONS OF NEW DENTAL MONOMERS FROM O-HYDROXYARYL PHOSPHONATES

by

Görçin Görkem Şahin

B.S., Chemistry, Boğaziçi University, 2006

Submitted to the Institute for Graduate Studies in
Science and Engineering in partial fulfillment of
the requirements for the degree of
Master of Science

Graduate Program in Chemistry
Boğaziçi University
2008

Babaanneme,

Erdal İnönü ve

Mustafa Kemal Atatürk'e…

ACKNOWLEDGEMENTS

I would like to express my sincere gratitude to my supervisor Prof. Duygu Avcı for her most valuable encouragement and scientific guidance throughout this study. I greatly appreciate her for giving me valuable opportunities. It was an invaluable experience for me to work with her.

I am also grateful to my committee members Prof. İlknur Doğan and Prof. Safiye Erdem for their careful and constructive review of the final manuscript.

I would like to thank my laboratory partners, Zeynep Saraylı Bilgici, Seda Edizer, Özlem Karahan and Bahar Yeniad for their help and friendship. I would like to extend my thanks to Dr. Ayla Türkekul and Burcu Selen Çağlayan for NMR analysis and Dr. Gökhan Çaylı for TGA analysis.

I would especially like to thank Assist. Prof. Aylin Ziylan Albayrak not only for her helps but also for her friendship and advice during my study. I also would like to express my heartfelt thanks to my dear friend Çimen Özgüç for her encouragement and friendship. I also thank to all members of Boğaziçi University Chemistry Department, my instructors, my friends, especially the secretary of the department Hülya Metiner for their help and friendship.

I would like to thank Güven Kurtuldu with all my heart for his help and love. Finally, my greatest thank is to my mother, father and especially my sister for their endless love, understanding, encouragement and support.

I would also like to thank TÜBİTAK for supporting me as a M.S. scholar during my master study.

ABSTRACT

SYNTHESIS AND PHOTOPOLYMERIZATIONS OF NEW DENTAL MONOMERS FROM O-HYDROXYARYL PHOSPHONATES

New phosphonate, phosphonic and carboxylic acid containing monomers were synthesized from o-hydroxyaryl phosphonates and dimethyl 2-hydroxyethyl phosphonate for use in dental adhesives and composites.

First set of monomers were synthesized from diethyl (2-hydroxyphenyl) phosphonate. Synthesis of the first monomer involved: (i) reaction of t-butyl α-bromomethacrylate (TBBr) and Bisphenol A, (ii) conversion to diacid chloride derivative using thionyl chloride, (iii) reaction of diacid chloride with diethyl (2-hydroxyphenyl) phosphonate. The second monomer was synthesized from the reaction of 2-chloromethacryloyl chloride (CMAC) and diethyl (2-hydroxyphenyl) phosphonate. Synthesis of the third monomer involved reaction of glycidyl methacrylate (GMA) with diethyl (2-hydroxyphenyl) phosphonate. Forth monomer was obtained by the ring opening reaction of bisphenol A diglycidylether with diethyl (2-hydroxyphenyl) phosphonate followed by reaction of the resulting diol with metharcyl chloride. Synthesis of the last monomer in this set involved reaction of diethyl (2-hydroxyphenyl) phosphonate with TBBr.

Hydrolysis of the phosphonate groups of the first and second monomers with trimethylsilyl bromide (TMSBr) gave new monomers with phosphonic acid functionality. Hydrolysis of both phosphonate and t-butyl groups of the fifth monomer gave a new monomer with both phosphonic and carboxylic acid functionality.

The homopolymerization and copolymerization behaviors of the synthesized monomers with 2,2-bis[4-(2-hydroxy-3-methacryloyloxy propyloxy)phenyl]propane (Bis-GMA) and glycerol dimethacrylate (GDMA) were investigated using photodifferential scanning calorimetry at 40 ^{o}C with 2,2'-dimethoxy-2-phenyl acetophenone (DMPA) as photoinitiator. The mono-functional (meth)acrylate

synthesized from GMA was found to homo and copolymerize rapidly to give crosslinked polymers. This monomer can be used as a reactive diluent for BisGMA and improve the cure efficiency, material properties and binding ability of dental composites.

The aqueous solutions of the acid monomers have a pH value in the range of acidity expected from a mild self-etching dental adhesive monomer (pH around 2.0). The interaction of the acid monomers with hydroxyapatite (HAP) was investigated using FT-IR technique.

The second set of monomers were synthesized from tetraethyl 2,5-dihydroxy-1,4-phenylene diphosphonate. Reaction of tetraethyl 2,5-dihydroxy-1,4-phenylene diphosphonate with TBBr gave a new phosphonated monomer which was hydrolyzed to give a monomer containing both carboxylic and phosphonic acid groups.

The copolymerization behaviors of the synthesized monomers with GDMA were first investigated in bulk using photodifferential scanning calorimetry at 40 ^{o}C with DMPA. Then solution copolymerization of the monomers with acrylamide in water was studied, indicating that the synthesized monomers were incorporated into the copolymers. The aqueous solutions of these monomers also have pH values (1.72-1.87) suitable for dental applications, therefore their interaction with HAP was also investigated, using ^{13}C-NMR and FT-IR techniques.

Last phosphonated monomer was synthesized from the reaction of dimethyl 2-hydroxyethyl phosphonate and CMAC and its photopolymerization reactivity was investigated.

ÖZET

O- HİDROKSİARİL FOSFONATLARDAN YENİ DİŞÇİLİK MONOMERLERİNİN SENTEZLENMESİ VE IŞIKLA POLİMERİZASYONU

Dişçilik kompozitlerinde ve yapıştırıcılarında kullanılmak üzere fosfonat, fosfonik ve karboksilik asit içeren yeni monomerler, o-hidroksiaril fosfonatlardan ve dimetil 2-hidroksietil fosfonattan sentezlendi.

İlk kısımdaki monomerler, dietil (2-hidroksifenil) fosfonattan sentezlendi. İlk monomerin sentezlenmesi üç adımda gerçekleştirildi. (i) t-bütil α-bromometil akrilat (TBBr) ve Bisfenol A'nın reaksiyonu, (ii) t-bütil gruplarının tionil klorür ile diasit klorür türevine dönüştürülmesi, (iii) diasit klorürün dietil (2-hidroksifenil) fosfonat ile reaksiyonu. İkinci monomer, 2-klorometil-akriloil klorür (CMAC) ve dietil (2-hidroksifenil) fosfonatın reaksiyonundan sentezlendi. Üçüncü monomer gilisidil metil akrilat (GMA) ile dietil (2-hidroksifenil) fosfonatın reaksiyonu sonucunda elde edildi. Dördüncü monomer, bisfenol A digilisidileterin (DER) dietil (2-hidroksifenil) fosfonatla halka açılma reaksiyonu sonucu oluşan diolün metakriol klorürle reaksiyonundan elde edilmiştir. Bu kısımdaki son monomer ise TBBr ile dietil (2-hidroksifenil) fosfonatin reaksiyonundan sentezlendi.

Birinci ve ikinci monomerlerin trimetilsilil bromür (TMSBr) ile hidrolizinden fosfonik asit fonksiyonuna sahip monomerler elde edildi. Beşinci monomerin t-bütil ve fosfonat esterlerinin her ikisinin hidrolizi ile hem difosfonik hem de dikarboksilik asit içeren yeni bir monomer sentezlendi.

Sentezlenen monomerlerin homopolymerizasyon ve 2-bis[4-(2-hidroksi-3-metakriloiloksi propiloksi fenil] propan (BisGMA) ve gliserol dimetakrilat (GDMA) ile homopolimerizasyon ve kopolimerizasyon davranışları 2,2'-dimethoxy-2-phenyl asetofenon (DMPA) fotobaşlatıcısı kullanılarak foto diferansiyel taramalı kalorimetre (photo-DSC) metoduyla 40 ^{o}C'de incelendi. GMA'dan sentezlenen mono-fonksiyonel metilakrilatın çok hızlı bir biçimde çapraz bağlı polimer vererek homo ve kopolimerleştiği bulundu. Bu monomer BisGMA için reaktif seyreltici olarak

kullanılabilir ve diş kompozitlerinin polimerleşme verimliliğini, malzeme özelliklerini ve bağlanma yeteneğini arttırabilir.

Asit monomerlerinin sulu çözeltilerinin pH değeri 2.0 civarında olup dişe nüfuz edici dolgu yapıştırıcı bir monomer için istenen seviyededir. Asit monomerlerinin hidroksiapatit (HAP) ile etkileşimi FT-IR tekniği kullanılarak incelenmiştir.

İkinci kısımdaki monomerler tetraetil 2,5-dihidroksi-1,4-fenilen difosfonattan sentezlendi. Tetraetil 2,5-dihidroksi-1,4-fenilen difosfonatın TBBr ile reaksiyonu yeni bir fosfonat monomeri vermiş, bu monomerin hidrolizi ile hem karboksilli hem de fosfonik asit içeren bir monomer elde edilmiştir.

Sentezlenen monomerlerin GDMA ile kopolimerizasyon davranışları foto diferansiyel taramalı kalorimetri (foto-DSC) ile 40 ^{o}C'de DMPA kullanılarak incelendi. Suda akrilamid ile çözelti kopolimerizasyonu yapıldı ve sentezlenen monomerlerin kopolimerlerin içine dahil olduğu gözlendi. Bu monomerlerin de sulu çözeltilerinin pH degeri (1.72-1.78) dişçilik uygulamalarına uygun olduğu için, bunların HAP ile etkileşimi de FT-IR ve ^{13}C-NMR tekniği kullanılarak incelendi.

Son olarak fosfonat grup içeren bir monomer, dimetil 2-hidroksietil fosfonat ve CMAC reaksiyonu ile sentezlendi. Bu monomerin ışıkla polimerizasyon davranışı, foto-DSC ile 40 ^{o}C'de DMPA kullanılarak incelendi.

TABLE OF CONTENTS

LIST OF FIGURES

LIST OF TABLES

LIST OF SYMBOLS/ABBREVIATIONS

DSC	Differential Scanning Calorimetry
FTIR	Fourier Transform Infrared Spectroscopy
GPC	Gel Permeation Chromatography
NMR	Nuclear Magnetic Resonance Spectroscopy
TGA	Thermal Gravimetric Analysis
UV	Ultraviolet Spectroscopy
k_{ct}	Chain transfer by hydrogen abstraction
k_p	Propagation rate constant
R_p	Rate of polymerization
T_g	Glass transition temperature
AIBN	2,2'azobis(isobutyronitrile)
DABCO	1,4-Diazobicyclo [2.2.2] octane
Irgacure 651	2,2'-dimethoxy-2-phenylacetophenone
TEA	Triethylamine
TMSBr	Bromotrimethylsilane
V-50	2,2'-azobis(N,N'-amidinopropane) dihydrochloride
Bis-GMA	2,2-Bis[4-(2-Hydroxy-3-Methacryloyloxy Propyloxy) Phenyl] Propane
CMAC	2-Chloromethyl-Acryloyl Chloride
DER	Bisphenol A Diglycidylether
GDMA	Gycerol Dimethacrylate
GMA	Glycidyl Methacrylate
TBHMA	tert-Butyl-α-Hydroxymethyl Acrylate
TBBr	tert-Butyl-α-Bromomethyl Acrylate

1. INTRODUCTION

1.1. Dental Materials

1.1.1. Tooth Anatomy

A human tooth has two main parts which are crown; the visible part of the tooth and root; the anchor of the tooth that extends into the jawbone. The region between the root and the crown is called neck. (Figure 1.1) [1].

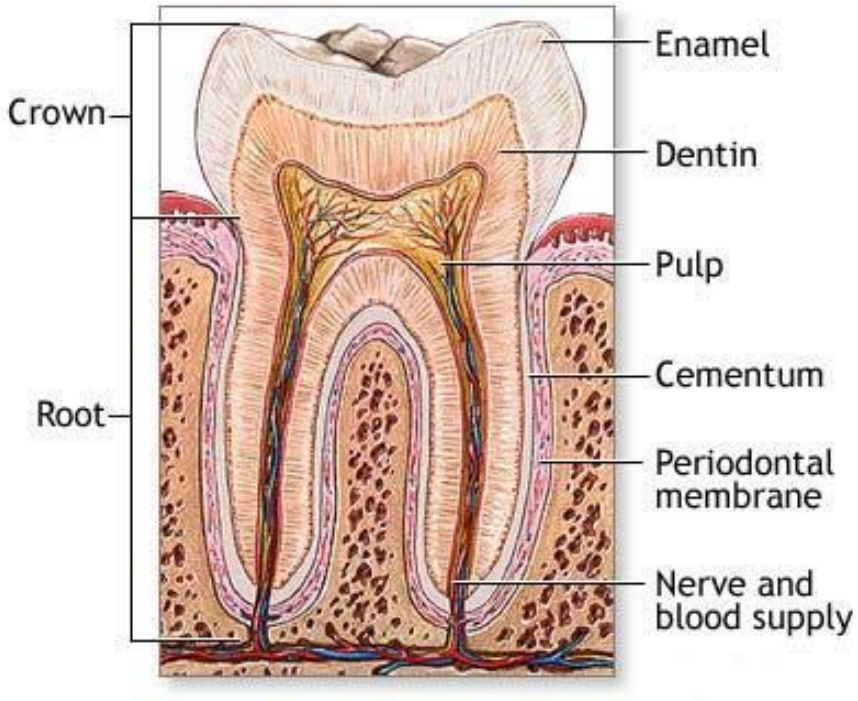

Figure 1.1. The anatomy of tooth

Enamel is the hardest and most highly mineralized substance of the body and is one of the four major tissues which make up the tooth, along with dentin, cementum, and dental pulp. It is visible and must be supported by underlying dentin. The normal color of enamel varies from light yellow to grayish white [2].

Dentin is the substance between enamel or cementum and the pulp chamber. Since it is softer than enamel, it decays more rapidly and is subject to severe cavities if not properly treated, but dentin still acts as a protective layer and supports the crown of the tooth [2].

Dentin and enamel are composed of hydroxyapatite, $Ca_{10}(PO_4)_6(OH)_2$ and collagen (Table 1.1). The collagen of the dentin provides hydroxyl, carboxyl and amino groups which can be utilized in bonding to this structure. Ninety-seven percent of enamel consists of mineral, with water and organic material composing the rest. Dentin is made up of 69 % inorganic materials, 20 % organic materials, and 10 % water by weight [3].

Table 1.1. Approximate composition of enamel and dentin

	Enamel	Dentin
Mineral phase (hydroxyapatite)	97 %	69 %
Organic phase (mainly collagen)	1 %	20 %
Water	2 %	11 %

When the dentin is cut by a dental instrument, a layer of loosely adhered debris is left covering the dentinal tubules. Due to its appearance, this layer, which contains the components of the ground dentin, is referred to as the *smear layer* [2].

The dental *pulp* is the central part of the tooth filled with soft connective tissue. This tissue contains blood vessels to supply nutrients to the tooth, and nerves to enable the tooth to sense heat and cold. The pulp also provides white blood cells to help fight bacteria via lymph vessels [4].

Cementum is a specialized bony substance covering the root of a tooth. It is approximately 45 % inorganic material (mainly hydroxyapatite), 33 % organic material (mainly collagen) and 22 % water. Its coloration is yellowish and it is softer than either dentin or enamel. The principal role of cementum is to serve as a medium by which the periodontal ligaments can attach to the tooth for stability [2].

1.1.2. General Properties of Ideal Dental Restorative Materials

Modern dental practice has been very dependent on its materials, such that the dentist's greatest challenge is choosing the right combinations of them for the benefit of their patients [3]. Properties for some materials differ from those for others, depending on their uses; however, a list of general properties can be generated for ideal dental restorative materials (Table 1.2) [5-7].

Table 1.2. General properties of ideal restorative dental materials

Physical/chemical properties	Consequences for dental practice
Mechanically stable and durable	Long-term durability of the filling
Biocompatible	Minimum toxicological risk for the patient
Dimensionally stable and low volume shrinkage	No marginal gap, minimally affected by temperature or solvents
Excellent resistance to oral conditions	Thermally and electrically stable, insulators
Coloration stability of the filling materials	Appearance like oral tissue
Easy to manipulate	Placement of the filling materials with reasonable time and effort
Adherent of tissue	Provide durable, tight union for retention and sealing
Tasteless and odorless	Not irritating or unpleasant taste in mount
Cleanable and repairable	Easily renewable and maintained
Low cost	Reasonable for patient’s budget

Dental personnel have appropriate materials for the many different situations that present, but there is not only one material that meets all of the requirements simultaneously [5].

1.1.3. Types of Dental Restorations

There are two types of dental restorations which are *direct* and *indirect* restorations (Table 1.3) [3].

Table 1.3. Dental restorative materials

Direct Restorative Materials	Indirect Restorative Materials
• Amalgams	• Porcelain
• Glass Ionomers	• Porcelain + Metals
• Composite Resins	• Gold Alloy
• Resin Ionomers	• Base Metal Alloys

Direct restorations are fillings placed immediately into a prepared cavity in a single visit. They include dental amalgam, glass ionomers, composite resin and resin ionomers fillings.

Indirect restorations generally require two or more visits. They include inlays, onlays, veneers, crowns and bridges fabricated with gold, base metal alloys, ceramics or composites. During the first visit, the dentist prepares the tooth and makes an impression of the area to be restored. The impression is sent to a dental laboratory, which creates the dental restoration. At the next appointment, the dentist cements the restoration into the prepared cavity and adjusts it as needed [8].

1.1.4. Direct Restorative Materials

Amalgam fillings are a mixture of mercury (from 43% to 54%) and powdered alloy made mostly of silver, tin, zinc and copper commonly called the amalgam alloy (Figure 1.2) [8, 9].

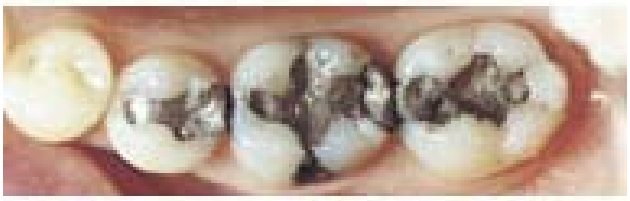

Figure 1.2. General appearance of amalgams

In preparing the alloy for dental amalgam, the components are melted together, usually under an inert atmosphere and then are homogenized at 400^{o}C for 6-24 hours. When the powdered amalgam alloy and mercury are freshly mixed, a paste-like material is obtained. The cavity is restored at this point and the chemical setting mechanism, which can be described by the following reaction, takes place in the cavity [10].

$$Ag_3Sn + Hg \longrightarrow Ag_2Hg_3 + Sn_{7\text{-}8}Hg$$

Dental amalgams are used by dentists for more than 150 years. This restorative type is the most thoroughly researched and tested restorative material in use therefore billions of dental amalgam fillings have been used to restore decayed teeth [3, 8, 11, 12]. They have many advantages over other materials. It is durable, easy to use, highly resistant to wear and relatively inexpensive in comparison to other materials. For those reasons, it remains a valued treatment option for dentists and their patients.

However, the major disadvantage of dental amalgams includes possible short-term sensitivity to hot or cold after the filling is placed. The silver-colored filling does not have as natural appearance as tooth. And to prepare the tooth, the dentist may need to remove more tooth structure to accommodate an amalgam filling than for other types of fillings [8].

Glass ionomer cement is the first aesthetic, tooth-colored filling materials appeared in the second decade of the 20th century and became available as a result of the studies of Alan Wilson and Brian Kent [13, 14].

Glass ionomer cements consist of an aqueous solution of poly (acrylic acid) at a concentration about 45 % and powder consisting of calcium fluoroaluminosilicate glass (CaFAlSi) and they gave an acid-base reaction [15, 16].

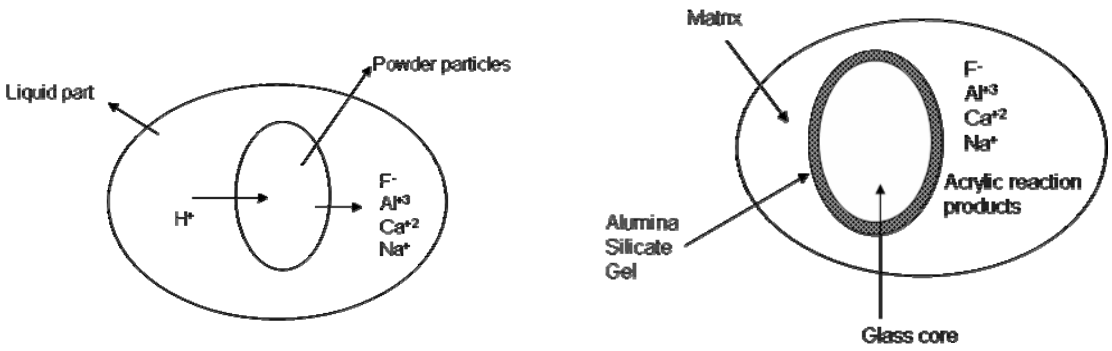

Figure 1.3. Ion migration and forming a matrix

When the components are mixed, the acidic protons from polymerizable acid rapidly attack the glass particles. Released Ca^{+2} and Al^{+3} ions form a silica gel area (Figure 1.3). The poly (alkenoic acis) chains chelae, i.e. form inter- and intramolecular salt bridges, forming a hard, cross-linked, ceramic- like cement (Figure 1.4) [15-17].

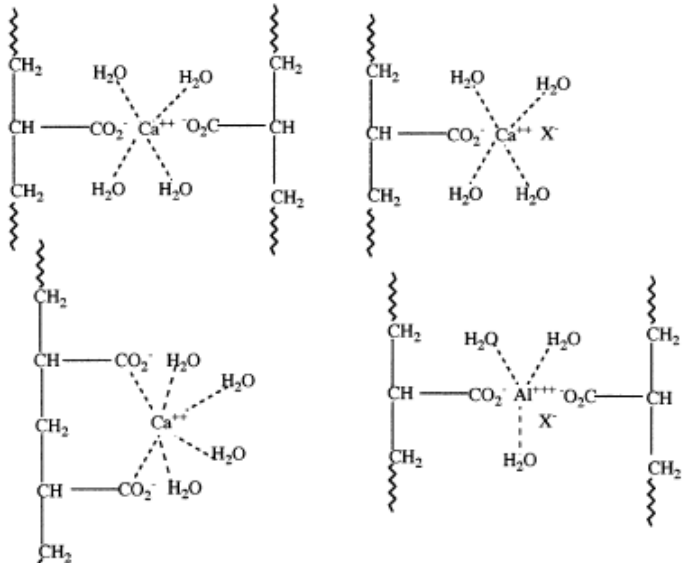

Figure 1.4. Possible intra- and intermolecular Ca^{+2} or Al^{+3} carboxylates (salt-bridges or molecular structure), where X represents OH^- or F^- anions

Glass-ionomer cements have a number of properties which make them highly suitable for application in dentistry [18]. Due to chemical bond between carboxylate groups on the poly (alkenoic acid)s backbone and the calcium ions on the surface of enamel or dentin, leakage around the filling and further decay is very low [17, 19]. They also displace phosphates from calcium hydroxyapatite surface so they have good biocompatibility [20].

Moreover, during the cement formation, fluoride ions in the glass are released into the aqueous acid phase and become trapped in the gel matrix [16]. Fluoride release protects against decalcification of the surrounding tooth structure and act as an anticorgenic agent [21, 22].

Main disadvantage is associated with early moisture sensitivity, which requires immediately placement with a varnish. Furthermore, glass ionomer cements show low resistance to wear and pressure, especially to abrasion, since matrix is ionically crosslinked, the possibility of water penetration into the matrix and acid erosion is high (Figure 1.5) [17].

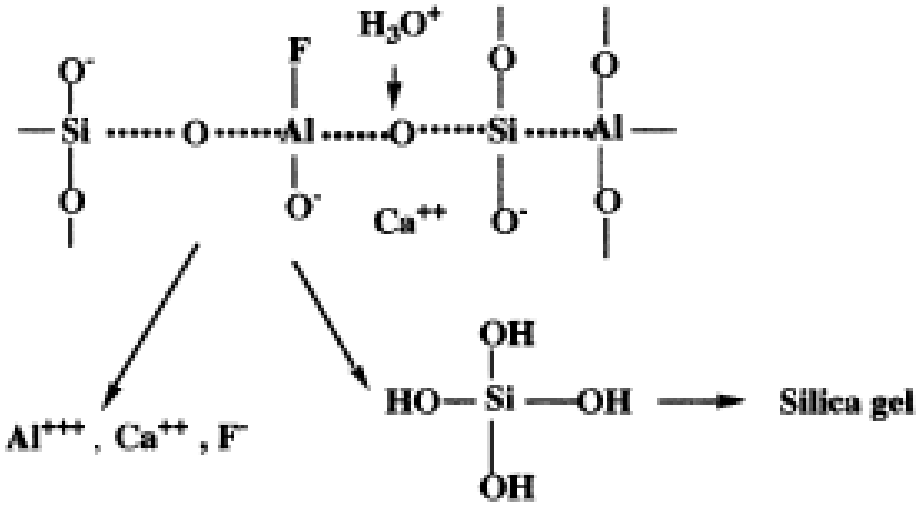

Figure 1.5. Acid hydrolysis or decomposition of glass powder

Composite resins are the most widely used of the aesthetic repair materials since their appearance on the dental scene in the early 1960s [12, 24]. These resins make excellent restorative materials because of their good resistance to wear and their excellent esthetics (Figure 1.6) [6, 8, 24].

Figure 1.6. Composite resins in dental application

Dental filling composites consist of two components; an organic matrix (15-20 wt %) and inorganic filler (85-80 wt %) [6, 24-28]. Organic matrix consists of free radically polymerizable bulky difunctional monomers, generally based on BisGMA (Figure 1.7) as patented by Bowen, initiator system and stabilizer. Inorganic fillers consist of quartz or finely divided silica powders and these powders are coated with a silane to promote bonding between the filler and the matrix in the set material [27].

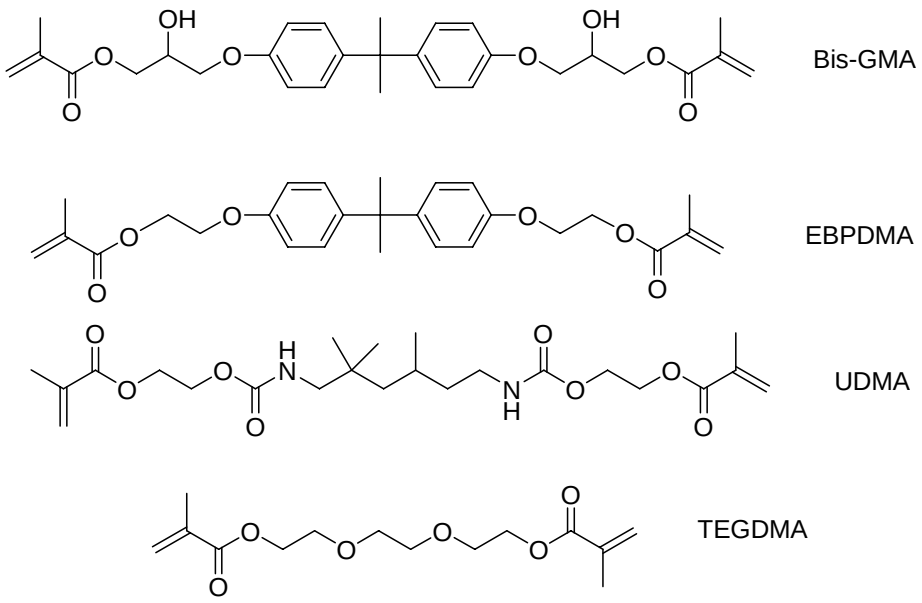

Figure 1.7. Chemical structures of dimethacrylate monomers used in dental application

Advantages of using Bis-GMA, its derivative EBPDMA or urethane dimethacrylate UDMA, over used small-sized dental monomers, such as methyl methacrylate, include less shrinkage, higher modulus and reduced toxicity due to its lower volatility and diffusivity into tissues. However, these monomers are very viscous liquid at room temperature, so to achieve more workable viscosity and to allow incorporation of sufficient powdered filler, diluent comonomer such as TEGDMA is used (Figure 1.7) [29, 30]. This also provides easier handling, higher filler loading and greater extent of polymerization. On the other hand, incorporation of these reactive diluents affects mechanical properties, volume shrinkage and water absorption [7, 31-33]

Moreover, organic matrix includes a photoinitiator (PI) or photoinitiating system. Monomers possess two terminal double bonds which are capable of undergoing addition polymerization with visible blue light of 470 nm wavelength [29]. This setting mechanism provides the property of "cure one command". Thus, initiation can be started and stopped almost at will. Initiator systems can be camphorquinone/amine system in visible (VIS) light curing composites. The amount of initiator system is usually very small, in the range of 0.1–1 wt % (Figure 1.8) [33-36].

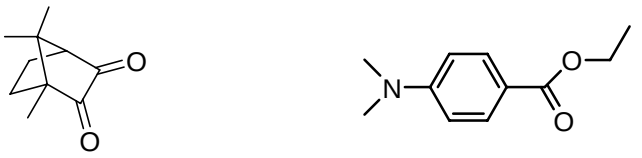

camphorquinone (CQ) Ethyl-4-dimethylaminobenzoate (DMAB)

Figure 1.8. Structures of camphorquinone and ethyl-4-dimethylaminobenzoate

However, the major disadvantage of composite resins is their lack of adhesion to dentine unless the tooth is acid-etched and a layer of thin plastic bonding resin is placed on the prepared surface first [37, 38].

Mou *et al.* synthesized phosphonic acid monomer for use in dental composites by the base-catalyzed rearrangement of the corresponding diethyl aryl phosphonate. They claimed that this aromatic monomer would yield materials with improved binding ability to tooth tissue and mechanical properties (Figure 1.9) [39].

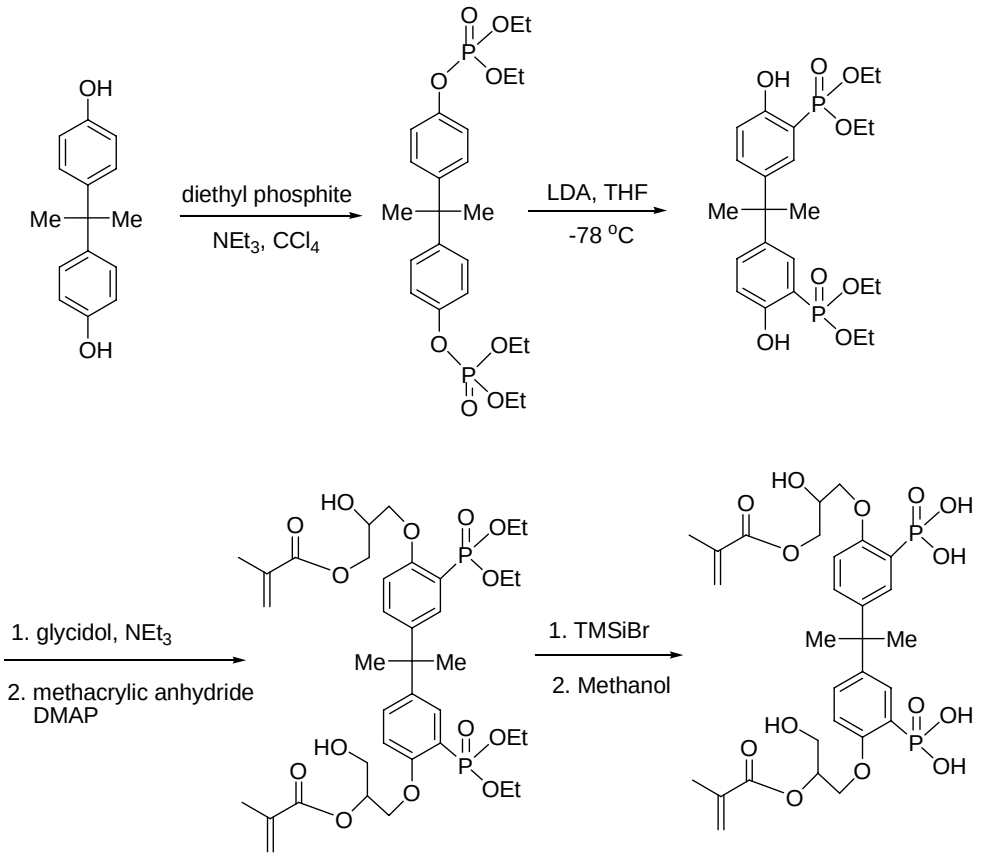

Figure 1.9. Synthesis of phosphonic acid containing dimethacrylate monomer

One disadvantage to standard resin systems is that unlike with Al-Fl-Si glass/acid mixtures, there is no way for fluoride to leach into the tooth structure offering a measure of decay resistance to the margins of the cavity preparation [40, 41].

Xu et al. synthesized fluoride-releasing dimethacrylate monomers to have high fluoride release and acceptable mechanical properties. Synthesized monomers have rigid, bulky backbone structures similar to Bis-GMA, can form crosslinked polymer matrix and have an anticariogenic effect with higher fluoride release (Figure 1.10) [42].

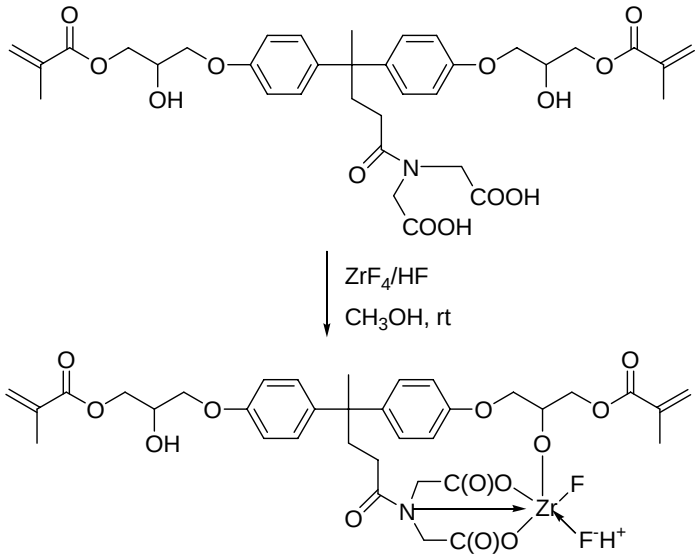

Figure 1.10. Synthesis of fluoride-releasing dimethacrylate monomer

Other disadvantage is that diluent monomers affect the properties of the matrix resin by increasing the water sorption and curing shrinkage. Investigations are being carried out in identifying new dimethacrylates, which will have moderately low viscosities to eliminate or minimize the use of the diluent monomer. [29, 43-45]

Stansbury et al. synthesized novel polymerizable dimethacrylate monomers with bulky substituent groups which could provide low volume shrinkage without sacrifice to degree of conversion and mechanical properties (Figure 1.11) [43].

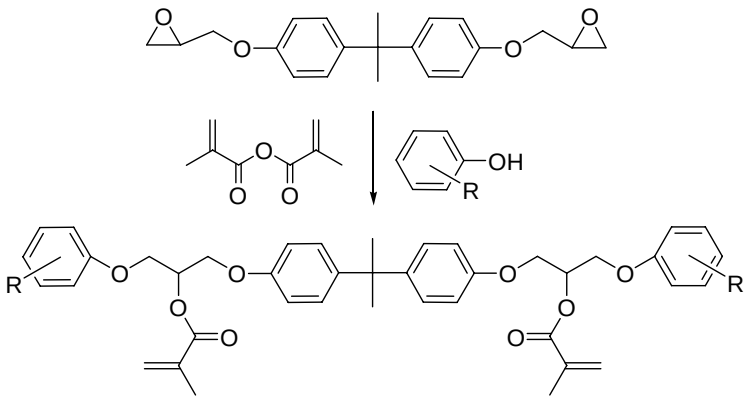

Figure 1.11. Novel low shrinkage monomers based on dimethacrylates

In the other study, they investigated fluorinated dimethacrylate monomers by the use of epoxy ring-opening monomers (Figure 1.12) [44].

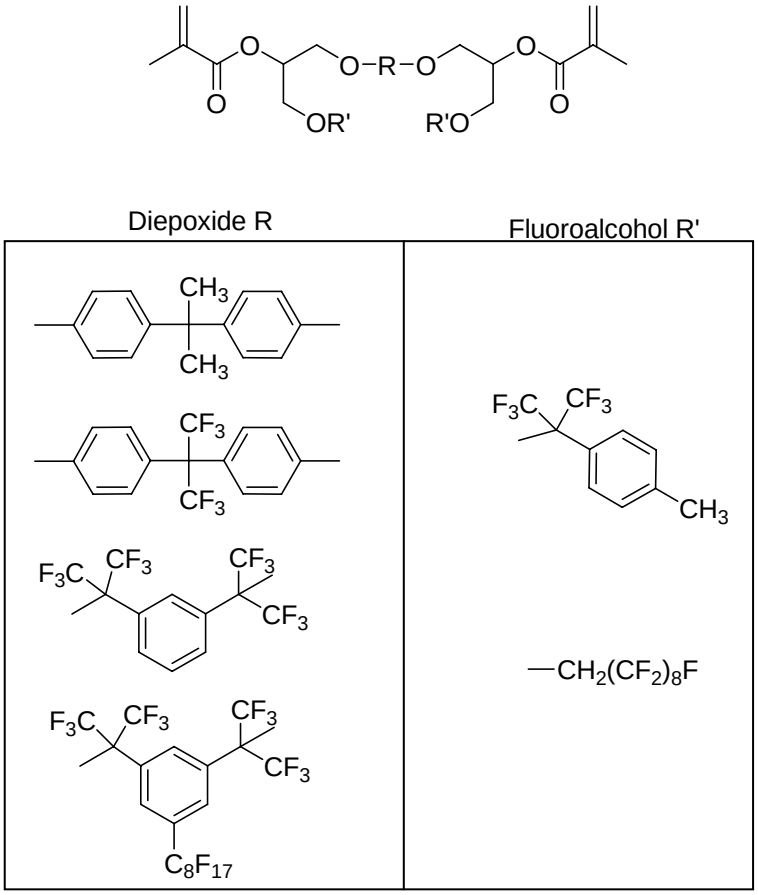

Figure 1.12. Fluorinated monomer structure

Taylor et al. synthesized several dimethacrylates based on structural modifications of Bis-GMA in the core and the side chain units are designated on the basis of the pendant side chains as -OH, -H and -CH_3 (Figure 1.13) [45].

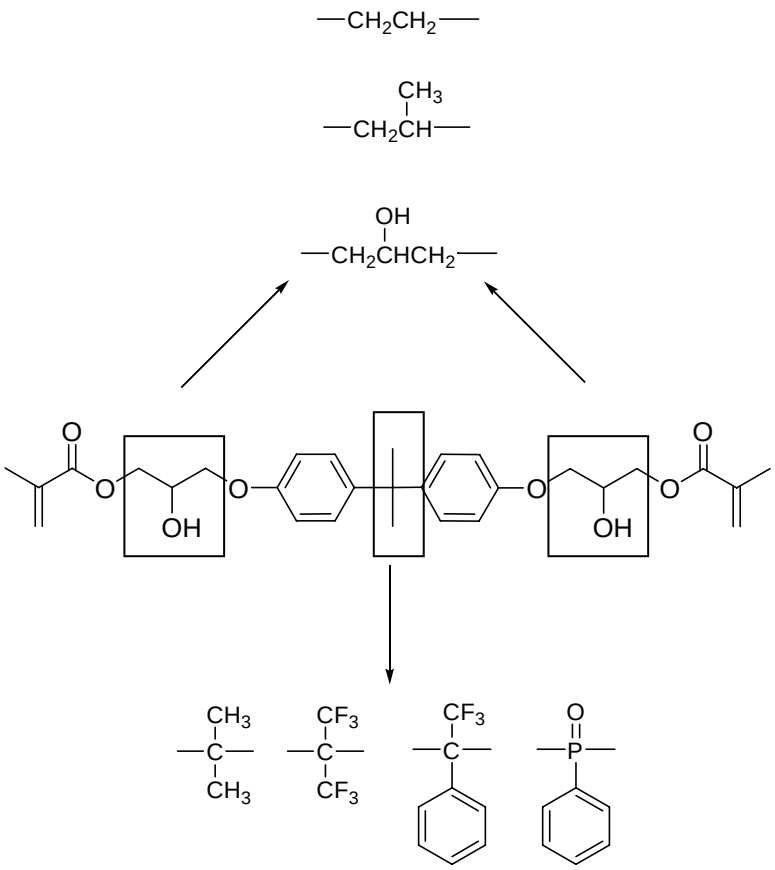

Figure 1.13. Modified Bis-GMA structure in novel monomers

Although dental composite resins have superiority in esthetic, mechanical properties, it is considered to be necessary to use an exclusive adhesive having strong adhesive properties to a tooth structure.

Hybrid materials, known also as polyacid-modified composite resins, are composed of ion-leachable glass embedded in a polymeric matrix. They are introduced to the profession in the early 1990s and presented as a new class of dental material designed to combine the aesthetics of traditional composite resins with the fluoride release and adhesion of glass-ionomer cements [23, 30, 46].

For hybrid materials, the combination of the words *comp*osite resin and glass iono*mer* results the term of compomer which is used to describe water free, single component, light cures composites consisting of acid-modified dimethacrylate reinforced

with silicate glass, for example $SrAlFSiO_4$. In hybrid systems, monomers are characterized by the presence of polymerizable methacrylic residue and acid groups (Figure 1.14) [7, 47, 48].

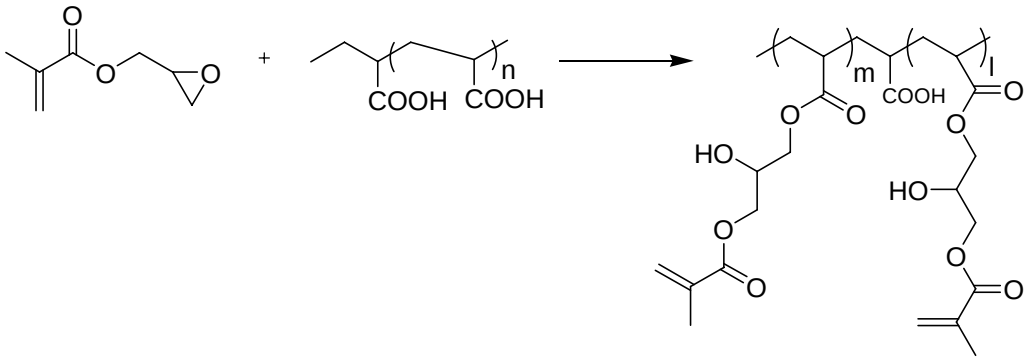

Figure 1.14. Synthesis of GMA-modified poly(acrylic acid)

Basically, the setting mechanism of hybrid materials involves both the free-radical polymerization of methacrylate groups and an acid-base neutralization reaction, with cations released from the glass particles in the presence of water.

However, all compomers showed a decrease in mechanical strength, which is caused by water induced degradation of matrix filler interface. Although hybrid materials were developed to combine the favorable properties of composite resins and glass ionomer cements, the dental restoration with hybrid materials is not a perfect way.

1.2. Adhesion in Dentistry

Various adhesives and pretreatments of the dentin have been used to obtain a strong and permanent bond between used synthetic material and the tooth substance (dentin and enamel). Current adhesives may be divided into major categories based on the number of clinical steps: “etch and rinse” and “self-etch” (Table 1.4) [49].

Table 1.4. Adhesive categories

Etch and Rinse Adhesives	Self-Etching Adhesives	
Three-step	Two-step	One-step
• conditioner • primer • bonding agent	• conditioner + primer • bonding agent	• conditioner + primer + bonding agent

1.2.1. Etch and Rinse Adhesives

“Etch and rinse” adhesives have been used since early 1990’s. These adhesives involve three steps that are etching, priming and bonding.

In etching step, the function of acidic conditioner is to remove smear layer by demineralizing the hydroxyapatite (HAP). A roughened surface with cavities which makes the tooth surface more permeable for the priming step is achieved (Figure 1.15). Besides a 37 per cent solution of phosphoric acid, some organic acids such as oxalic, citric, maleic or lactic acid can also be used as acid conditioner. After it is applied, washing with water and drying of tooth surface are essential. [5, 50]

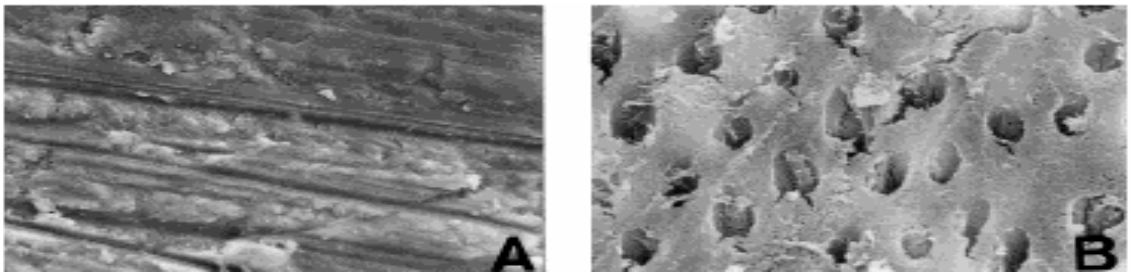

Figure 1.15. SEM images of the treated dentin: (A) ground dentin surface, (B) 37 wt per cent H_3PO_4, water-rinse, air-dried; smear layer was removed and dentin tubules were opened

In priming step, primer serves as an agent to wet and penetrate the etched dentin and prepares to receive the bonding agent. Primer is usually a hydrophilic monomer such as 2-hydroxy-ethylmethacrylate (HEMA). Since much of mineral has been removed in the etching step, primer restores a mostly organic material composed of collagen fibrils [5].

Final step is to apply bonding agent. The composition of bonding agent is similar to the composition of composite resin except the presence of hydrophilic monomers [27]. Bonding agent is brushed onto the prepared dentin surface and then light cured. Adhesive monomers bond to the dentin composed of the exposed collagen fibrils [5].

Major advantage of "etch and rinse" adhesives is the availability of favorable long-term clinical studies. However, these systems are sensitive to the level of dentin wetness after rinsing off the acidic conditioner, too little or too much remaining water may lead to reduced adhesion [51].

1.2.2. Self-Etching Adhesives

"Self-etching" adhesives have been used in dentistry due to their ease and less technique sensitivity more than 10 years. They are divided into one- and two-step systems.

Two-step self-etching adhesives combine etching and priming steps in the initial step. Firstly, self-etching primer is applied to the tooth and then bonding agent is applied to the conditioned surface [49]. The etching potential of enamel or dentin is strongly dependant on the type of acidic groups such as phosphoric, phosphonic or carboxylic acid (Figure 1.16) [52].

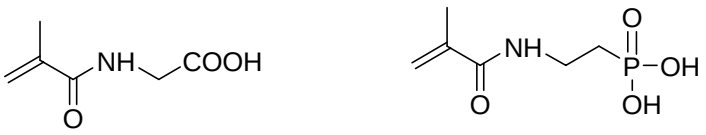

NMGLY NMEP

Figure 1.16. Examples of self-etching primers; N-methacryloyl glycine (NMGLY) and N-methacryloyl-2-aminoethyl phosphonic acids (NMEP)

New generation bonding system that is introduced to the market and called *self-etching adhesives* is caused by the further reduction in the number of clinical steps. Major advantage of self-etching adhesives is that there is no need to be rinsed off. Commercial self-etching enamel-dentin adhesives consist of a mixture of self-etching adhesive monomers, crosslinkers, additional monofunctional co-monomers and additives (Figure 1.17) [53, 54].

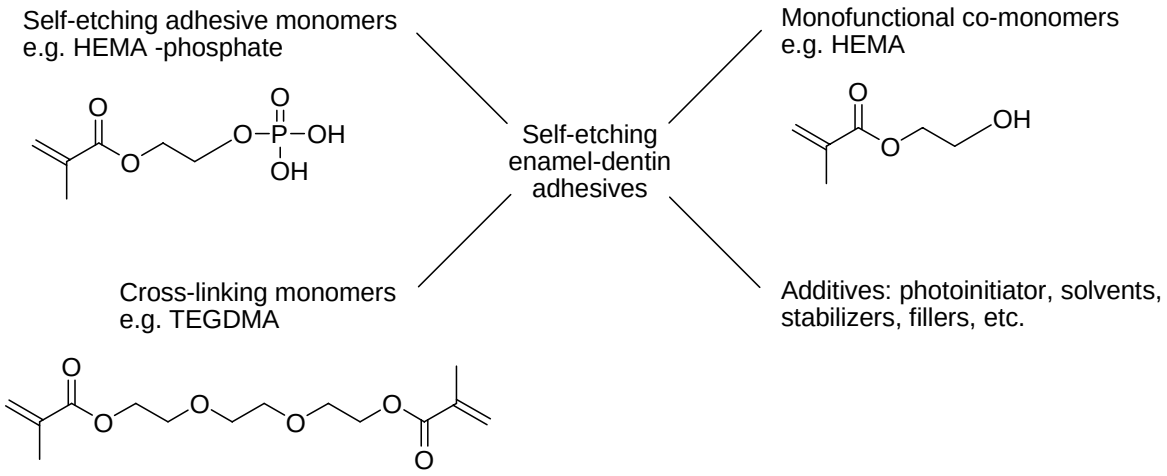

Figure 1.17. Components of currently available self-etching enamel-dentin adhesives

Self-etching enamel-dentin adhesives have to meet the following general requirements:

- High rate of free radical polymerization with the other monomers.
- Miscibility with aqueous solutions of acetone and ethanol, which are mainly used as solvents in commercial adhesive systems.
- Sufficient stability of both the monomer and the formed polymer against degradation by oxygen, heat, light and of course water during storage.
- Minimal water uptake and low swelling degree of the formed polymer.
- Low polymerization shrinkage or thermal stress in the adhesive layer.
- Low oral toxicity and cytotoxicity of the monomers.

There are three different monomer groups in the self-etching enamel-dentin adhesives: adhesive monomers, cross-linking monomers, monofunctional co-monomers.

1.2.2.1. Adhesive Monomers. The function of adhesive monomers is forming specific interaction between adhesive and dental hard tissue. Therefore, beside the above mentioned general requirements for the adhesive monomers, they should meet the following additional demands [53, 54]:

- Capability of self-etching the enamel surface in a relatively short time while forming a surface with increased roughness that enables micromechanical bonding of the adhesive on enamel.
- Optimal wetting and film forming behavior on the tooth surface and the ability of penetrating, for example, into the dental tubules.
- Fast ionic or covalent interaction with components of the dental hard tissue, e.g., the formation of low soluble calcium salts or formation of covalent bonds with collagen.

Generally, these bonding agents contain a polymerizable group P, which can react both with the other monomers of the adhesive and the restorative material by

copolymerization, an adhesive group AD, such as a strong acidic group capable of both etching the dental hard tissues and interacting with the tooth substance, and a spacer group R, designed to influence the solubility, flexibility and the wetting properties of the adhesive monomer (Figure 1.18) [55].

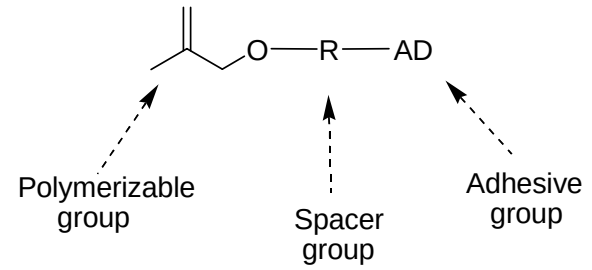

Figure 1.18. Design of a self-etching adhesive monomer

Various free-radically polymerizable groups are shown in Figure 1.19. Methacrylate functions have sufficient reactivity; however, they may increase the toxicological risk of the monomers. Methacrylamides provide easier access to synthetics with enhanced hydrolytic stability under acidic conditions. Vinyl and styryl monomers are less reactive in the free radical photopolymerization and often it is more difficult to synthesize additional functionalized derivatives of these monomers. Allyl monomers exhibit a low tendency towards homopolymerization and in the mixture of other monomer they show a degradative chain transfer reaction [55].

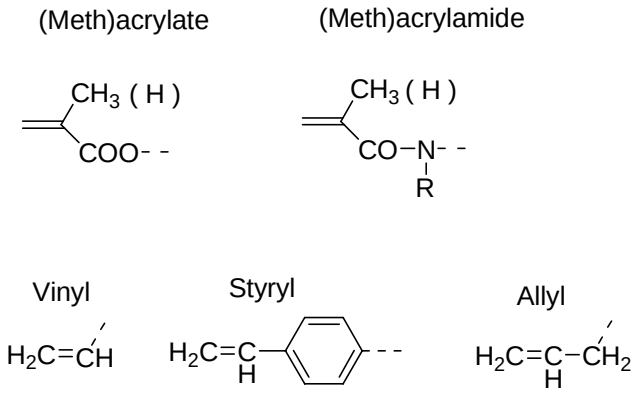

Figure 1.19. Polymerizable groups in monomers for adhesives

The structure of spacer groups influences the properties of the resulting polymers, such as hydrophilicity, swelling properties, flexibility or stiffness (Figure 1.20) [55].

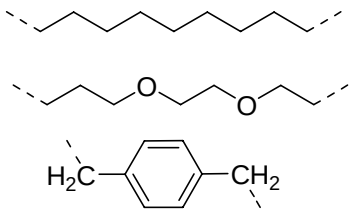

Figure 1.20. Examples of spacer groups R in adhesive monomers

Suitable adhesive groups containing acidic groups are shown in Figure 1.21. The general potential to etch enamel largely depends on the acidity of the monomers that increases in the following order: carboxylic acids < phosphonic acids < acid phosphates < sulfonic acid. Acid groups can form ionic bonds and chelating groups can form coordinative linkages with the calcium ions in enamel or dentin. Also, as dentinal collagen contains reactive groups such as amino or hydroxyl, the reaction of covalent coupling groups with the dentin can form covalent bonds with the collagen fibers if the conditions are mild. Moreover, Van der Waals forces, London dispersion forces, hydrogen bonding or charge-transfer interactions may additionally contribute to the physical adhesion [55].

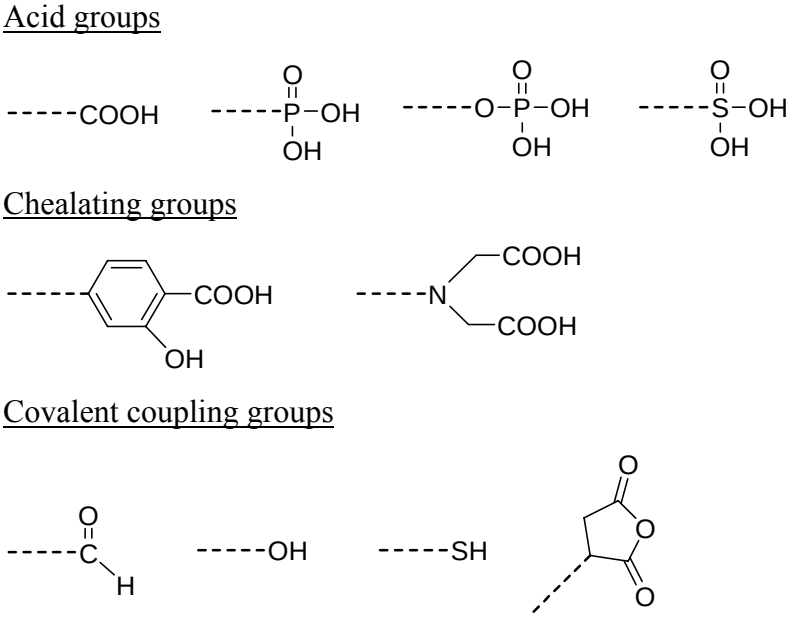

Figure 1.21. Adhesive groups (AD)

In general, phosphorus-containing monomers are capable of etching enamel and dental and promote monomer diffusion. Among the phosphorus-containing monomers, polymerizable phosphonic acid or phosphoric acids are commonly used.

Polymerizable phosphoric acids: Phosphoric acid esters are favorable as components of dentin adhesives because they are able to remove the smear layer on the dentin and achieve a strong bond between restorative material and tooth substance. One of the first chemical compounds proposed to improve bonding to human dentin was the glycerol dimethacrylate ester of phosphoric acid (GDMP) [55]. Further commercially available examples are methacryloyloxyethyl phenyl hydrogen phosphate (MEP-P), 10-methacryloyloxy methacrylate MDP, and methacryloyloxyethyl dihydrogen phosphate (MEP, HEMA-phosphate) (Figure 1.22) [27, 56].

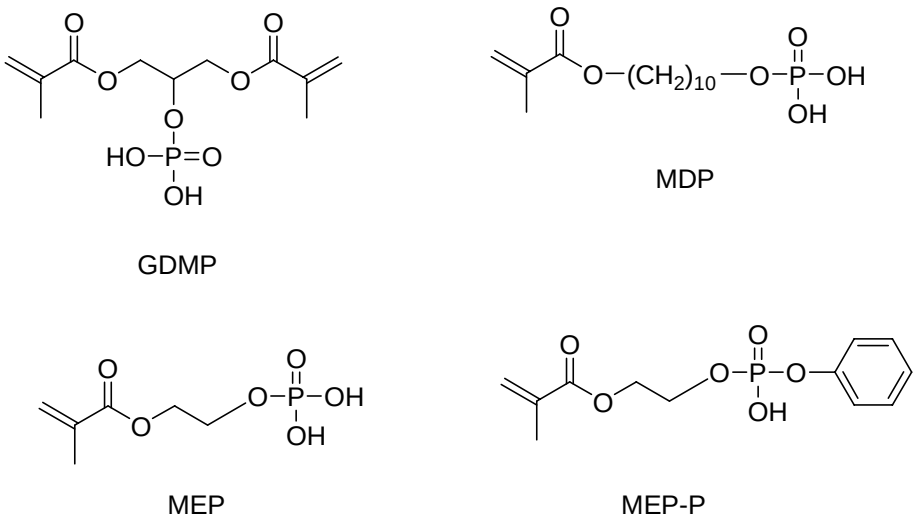

Figure 1.22. Examples of polymerizable acidic phosphates used in dentin adhesives

However, low hydrolytic stability of polymerizable phosphoric acids is major disadvantage [57, 58].

In general, the hydrolytic stability of the phosphoric acid esters increases in the following order: dialkyl hydrogen phosphate < trialkyl phosphate < monoalkyl dihydrogen phosphate (Figure 1.23).

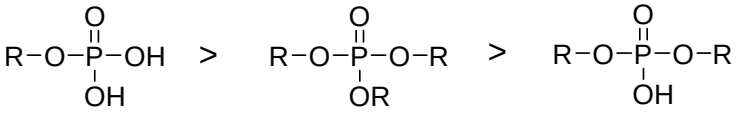

Figure 1.23. Order of hydrolytic stability of the phosphoric esters

In the case of acidic methacrylate phosphates, an additional hydrolytic instability results from the hydrolysis of the methacrylate ester bond. For MEP, even though hydrolysis of the phosphate ester bond was not expected, it was found that the hydrolysis of both the methacrylate and phosphate ester bonds resulted in the formation of methacrylic acid and HEMA (Figure 1.24) [53].

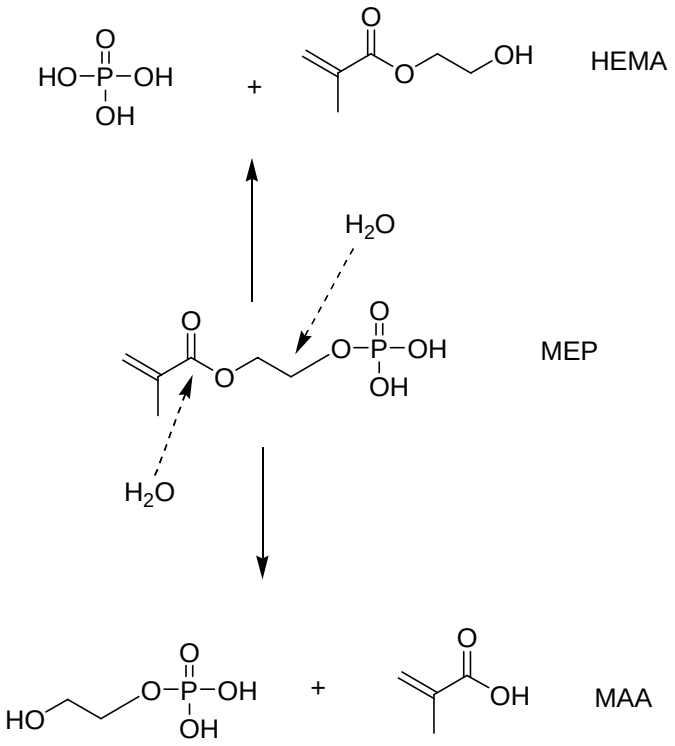

Figure 1.24. Hydrolysis of MEP in the presence of water

Polymerizable phosphonic acids: In order to solve the hydrolytic instability of methacrylate phosphates, monomers that contain more hydrolytically stable bonds achieved by the use of phosphonates are designed.

A first evaluation of polymerizable phosphonates for dental adhesives was carried out by Anbar *et al.* [59, 60]. They proved that vinyl phosphonic acid (VPA) and 4-vinylbenzyl phosphonic acid (VBPA) can improve the adhesion of the filling composites on etched enamel (Figure 1.25). Unfortunately, VPA and VBPA are less reactive than methacrylates in radical polymerization.

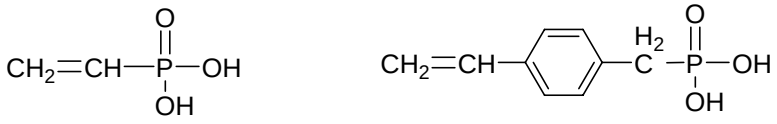

VPA VBPA

Figure 1.25. Structure of monomeric phosphonic acids VPA and VBPA

Moszner *et al.* synthesized a number of new monomers containing more hydrolytically stable bonds (Figure 1.26) [55].

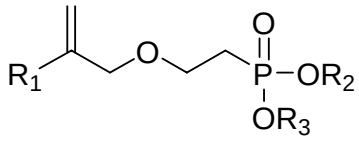

	R_1	R_2	R_3
1	$CO\text{-}OC_2H_5$	H	H
2	$CO\text{-}OC_2H_5$	H	CH_3
3	COOH	H	H
4	COOH	CH_3	CH_3/ C_2H_5
5	COOH	H	CH_3
6	CN	CH_3	CH_3
7	CN	H	H
8	$CO\text{-}N(C_2H_5)_2$	CH_3	CH_3
9	$CO\text{-}N(C_2H_5)_2$	H	H

Figure 1.26. Examples of phosphorus containing monomers

Among the synthesized monomers, 2-[4-(dihydroxyphosphoryl)-2-oxa butyl] acrylate (entry 1) shows the best dentin adhesive properties, whereas the carboxylic acid and nitrile derivatives, 2-[4-(dihydroxyphosphoryl)-2-oxabutyl]acrylic acid (entry 3) and 2-[4-(dihydroxyphosphoryl) -2-oxabutyl]acrylonitrile (entry 7), exhibited less adhesive action. These monomers are hydrolytically stable in aqueous solutions at room temperature.

Recently, U.S. Patent No. 6,902,608 B2 shows the synthesis of new dental materials which have good adhesive properties and high resistance to hydrolysis (Figure 1.27) [61]. The dental materials comprise phosphonic acids with the general structures given below:

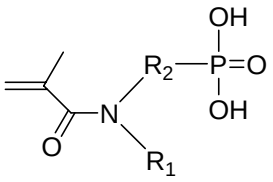

R_1= H, Methyl, Ethyl, Isopropyl

R_2= Alkyl group with 4-18 C-atoms

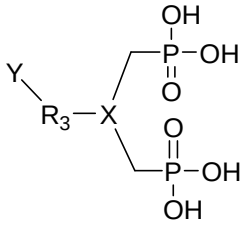

X= N, B or CH group.

R_3= Alkyl group with at least 3C atoms, aryl group, polyether group with 1-10 polyether units.

Y= CH_2=CH-O-,styrene, methacrylamide and CH_2=C($COOR_4$)-CH2-

R_4= H, methyl, ethyl, isopropyl or butyl.

Figure 1.27. General adhesive monomer structures of the invention

Polymerizable carboxylic acids: Only a few polymerizable carboxylic acids are used commercially as a self-etching adhesive. Examples are 4-methacryloyloxyethyl trimellitic acid (4-MET), 10- methacryloyloxydecyl malonic acid (MAC-10), N-acryloyl aspartic acid (NAASP), N-methacryloyl-1-aminosalicylic acid (MASA), N-(vinylbenzyl)iminodiacetic acid (NVBIDA) and N-methacryloyl glycine (NMGLY) (Figure 1.28) [50, 62, 63].

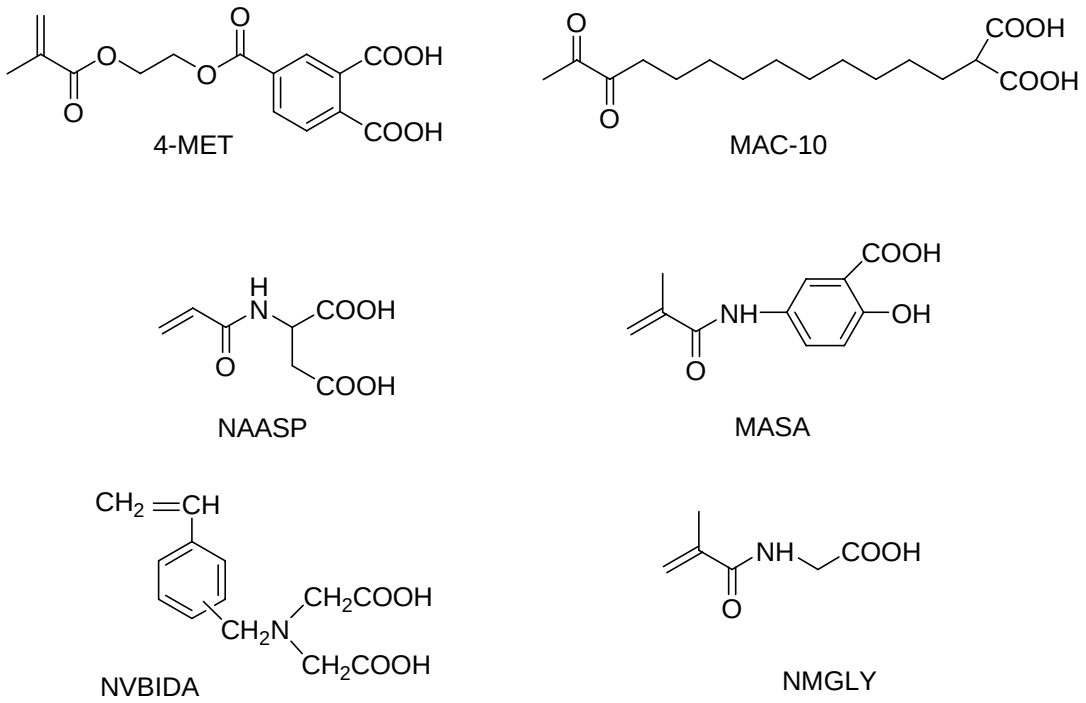

Figure 1.28. Examples of COOH-containing adhesive monomers

1.1.2.2. Monofunctional Co-monomers. HEMA is the most frequently used monofunctional monomer (Figure 1.17). Its hydrophilic nature improves the miscibility and solubility of the adhesive components and the wetting behavior of the adhesive on the dental hard tissue.

Nishiyama *et al.* showed that, HEMA solution was applied to etched dentin in order to achieve an increase in the bond strength. However, the bond strength was strongly dependent on the pH of the aqueous solution. The interaction between the ester carbonyl portion in the HEMA and the undissociated carboxylic acid of the collagen functional group became stronger when the pH was decreased [64, 65].

Also, different substitutes of HEMA, N-(2-hydroxyethyl)-methacrylamide (HEMAM) and N-methyl-N-(2-hydroxyethyl)-acrylamide (MHEAM) were synthesized as they have improved hydrolytic stability and showed very low cytotoxicity [53].

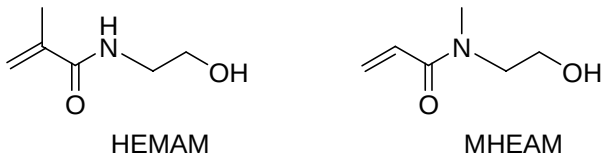

Figure 1.29. Structure of HEMA substitutes with improved hydrolytic stability

1.1.2.3. Cross-Linking Monomers. Cross-linking dimethacrylates, such as Bis-GMA, TEGDMA, urethane dimethacrylate (UDMA) and glycerol dimethacrylate (GDMA) are used in order to improve the polymerization rate of the adhesive because of the gel effect and the mechanical properties of the adhesive layer formed as used in composite resin restorative materials. Finally, the formed cross-linked layer is not water soluble and the degree of swelling decreases with the increasing polymer network density. Bis-GMA shows high reactivity but it has high viscosity and low water solubility. In contrast, TEGDMA and GDMA exhibit low viscosity and better solubility in water (Figure 1.7).

Unfortunately, all these dimethacrylates are not hydrolytically stable in aqueous acidic solutions and degrade forming the corresponding diols and methacrylic acid. So, new cross-linking bisacrylamides with improved hydrolytic and storage stability were synthesized (Figure 1.30). N,N'-diethyl-1,3-bis(acrylamido)-propane (DEBAAP) remained stable in aqueous ethanol in the presence of 20 wt per cent of phosphoric acid at 37 ºC for a test period of 4 months whereas GDMA was not stable after one day. These bis(acrylamide)s are completely soluble in water and ethanol and show similar reactivity with GDMA. However, bis(methacrylamide)s are less reactive than the corresponding bis(acrylamide)s [66].

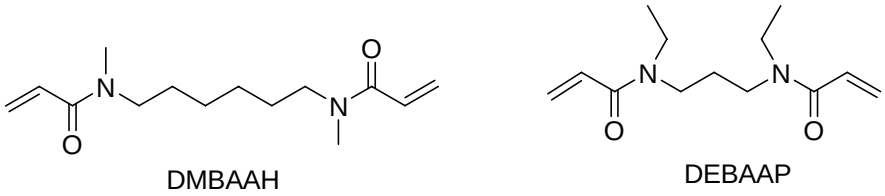

Figure 1.30. Structure of bis(acrylamide)s with improved hydrolytic stability

1.2.2.4. Additives. Various dental adhesive systems are available with significant amount of additives on market.

The most important additive is photoinitiator or photoinitiating system. As mentioned before in composite resins, setting mechanism provides the property of "cure on command".

Fillers are also used as additives in order to improve mechanical properties. However, compared to other restorative filling materials, filler content and composition play a minor role in dental adhesive systems. Silica, alumina, ceramics, clay minerals, ZrO_2, TiO_2, quartz powder, glass ceramic powder or glass powder etc. are often used [67]. Adhesive systems with fluoroalumino silicate glass powder continuously release flouride ions so that an effective reinforcement of the tooth structure and inhibition of secondary caries can be expected [68].

Some manufacturers add different dyes to their adhesive formulations. In two component systems, dyes are used to indicate to the clinician that if both components have been properly mixed by featuring a color change. The color is also useful for facilitating the control of homogenous tooth coverage. When the adhesive system is light cured, the color fades out [53].

During the last years, it was shown that total etch and self etch adhesive systems possess short term inherent antibacterial activity due to their low pH values during the acid etch procedure [69]. But, addition of antibacterial components to the adhesive formulations is manifold to ensure the biological sealing of the restoration as oral bacteria can penetrate through micro gaps in between restoration and tooth generating secondary caries and pulp damage. For many years, glutaraldeyhde has been used as a disinfectant, which features antibacterial properties. Due to the fact that gluteraldehyde can not be polymerized into the adhesive matrix, the antibacterial effect persists after polymerization because the molecules are leaching. In contrast, a polymerizable antibacterial monomer 12-methacryloyloxy dodecylpyridiunium bromide (MDPB) was introduced by Kuraray Company (Figure 1.31). If this monomer is used in the adhesive system, it will provide

antibacterial effects before polymerization and polymerized adhesive will have bacteriostatic activity as a contact antimicrobial [70].

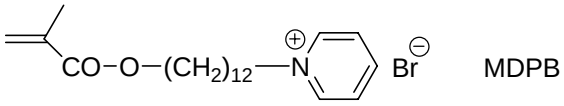

Figure 1.31. A polymerizable antimicrobial agent

1.2.3. Adhesion to and Decalcification of Hydroxyapatite by Acids

In dentistry, acids are generally applied to teeth for two distinct purposes. Polyalkenoic acid possesses the unique property of self-adherence to human calcified tissue and form an essential feature of glass-polyalkenoate cements. Other acids, such as phosphoric, citric and maleic acid, are merely used to enhance the surface energy of enamel and dentin and provide the initial step of the application procedure by which resin composites bond to tooth tissue [71].

Inherent mechanisms of the interaction of acids with hard tissues have never been fully elucidated. Yoshida et al. proposed a concept called "Adhesion-Decalcification Concept" as shown schematically in Figure 1.32 in order to explain why carboxylic acids either adhere to or decalcify hydroxyapatite (HAP). In the first phase, carboxyl groups of the acids form ionic bonds to calcium at the HAP surface. This step may largely be determined by the pKa of the acids. At the same time, PO_4^{-3} and OH^- are extracted by H_3O^+ from the HAP surface and brought into solution. In the second phase, the acids investigated either remained attached to the HAP surface, with only a limited decalcification step, or de-bonded with a significant decalcification effect. From this study, it appears that the fact the acids either adhere or decalcify HAP may depend on the dissolution rate of the respective calcium salts in the acidic solution, regardless of concentration or pH [71]. The less soluble the calcium salt of the acidic molecule, the more intense and stable the molecular adhesion to a hydroxyapatite-based substrate.

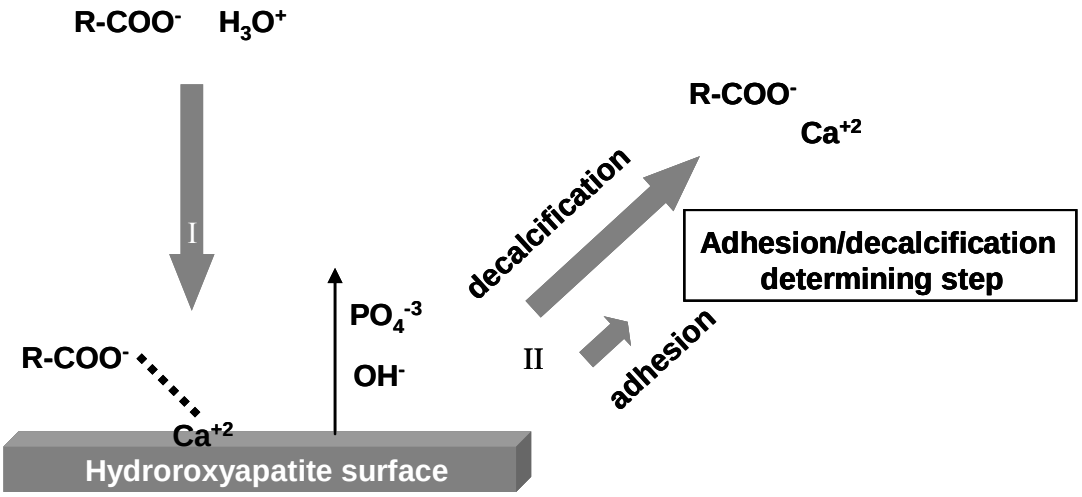

Figure 1.32. Schematic presentation of the adhesion/decalcification concept

Yoshida *et al.* characterized the adhesive interaction of monomers, MDP, 4-MET and MEP-P (see Figures 1.22 and 1.28), with synthetic hydroxyapatite, using x-ray photoelectron spectroscopy and atomic absorption spectroscopy (AAS) [72]. MDP has a high chemical bonding potential to hydroxyapatite within a clinically reasonable application time. The chemical bonding capacity of 4-MET is weaker and it is doubtful that 4-MET within a short application time, is capable of chemically bonding to hydroxyapatite. The chemical bonding efficiency of MEP-P is the lowest among the functional monomers investigated. In accordance to the adhesion-decalcification concept, AAS results showed that calcium salt of MDP was hardly soluble; the calcium salt of 4-MET could be dissolved more easily, whereas MEP-P was very soluble in water.

Albayrak *et al.* examined the amount of decalcification of the hydroxyapatite in synthesized phosphonic and carboxylic acid containing monomer (Figure 1.33).

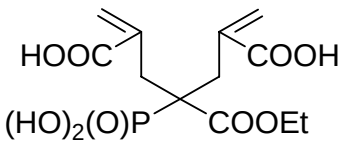

CA-PA

Figure 1.33. Synthesized phosphonic and carboxylic acid containing monomer

The pH dependencies on the chemical shifts of the carbonyl carbon and the α-methylene carbon to the phosphorus were examined. When CA-PA was titrated with NaOH, α -methylene carbon peaks were shifted to a lower field reflecting the formation of an acid-base interaction (Figure 1.34). The titration curve showed three jumps in the chemical shift difference of the α-methylene carbon. First, one hydroxyl group of phosphonic acid dissociates (0.46 ppm), then carboxylic acid (0.73 ppm), and finally the remaining hydroxyl group of phosphonic acid (0.47 ppm) dissociates according to the chemical shifts of α -methylene carbon [73].

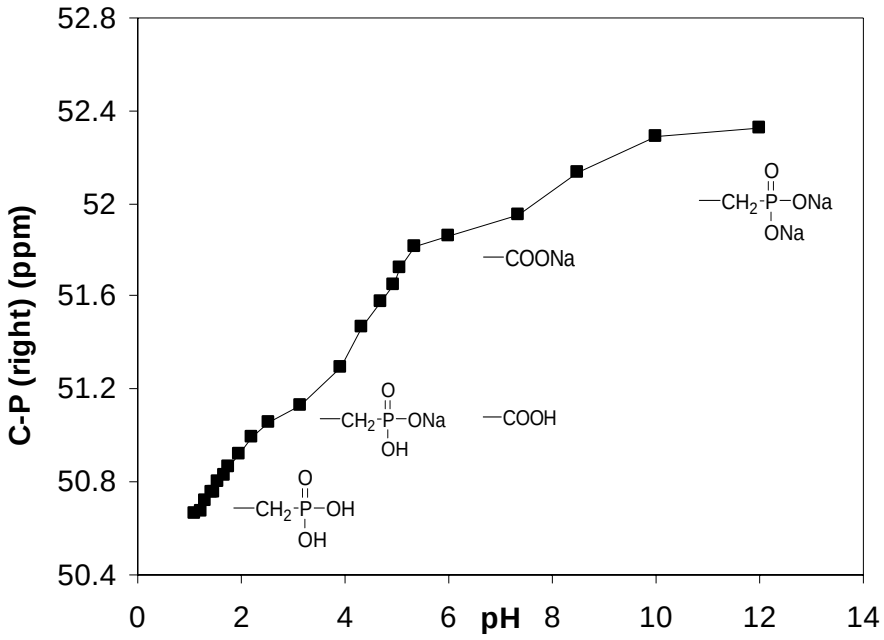

Figure 1.34. pH Dependencies of the chemical shift of the α-methylene peak to the phosphorus and carbonyl carbon peak in CA-PA

In order to evaluate interactions of CA-PA with the calcium in tooth, two different amounts of HAP were added to the aqueous solution of the monomer. The chemical shift differences of CA-PA with 25 mg HAP (0.37 ppm for the α-methylene carbon and 0.80 ppm for the carbonyl carbon) are below the value for the start of the second dissociation due to the carboxylic acid group. Interacted amount of the first OH group of the phosphonic acid was 78.7 per cent when calculated with respect to the α-methylene carbon shifts and 80.6 per cent when calculated with respect to the carbonyl carbon shifts.

When the HAP amount is doubled, the chemical shift differences increase such that, all the first OH group of the phosphonic acid was interacted and 11.7 per cent of the two carboxylic acids started to interact when calculated with respect to the carbonyl carbon shifts. But, interacted amount of carboxylic acid was turned out to be 5.2 per cent when calculated with respect to the α-methylene carbon shifts (Table 1.5.) [73].

Table 1.5. Interaction of CA-PA with HAP

			In the presence of HAP			
Monomer	HAP[a] (mg)	pH	. α-CH_2 (right)		-COOH	
			S.D.[b]	I.A.(%)[c]	S.D.[d]	I.A.(%)[e]
CA-PA	25	2.63	0.366	78.7	0.800	0
CA-PA	50	3.39	0.503	100	1.509	5.2-11.7

[a]Amount of HAP added to monomer solution

[b]Chemical shift difference for the α -CH_2 peak in CA-PA after addition of HAP

[c]Interacted amounts of the phosphonic acid groups in CA-PA with HAP

[d]Chemical shift difference for the carbonyl carbon of the carboxylic acid in CA-PA after addition of HAP

[e]Interacted amounts of the carboxylic acid groups in CA-PA with HAP

In the other study, Nishiyama *et al.* examined the amount of decalcification of the hydroxyapatite or dentin in NMGLY (see Figure 1.28) as a self-etching primer [74].

1.2.4. Bonding Effectiveness

In the literature, it was demonstrated that acid etchant causes demineralization of the hydroxyapatite by removing the smear layer and expose the collagen tubules, leading to more roughened surface. The surface changes greatly, becoming chalky, due to the development of microporosity within the surface. The achievement of the bond between bonding resin and dentin depends on the penetration of the bonding resin into the microporosities of the conditioned dentine surface in order to create a micro-mechanical interlocking between the dentinal collagen and resin to form a hybrid layer [75]. So the

extent and the depth of the etching pattern as well as the ionic, covalent or physical interactions between the dentin and the resin should influence the bonding performance of an adhesive.

Strong self-etch adhesives (pH<1), like etch and rinse adhesives, completely remove smear layer from dentin. Dentinal tubules were opened and devoid of smear plugs. In applying a bonding agent to the dentin surface, several micrometers thick, relatively deep resin-dentin hybrid zone is formed (Figure 1.35). However, as mild self-etch adhesives (pH around 2 or more) can only partially demineralize the dentin surface, the etching pattern was not deep enough to obtain good penetration of bonding resin and therefore adhesion of the bonding agent is obtained micro-mechanically through shallow hybridization [76].

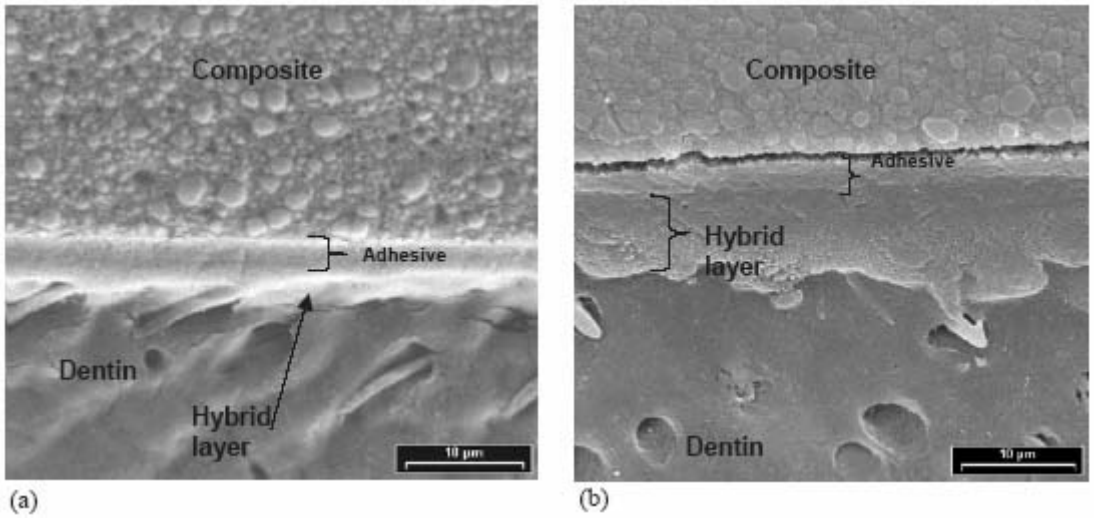

Figure 1.35. a) SEM image of a self-etching sample showing a thin hybrid layer and b) SEM image of a etch and rinse sample showing a thick hybrid layer

Nishiyama *et al.* proposed an adhesion mechanism of the resin to the acid-etched dentin treated with NMGLY primer. The application of the primer facilitated the restoration of the dentinal collagen which had collapsed during the air-drying process. Further, the amide group and/or the carboxylic acid group in the NMGLY molecule hydrogen bonded with the dentinal collagen (Figure 1.36). Since the interaction of the NMGLY molecule promoted the hybridization of the resin to the dentinal collagen

molecule at the interface, it enhanced the bonding of the resin to the dentinal collagen fiber and provided noticeably higher bond strength [77].

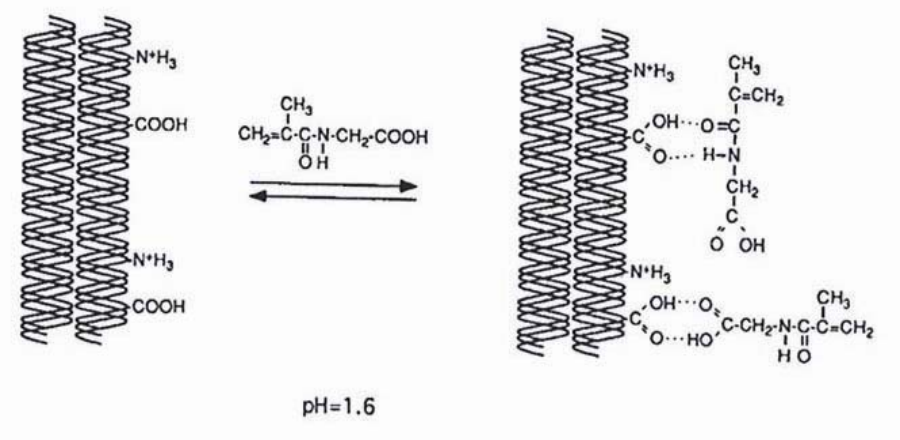

Figure 1.36. Model of hydrogen bonding between NMGLY and dentinal collagen

1.3. Photopolymerization

In dentistry, one of the most important requirements which dental filling systems must fulfill is a fast process at room temperature. Since photopolymerization satisfies this requirement, it is widely used in polymerizable dental systems.

Dental polymerizable systems are usually made of three main components [78].

- A photoinitiator that effectively absorbs the incident light and generates radicals or ions,
- Functionalized monomer or oligomer that will polymerize
- A reactive diluent to adjust viscosity.

Photopolymerization is mainly classified into two groups, depending whether on the reaction proceeds by cationic type or radical type mechanism (Table 1.6). In photoinduced radical polymerization, aromatic ketones are used as initiators which decompose to generate free radical. The produced radicals initiate the polymerization of vinyl monomers by a chain growth addition mechanism. On the other hand, in

photoinduced cationic polymerization, a protonic acid is generated by photolysis of triarylsulfonium (TAS) or diaryliodonium salts to initiate the polymerization of epoxides or vinyl ethers [78]. Radical polymerization type of curing is the most popular and most widely applied [79].

Table 1.6. Different types of photo-curable resins

Mechanism	RADICAL	CATIONIC
Photoinitiator	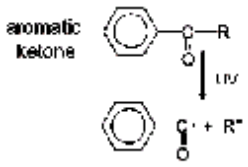	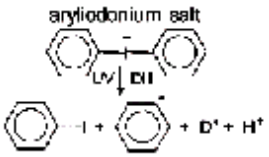
Monomers and functionalized polymers	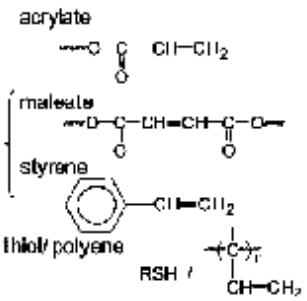	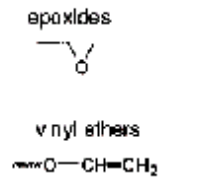

1.3.1. Photoinitiators

Photoinitiators govern the rate of initiation and penetration of light into the sample, and therefore control the depth of the cure. The essential point is to select the initiator which shows the highest initiation efficiency and undergoes a fast photobleaching upon UV exposure in order to achieve a deep-through cure [78].

Classification of photoinitiators is based on the type of polymerization system i.e. free radical or cationic. There are also a few cases of initiators (e.g. iodonium and sulphonium salts, arene complexes), which are able to initiate polymerizations via both cationic and radical processes.

Radical photoinitiating systems are commonly classified according to the nature of the mechanism that produces the free-radical intermediates upon irradiation of the initiators [58].

Photofragmentation generates radical pairs through a highly efficient α-cleavage process (type-I) and the H abstraction process from donor molecules (type-II). Type-I class includes aromatic carbonyl compounds that are known to undergo a homolytic C-C bond scission upon UV exposure (Figure 1.37).

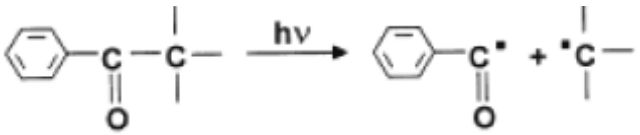

Figure 1.37. Example to type-I photoinitiator

The benzoyl radical is the major initiating species, while the other fragment may, in some cases, also contribute to the initiation. The most efficient photointiators include benzoin ether derivatives, benzyl, ketals, hydroxyalkylpheneones, L-aminoketones, and acylphosphine oxides.

Type-II systems usually consist of two components: An aromatic ketone with a H donor molecule. Aromatic ketones, when promoted to their excited states by irradiation, do not undergo a fragmentation but rather abstract a H atom from a H-donor molecule to generate a ketyl radical and a donor radical. The donor radical initiates polymerization. In Figure 1.38, there is a typical example, benzophenone.

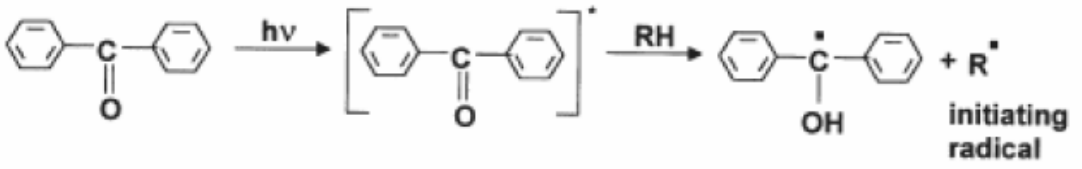

Figure 1.38. Example to type-II photoinitiator

Other examples are; xanthones and thioxanthones, aromatic diketones, phenyl glyoxalates, 3-ketocoumarins, camporquinone, etc.

Figure 1.39 gives the structures of some photoinitiators which are commonly used in both dentistry and other applications [79].

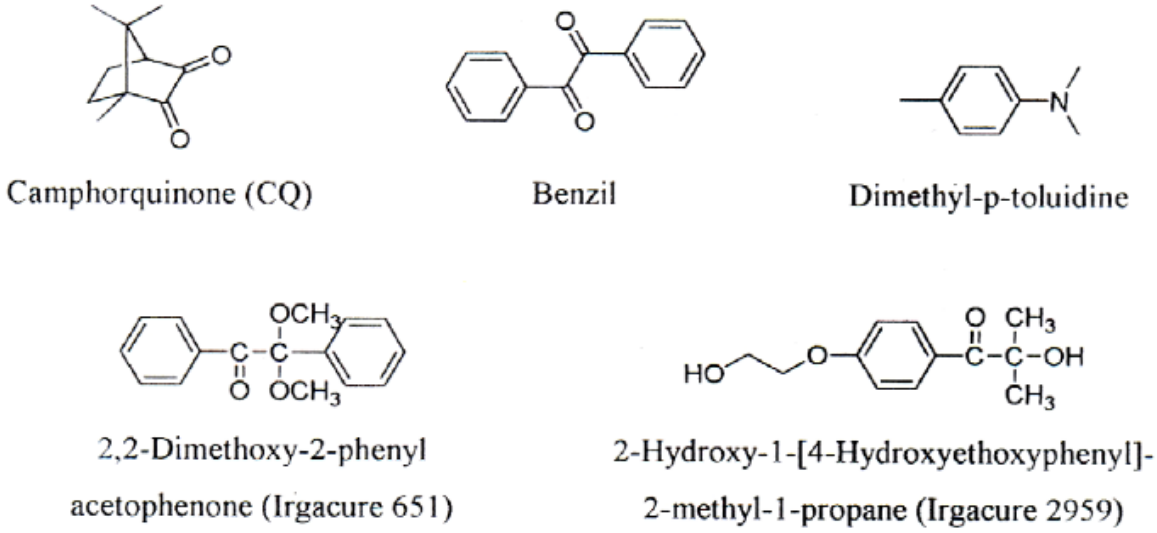

Figure 1.39. Commonly used photoinitiators

1.3.2. Monomers

Widely used monomers in photopolymerization are multifunctional acrylates and methacrylates due to high reactivity and low volatility [59]. Figure 1.40 shows the general structure of the commonly used acrylate/methacrylate based on resin systems [79].

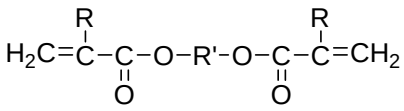

R = H, CH_3
R' = polyether, polyester, polymethane

Figure 1.40. Commonly used (meth)acrylate monomers for light curable systems

The polymerization of dimethacrylate monomer, initiated by UV- generated benzoyl radicals, is assumed to develop according to following scheme (Figure 1.41).

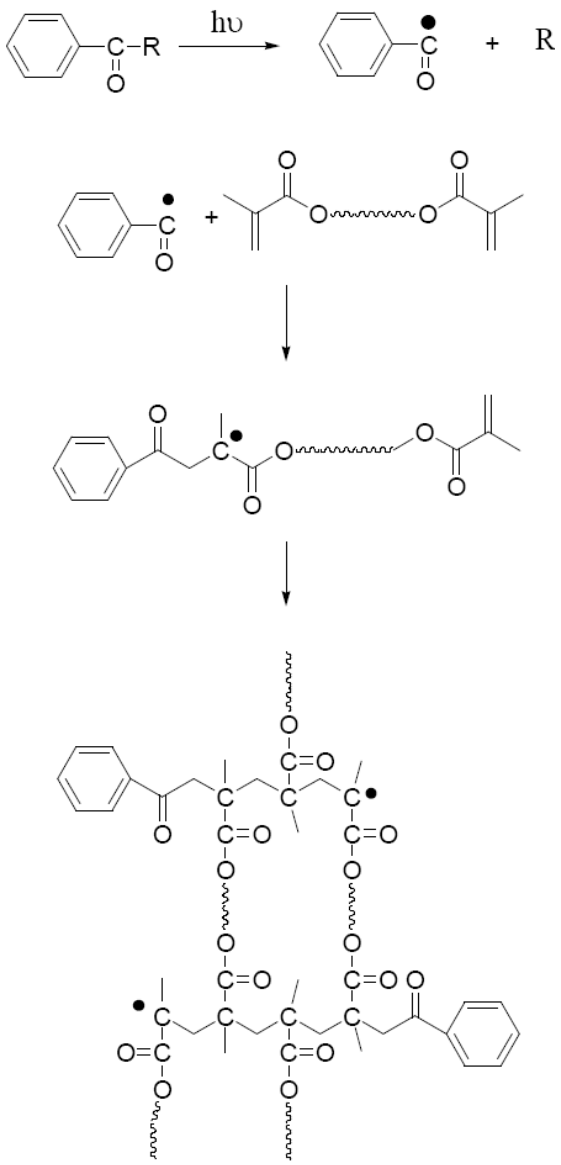

Figure 1.41. Mechanism of the photopolymerization of a dimethacrylate monomer

The rate of polymerization initially depends on the reactivity of the functional group, its concentration and the viscosity of the resin. The chemical structure, distance and flexibility between the functional groups, and the functionality of both monomer and/or oligomer are also important. These factors determine the final degree of polymerization, as well as the physical and chemical characteristics of the UV-cured polymer [80]. For instance, monomers capable of hydrogen bonding generally shows higher rate of polymerization (R_p) compared to their non-hydrogen bonding analogues. A plausible explanation for this enhanced polymerization rate is that hydrogen bonding

results in preorganization in the monomers, by forcing the double bonds to get close with each other. As a consequence, the propagation rate constant (k_p) will be enhanced [81]. Furthermore, hydrogen bonding will increase the overall viscosity of the bulk monomer solution, thus hindering radical termination and causing an increase in radical concentration. The result is an increase in polymerization rate [82]. However, there is a critical distance between double bond and the hydrogen bonding moiety (alkyl bridge length) beyond which there is no effect on R_p in the case of the preorganization theory. This is because conformational mobility of the skeletal bonds between the hydrogen-bonding moieties, the double bond will reach a level whereby the double bond can be regarded as isolated from the hydrogen bonding moiety [81, 82].

Coinitiators are secondary components in the photopolymerization systems. The amines used as coinitiator are both toxic and mutagenic, but they are necessary components of the camphorquinone visible light photoinitiating system. Though work has been done to improve the amine coinitiator, the major purpose has been to decrease the toxicity and improve the polymerization process. Generally, a commercial amine without a methacrylate group has been used as the coinitiator. To enhance the biocompatibility of the coinitiator further, some studies involve the synthesis of monomers which contains two methacrylate groups and two amine groups that could be polymerized to form a more biocompatible polymer system (Figure 1.42) [83].

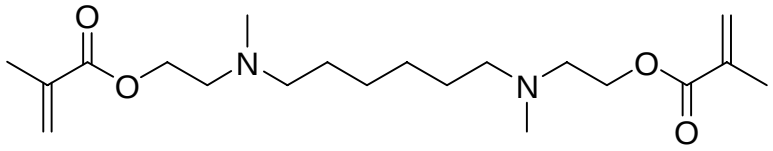

Figure 1.42. N,N'-dimethyl,-N,N'-di(methacryloxyethyl)-1,6-hexanediamine (NDMH)

NDMH has two different kinds of functional groups: methacrylates, which can be free radically polymerized, linking the NDMH to the crosslinked polymer chain; and the amines which serve as coinitiators for hydrogen abstraction.

There is a major drawback of the photocurable composites; volumetric shrinkage of 2-5% during polymerization. Polymerization shrinkage is caused mainly by changing the distance between the free monomer molecules loosely bonded by weak van der Waals force to the distance between the monomers tightly linked by a covalent bond in a polymer. This polymerization shrinkage during a direct composite restorative procedure creates a detrimental strong stress at the interface between the cavity wall and the composite restoratives, which often cause adhesion failure or micro cracking of the enamel margin. Consequently, the micro gap induced by the setting stress of composites between the restorative and the cavity wall may give rise to postoperative hypersensitivity, secondary caries and pulpits. Many researchers have developed various clinical restorative techniques such as incremental filling, slow start polymerization and delayed curing to reduce or eliminate polymerization shrinkage during the restorative procedure [84].

1.3.3. Light Sources

Since the initiation rate of photopolymerization can be varied by changing the light intensity, light source is another significant factor in the photo-curing process. Simply, increase in light intensity will lead to an increase in polymerization rate. In general, there are two major light sources that are used.

- Arc light
- Laser light

An arc lamp is the general term for a class of lamps that produce light by an electric arc (or voltaic arc). The lamp consists of two electrodes typically made of tungsten which are separated by a gas. The type of lamp is often named by the gas contained in the bulb; including neon, argon, xenon, sodium, metal halide, and mercury.

The gas pressure can be low (10-3 torr), medium (1-2 atm), or high (> 2 atm). The medium-pressure mercury lamp is the most important light source used in the photo- or UV-curing industry [85]. The common flourescent lamp is actually a low-pressure

mercury arc lamp where the inside of the bulb is coated with light-emitting phosphorus. Lightning could be thought of as a type of natural arc lamp, or at least a flash lamp.

Lasers offer the prospect of an excitation source of exceedingly high intensity compared to classical light sources. The output of a laser can be pulsed or a continuous beam; visible, IR, or UV; with power ranging from less than a milliwatt to millions of watts. Some lasers offer fixed wavelength, whereas some others offer tunable wavelengths [85].

In dentistry, 420-500 nm light in visible region is used [86].

1.3.4. Photopolymerization Kinetics of Monomers

Photopolymerization kinetics can be studied in various methods such as differential scanning calorimetry, dilatometry, fluorescence spectroscopy, and RT-FTIR spectroscopy. By these techniques, heat evolved, volume shrinkage, increase in viscosity or disappearance of the reactive groups are monitored. The rate of polymerization, propagation, and termination rate constants can be calculated from heat flow during polymerization according to the following equations by using differential scanning calorimetry technique (Figure 1.43):

$$R_p = \frac{(Q/s)\ M}{n\ \Delta H_p\ m} \qquad \frac{k_p}{k_t^{1/2}} = \frac{R_p}{[M]\ (\Theta I_0 \varepsilon [A])^{1/2}}$$

(Q/s)	: heat flow per second during reaction
M	: molar mass of the monomer
n	:number of double bonds per monomer molecule
ΔH_p	: heat released per mol of double bonds reacted
m	: the mass of the monomer in the sample
Θ	: the initiator efficiency
[M]	: molar concentration of the double bonds
I_0	: incident light intensity
ε	: extinction coefficient of the initiator
[*A*]	: initiator concentration

Figure 1.43. Equation of the rate of polymerization

At the very beginning of the irradiation autoacceleration occurs because of the rapid increase in viscosity until the reaction reaches its maximum rate value. It is followed by a period where the polymerization develops, the time after which autodeceleration starts to take place when propagation becomes diffusion controlled. Ultimately, vitrification leads to a complete stop of the curing process through the end of the polymerization. A certain amount of unreacted acrylic double bonds remains in the crosslinked polymer, which may affect the long term properties of the UV-cured material [85] (Figure 1.44).

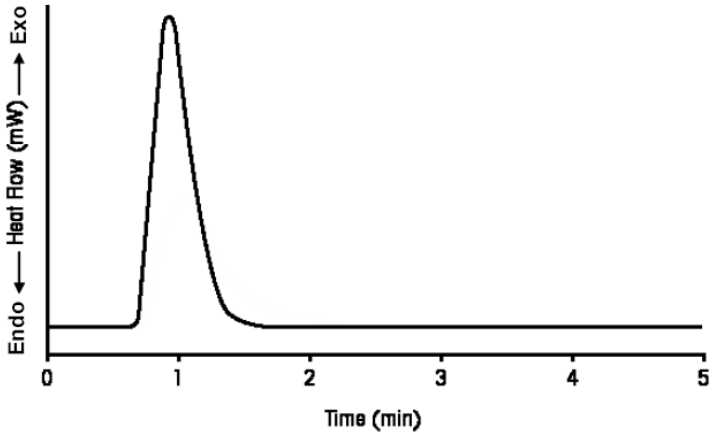

Figure 1.44. Representative heat flow versus time plot obtained from differential scanning calorimeter technique

1.3.5. Other Applications of Photopolymerizing Systems

Photocuring technology has been used in a variety of industrial applications due to the unique properties, such as high speed, solvent-free formulations, low energy consumption, ambient temperature operations, and tailor-made properties of the photocured polymers. Besides its wide use in dental restorative filling systems, photopolymerization has also found application areas in coating industry, for instance fast-drying varnishes, paints or printing inks, quick-setting adhesives, sealants; and also optical disks, microcircuits, and contact lenses are some of the other areas which photocuring technology is used [77, 87, 88].

2. OBJECTIVES

The purpose of this study is to develop novel self-etching adhesive and crosslinking dental monomers aiming for all the properties that are desired in a good dental monomer, namely a) ability to form bonds with dental tissues, b) high rate of polymerization and copolymerization with common monomers used in dentistry, c) biocompatibility, d) hydrolytic and storage stability, e) solubility in water and ethanol, f) good mechanical properties in polymeric form, g) low volume of shrinkage in polymeric form.

The phosphonate, phosphonic and carboxylic acid containing monomers were synthesized from reactions of o-hydroxyaryl phosphonates with alkyl α-hydroxyl methacrylate derivatives. The homo- and copolymerization behavior of these monomers with BisGMA and GDMA were investigated using photodifferential scanning calorimeter. Acidities and interactions of the acid monomers with HAP were evaluated.

3. EXPERIMENTAL

3.1. Materials and Apparatus

3.1.1. Materials

tert-Butyl acrylate (Aldrich, 98 per cent), paraformaldehyde (Merck), 1,4-diazobicyclo [2.2.2] octane (DABCO) (Aldrich), thionyl chloride (Acros, 99.5 per cent), phenol (Aldrich), acrylamide (Aldrich), hydroquione (Aldrich), 2,2 Bis-(4-hydroxyphenyl)-propane (Bisphenol A) (Aldrich), diethyl phosphate (Aldrich), (2-hydroxy-ethyl)-phosphonic acid diethyl ester (Ivoclar Vivadent), bisphenol A diglycidyl ether (DER) (Aldrich), glycidyl methacrylate (GMA) (Aldrich), lithiumdiisopropylamide (LDA) (Aldrich), phosphorus tribromide (Aldrich), bromotrimethylsilane (TMSBr) (Aldrich, 97 per cent), trifluoroacetic acid (Aldrich, 99 per cent), methacrloyl chloride (Merck), ammonium chloride (NH_4Cl) (Merck), K_2CO_3 (Merck), anhydrous $CaCl_2$ (Merck), NaCl (Merck), anhydrous Na_2SO_4 (Merck), triethyl phosphite (Fluka, 97 per cent), triethylamine (Aldrich, 99 per cent) were used as received without purification.

The photoinitiator, 2,2'-dimethoxy-2-phenylacetophenone (Irgacure 651 or DMPA from Aldrich) and the thermal initiators 2,2'-azobis(isobutyronitrile) (AIBN) and 2,2'-azobis(N,N'-amidinopropane) dihydrochloride (V-50) were used as received.

Dichloromethane for hydrolysis reactions and tetrahydrofuran for rearrangement reactions were used as freshly dried under Ar. Ethyl acetate, dichloromethane, hexane and methanol used for column chromatography were received from Cakir Kimya and distilled before use. All other solvents were obtained from Aldrich, Merck or J.T. Baker and used as received.

3.1.2. Apparatus

^{1}H, ^{13}C and ^{31}P nuclear magnetic resonance (NMR) spectra were recorded using Varian Gemini 400 MHz spectrometer. Infrared analysis was performed on a Perkin Elmer 1600 FT-IR spectrometer using NaCl windows or KBr dics. The maximum absorbance of some monomers was measured with an ultraviolet-visible spectrophotometer (UNICAM-UV2). Photopolymerizations were carried out by TA Instruments differential photocalorimeter (DPC) (Q100) containing a high pressure mercury lamp. Gel permeation chromatography (GPC) analysis was done using HP 1050 series GPC with polyethylene oxide standarts.Thermogravimetric analysis (TGA) was carried out on a TA Instruments Q50.

3.2. Synthesis of Starting Materials

3.2.1. Synthesis of tert-Butyl-α-Hydroxymethyl Acrylate (TBHMA)

tert-Butyl acrylate (128.2 g, 1.0 mol), paraformaldehyde (30 g, 1.0 mol) and 1,4-diazobicyclo [2.2.2] octane (DABCO) (14 g, 0.12 mol) were added to a mixture of DMSO (227 ml) and H_2O (85 ml). The mixture was heated at 100 °C for 30 minutes under N_2. Then it was cooled to ambient temperature and aqueous phase was separated. The organic phase was washed with 1 wt per cent HCl (2x100 ml), dried with anhydrous $CaCl_2$ and filtered. The solution was distilled under reduced pressure in the presence of $CuCl_2$ as a free radical inhibitor and pure TBHMA was collected as a colorless liquid in 45-50 per cent yield.

^{1}H-NMR ($CDCl_3$): δ= 1.49 (s, 9H, CH_3), 2.68 (s, 1H, O-H), 4.25 (s, 2H, CH_2-O), 5.72, 6.12 ppm (d, 2H, CH_2=C).

^{13}C-NMR ($CDCl_3$): δ= 28.1 (CH_3), 62.4 (CH_2-O), 81.2 [*C*-$(CH_3)_3$], 124.4 (C=*C*H_2), 140.6 (*C*=CH_2), 165.4 ppm (C=O).

FT-IR (neat): 3500-3000 (OH), 2978 (C-H), 1709 (C=O), 1639 cm^{-1} (C=C).

3.2.2. Synthesis of tert-Butyl-α-Bromomethyl Acrylate (TBBr)

PBr_3 (5.3 ml, 0.056 mol) was added dropwise to a solution of TBHMA (19.2 g, 0.12 mol) in 115 ml of ether on ice, under nitrogen. After 3 h of mixing at room temperature, 69 ml of H_2O was added dropwise in an ice bath and the aqueous phase was separated. Then it was extracted with hexane (3x23 ml). The organic phases were combined, washed with saturated NaCl solution (2x23 ml) and dried with anhydrous $CaCl_2$. After removal of ether by rotary evaporator, distillation was done under reduced pressure to obtain pure product as a colorless liquid in 72 per cent yield.

^{1}H-NMR ($CDCl_3$): δ= 1.47 (s, 9H, CH_3), 4.09 (s, 2H, CH_2-Br), 5.79, 6.16 ppm (d, 2H, CH_2=C) .

^{13}C-NMR ($CDCl_3$): δ= 28.4 (CH_3), 30.2 (CH_2-Br), 81.9 [*C*-$(CH_3)_3$], 128.1 (C=*C*H_2), 139.0 (*C*=CH_2), 164.1 ppm (C=O).

FT-IR (neat): 2978 (C-H), 1717 (C=O), 1632 (C=C), 720 cm^{-1} (C-Br).

3.2.3. Synthesis of 2-Chloromethyl-Acryloyl Chloride (CMAC)

Thionyl choride (15 ml) was added dropwise to TBHMA (4.45 g, 0.028 mol) in an ice bath under nitrogen. The mixture was stirred at room temperature for 1 day. After removal of thionyl chloride CMAC was obtained as a colorless liquid in 35per cent yield.

^{1}H-NMR ($CDCl_3$): δ= 4.26 (s, 2H, CH_2-Cl), 6.41, 6.74 ppm (2H, CH_2=C).

^{13}C-NMR ($CDCl_3$): δ= 41.99 (CH_2-Cl), 136.21 (C=*C*H_2), 141.44 (*C*=CH_2), 166.90 ppm (C=O).

FT-IR (neat): 2966 (C-H), 1747 (C=O), 1640 (C=C), 896 cm^{-1} (C-Cl).

3.2.4. Synthesis of Diethyl (2-Hydroxyphenyl) Phosphonate

To a mixture of phenol (8.80 g, 93.5 mmol) and diethylphosphite (18 ml, 143.5 mmol) in 40 ml carbontetrachloride, triethylamine (20 ml, 143.5 mmol) was added dropwise at 0 ^{o}C. The reaction mixture was stirred overnight at room temperature. Then, it was extracted with water (3x15 ml) and the organic layer was dried with anhydrous Na_2SO_4. Removal of solvent gave diethyl phenyl phosphate as a pure yellow liquid in 86 per cent yield.

^{1}H NMR ($CDCl_3$): δ= 1.31 (t, 6H, CH_2-CH_3), 4.17 (q, 4H, CH_2-CH_3), 7.12 (dd, 1H, Ar-CH) 7.18 (t, 2H, Ar-CH), 7.29 ppm (dd, 2H, Ar-CH).

^{13}C NMR ($CDCl_3$): δ= 16.4 (CH_3-CH_2), 64.7 (CH_3-CH_2), 120.1(Ar-CH), 125.3 (Ar-CH), 129.9 (Ar-CH), 151.1 ppm [C(Ar)-O].

FT-IR (NaCl): 2986 (m, C-H), 1593, 1491 (m, C=C), 1271 (s, P=O), 1165, 969 cm^{-1} (vs, P-O-Et).

To a mixture of 25 ml THF and 25 ml lithiumdiisopropylamide (LDA) (2M, 0.050 mol) at –78 ^{o}C diethyl phenyl phosphate (5.23 g, 0.023 mol) in 25 ml THF was added. The mixture was stirred at –78 ^{o}C for 1 h and stirring was continued at 0 ^{o}C for an additional 30 min. The mixture was poured to a mixture of 75 ml of saturated aqueous NH_4Cl and 75 ml ether. The organic layer was separated and dried with anhydrous Na_2SO_4. After removal of solvents a red liquid was obtained. The pure product (diethyl (2-hydroxyphenyl) phosphonate) was obtained as a yellow viscous liquid after column chromatography, CH_2Cl_2: MeOH (99:1) elutant in 85 per cent yield.

^{1}H NMR ($CDCl_3$): δ= 1.26 (t, 6H, CH_2-CH_3), 4.04 (m, 4H, CH_2-CH_3), 6.84 (dd, 1H, Ar-CH), 6.89 (t, 1H, Ar-CH), 7.29 (dd, 1H, Ar-CH), 7.38 (t, 1H, Ar-CH), 10.19 ppm (s, 1H, -OH).

^{13}C NMR ($CDCl_3$): δ= 16.6 (CH_3-CH_2), 63.1 (CH_3-CH_2), 107.9, 109.8 (d, C-P), 118.0 (Ar-CH), 119.8(Ar-CH), 131.9 (Ar-CH), 135.4 (Ar-CH), 162.4 ppm [C(Ar)-O].

^{31}P NMR ($CDCl_3$): δ= 23.4 ppm.

FT-IR (NaCl): 3075 (b, -OH), 2984 (m, C-H), 1598, 1446 (m, C=C), 1391, 1197 (m, C-O), 1250 (m, P=O), 1163, 974 cm^{-1} (vs, P-O-Et).

3.2.5. Synthesis of Tetraethyl 2,5-Dihydroxy-1,4-Phenylene Diphosphonate

To a mixture of hydroquinone (1.32 g, 12.0 mmol), diethylphosphite (3.46 g, 25.1 mmol) in 8 ml CCl_4, triethylamine (2.52 g, 25.0 mmol) was added dropwise in an ice bath under nitrogen. The mixture was stirred overnight at room temperature. Then, it was extracted with water (3x15 ml) and the organic layer was dried with anhydrous Na_2SO_4. Removal of solvent gave 1,4-phenylene tetraethyl diphosphate as a pure colorless liquid in 72 per cent yield.

^{1}H NMR ($CDCl_3$): δ= 1.34 (t, 12H, CH_2-C*H*$_3$), 4.19 (m, 8H, C*H*$_2$-CH_3), 7.18 ppm (s, 4H, Ar-CH).

^{13}C NMR ($CDCl_3$): δ= 14.8 (*C*H_3-CH_2), 63.4 (CH_3-*C*H_2), 119.9 (Ar-CH), 149.3 ppm [C(Ar)-O].

FT-IR (NaCl): 2985 (m, C−H), 1502 (m, C=C), 1394, 1198 (w, C−O, arom.), 1277 (s, P=O), 1165, 961 cm^{-1} (vs, P−O−Et).

To a mixture of 25 ml THF and 25 ml LDA (2M, 0.050 mol) at −78 ^{o}C 1,4-phenylene tetraethyl diphosphate (4.29 g, 0.011 mol) in 25 ml THF was added. The mixture was stirred at −78 ^{o}C for 1h and stirring was continued at 0 ^{o}C for an additional 30 min. The mixture was poured to a mixture of 50 ml of saturated aqueous NH_4Cl and 50 ml ether. The organic layer was separated and dried with anhydrous Na_2SO_4. After removal of solvents a red liquid was obtained. The pure product was obtained as a light yellow solid after recrystalization in ethyl acetate in 86 per cent yield.

^{1}H NMR ($CDCl_3$): δ= 1.34 (t, 12H, CH_2-C*H*$_3$), 4.19 (q, 8H, C*H*$_2$-CH_3), 7.10 (s, 2H, Ar-CH), 9.62 ppm (s, 2H, OH).

^{13}C NMR ($CDCl_3$): δ= 15.2 (CH$_3$-CH$_2$), 62.2 (CH$_3$-CH$_2$), 114.1, 116.2 (d, C-P), 118.4 (Ar-CH), 152.5 ppm [C(Ar)-O].

FT-IR (NaCl): 3076 (b, −OH), 2985 (m, C−H), 1523 (m, C=C), 1406, 1198 (m, C−O, arom.), 1284 (m, P=O), 1162, 974 cm^{-1} (vs, P−O−Et).

3.3. Synthesis of Monomers from Diethyl (2-Hydroxyphenyl) Phosphonate

3.3.1. Synthesis of Monomers 1a and 1b

3.3.1.1. Synthesis of Di-tert-butyl 2,2'-(4,4'-(Propane-2,2-diyl)bis(4,1-Phenylene)) bis(Methylene) Diacrylate (Monomer A). To a mixture of Bisphenol A (6.48 g, 28.38 mmol) and triethylamine (TEA) (10.20 g, 0.1 mol) in THF (30 ml), TBBr (12.42 g, 56.2 mmol) was added dropwise in an ice bath under nitrogen. After 24 h of stirring at 60 ºC, THF was evaporated. The residue was diluted with 50 ml of methylene chloride (CH_2Cl_2) and 4 ml of 1 wt % NaOH was added in an ice bath. Then, the solution was extracted with water (3x24 ml), dried with anhydrous Na_2SO_4. After removal of CH_2Cl_2 the residue was recrystallized from methanol to give pure product as a white solid in 75.5 per cent yield. (mp. 66-67 ºC)

^{1}H NMR ($CDCl_3$): δ= 1.42 (s, 18H, [(CH$_3$)$_3$-C]), 1.54 (s, 6H, [(CH$_3$)$_2$-C]), 4.59 (s, 4H, CH$_2$-O), 5.84, (s, 2H, CH=C), 6.21 (s, 2H, CH=C), 6.75 (d, 4H, Ar-CH), 7.05 ppm (d, 4H, Ar-CH).

^{13}C NMR ($CDCl_3$): δ= 28.4 [(CH$_3$)$_3$-C], 31.4 [(CH$_3$)$_2$-C], 41.9 [C-(CH$_3$)$_2$], 66.5 (CH$_2$-O), 81.5 [C-(CH$_3$)$_3$], 114.4 (Ar-CH), 125.4 (CH$_2$=C), 128.2 (Ar-CH), 137.9 (Ar-C), 143.8 (CH$_2$=C), 156.5 [C(Ar)-O], 165.2 ppm (C=O).

FT-IR (NaCl): 2973, 2932 (m, C−H), 1720 (s, C=O), 1637 (m, C=C), 1582, 1477 (w, C=C, arom.), 1393, 1180, (w, C-O, arom.), 1149 cm^{-1} (vs, C-O).

3.3.1.2. Synthesis of 2,2'-(4,4'-(Propane-2,2-diyl)bis(4,1-Phenylene))bis(Methylene) Diacryloyl Chloride (Monomer B). To monomer A (3.86 g, 7.59 mmol) thionyl chloride (10 ml) was added dropwise in an ice bath under nitrogen purge. The mixture was stirred at room temperature for 1 day under nitrogen. After evaporation of excess $SOCl_2$, the diacid chloride intermediate was obtained as a light brown solid in 80 per cent yield.

^{1}H NMR ($CDCl_3$): δ= 1.54 (s, 6H, [$(CH_3)_2$-C]), 4.65 (s, 4H, CH_2-O), 6.38 (s, 2H, CH=C), 6.68 (s, 2H, CH=C), 6.73 (doublet of doublet, 4H, Ar-CH), 7.05 ppm (doublet of doublet, 4H, Ar−CH).

^{13}C NMR ($CDCl_3$): δ= 31.2 [(CH$_3$)$_2$-C], 41.8 [C-(CH_3)$_2$], 66.0 (CH_2-O), 114.4 (Ar-CH), 128.1 (Ar-CH), 134.8 (C=CH$_2$), 140.8 (Ar-C), 144.4 (C=CH_2), 155.9 (Ar-C-O), 167.7 ppm (C=O).

FT-IR (NaCl): 3037, 2967 (m, C−H), 1745 (s, C=O), 1636 (m, C=C), 1582, 1457 (w, C=C, arom.), 1384, 1182 cm^{-1} (w, C-O, arom.).

3.3.1.3. Synthesis of Monomer 1a. To a mixture of diethyl (2-hydroxyphenyl) phosphonate (1.18 g, 5.1 mmol) and triethyl amine (TEA) (0.52 g, 5.1 mmol), monomer B(1.0 g, 2.3 mmol) in 4 ml THF was added dropwise in an ice bath under nitrogen purge. After 24 h of stirring at room temperature, THF was evaporated. The solution was diluted with 12 ml of CH_2Cl_2 and extracted with 5 wt % $NaHCO_3$ (2x5 ml) and with 5 ml water. The organic layer was dried with anhydrous Na_2SO_4. Removal of solvent left thick brown paste (97 per cent yield) and it was washed with petroleum ether to remove excess diethyl (2-hydroxyphenyl) phosphonate. The pure product was obtained as a light yellow viscous liquid after column chromatography (silica gel 0.063-0.200 mm), starting ethylacetate:hexane (50:50) elutant and changing to EtAc:MeOH (99:1) in 45 per cent yield.

^{1}H NMR ($CDCl_3$): δ= 1.18 (t, 12H, CH_2-CH_3), 1.56 (s, 6H, [(CH_3)$_2$-C]), 3.95 (m, 8H, CH_2-CH_3), 4.81 (s, 4H, CH_2-O), 6.15, 6.62 (s, 4H, CH_2=C), 6.81, 7.08 (d, 8H, Ar-CH),

7.16 (dd, 2H, Ar-CH), 7.27 (td, 2H, Ar-CH), 7.53 (t, 2H, Ar-CH), 7.90 ppm (qd, 2H, Ar-CH).

^{13}C NMR ($CDCl_3$): δ= 15.2 (CH_3-CH_2), 30.0 [(CH_3)$_2$-C], 40.7 [C-(CH_3)$_2$], 61.2 (CH_3-CH_2), 64.8 (CH_2-O), 113.1 (Ar-CH), 119.4, 121.2 (d, C-P), 122.8, 125.0 (Ar-CH), 126.7 (Ar-CH), 127.6 (C=CH_2), 132.8, 133.9 (Ar-CH), 134.5 (Ar-C), 142.6 (C=CH_2), 151.0, 155.2 [C(Ar)-O], 162.6 ppm (C=O).

^{31}P NMR ($CDCl_3$): δ= 16.1 ppm

FT-IR (NaCl): 2964 (m, C−H), 1745 (s, C=O), 1641 (m, C=C), 1599, 1475 (w, C=C, arom.), 1391, 1200 (w, C−O, arom.), 1257 (vs, P=O), 1087 (s, C−O), 1021, 972 cm^{-1} (vs, P−O−Et).

3.3.1.4. Synthesis of Monomer 1b. TMSBr (0.21 g, 1.36 mmol) was added dropwise to a solution of monomer 1a (0.25 g, 0.31 mmol) in 0.5 ml freshly dried CH_2Cl_2 in an ice bath under nitrogen, and then the solution was refluxed for 2 h. After the evaporation of the solvent, 4 ml of MeOH was added and the mixture was stirred at room temperature for 18 h. Methanol was removed by the rotary evaporator. In order to reduce water content of the crude product, acetonitrile was added and evaporated immediately. This procedure was repeated four times, finally residual solid was washed with acetonitrile and pure product was obtained in 79 per cent yield.

^{1}H NMR ($CDCl_3$): δ= 1.52 (s, 6H, [(CH_3)$_2$-C]), 4.83 (d, 4H, CH_2-O), 6.04, 6.55 (s, 4H, CH_2=C), 6.81, 7.05 (d, 8H, Ar-CH), 7.19 (t, 2H, Ar-CH), 7.28 (t, 2H, Ar-CH), 7.53 (t, 2H, Ar-CH), 7.81 ppm (dd, 2H, Ar-CH).

^{13}C NMR ($CDCl_3$): δ= 30.5 [(CH_3)$_2$-C], 41.6 [C-(CH_3)$_2$], 66.1(CH_3-CH_2), 114.3 (Ar-CH), 125.4, 123.5 (d, C-P), 117.2, 123.8, 126.1 (Ar-CH), 127.8 (Ar-CH), 127.8 (C=CH_2), 133.3 (Ar-CH), 136.2 (Ar-C), 143.8 (C=CH_2), 152.2, 156.4 [C(Ar)-O], 164.1 ppm (C=O).

FT-IR (NaCl): 2964 (m, C−H), 1715 (s, C=O), 1644 (m, C=C), 1602, 1445 (w, C=C, arom.), 1398, 1179 (w, C−O, arom.), 1262 (vs, P=O), 1087 cm^{-1} (s, C−O).

3.3.2. Synthesis of Monomers 2a and 2b

3.3.2.1. Synthesis of Monomer 2a. To a stirring mixture of diethyl (2-hydroxyphenyl) phosphonate (0.4 g, 1.74 mmol) and TEA (0.23 g, 2.2 mmol) in 2 ml dry THF in an ice bath CMAC (0.11 g, 0.72 mmol) was slowly added in an ice bath. After 24 h of stirring at 55^{o}C, THF was evaporated. The solution was diluted with 10 ml of CH_2Cl_2 and extracted with 3x5 ml water. The organic layer was dried with anhydrous Na_2SO_4. Removal of solvent left thick brown paste and it was washed with petroleum ether to remove excess diethyl (2-hydroxyphenyl) phosphonate. The pure product was obtained as a light yellow viscous liquid after reversed phase column chromatography (C18), starting H_2O:MeOH (70:30) elutant and changing to 100% MeOH gradually in 45 per cent yield.

^{1}H-NMR ($CDCl_3$): δ= 1.29 (m, 12H, CH_2-C*H*$_3$), 4.12 (m, 8H, C*H*$_2$-CH_3), 5.01 (s, 2H, CH_2-O), 6.59, 6.76 (s, 2H, CH_2=C), 7.07 (m, 2H, Ar-CH), 7.27, 7.37 (m, 2H, Ar-CH), 7.51, 7.61 (t, 2H, Ar-CH), 7.88, 7.98 ppm (dd, 2H, Ar-CH).

^{13}C NMR ($CDCl_3$): δ= 14.1 (*C*H_3-CH_2), 59.7, 60.0 (CH_3-*C*H_2), 63.6 (CH_2-O), 109.8 (Ar-CH), 113.2, 115.0 (d, C-P), 117.9, 119.7 (d, C-P), 118.6, 121.3, 123.7 (Ar-CH), 126.7 (C=*C*H_2), 131.7, 132.1, 132.2 132.7 (Ar-CH), 133.0 (*C*=CH_2), 149.5, 157.3 [C(Ar)-O], 161.1 ppm (C=O).

FT-IR (NaCl): 2983 (m, C-H), 1746 (s, C=O), 1643 (m, C=C), 1593 (w, C=C, arom.), 1250 (vs, P=O), 1091 (s, C-O), 1023 cm^{-1} (vs, P-O-Et).

3.3.2.2. Synthesis of Monomer 2b. TMSBr (0.39 g, 2.6 mmol) was added dropwise to a solution of monomer 2a (0.31 g, 0.59 mmol) in 1 ml freshly dried CH_2Cl_2 in an ice bath under nitrogen, and then the solution was refluxed for 2 h. After the evaporation of the solvent, 4 ml of MeOH was added and the mixture was stirred at room temperature overnight. Then MeOH was evaporated pure light brown solid in 60 per cent yield.

^{1}H-NMR ($CDCl_3$): δ= 5.08 (s, 2H, CH_2-O), 6.43, 6.66 (s, 2H, CH_2=C), 7.05, 7.17 (m, 2H, Ar-CH), 7.32, 7.38 (m, 2H, Ar-CH), 7.54, 7.63 (t, 2H, Ar-CH), 7.80, 7.90 ppm (dd, 2H, Ar-CH).

^{13}C NMR ($CDCl_3$): δ= 66.3 (CH_2-O), 112.5 (Ar-CH), 115.9, 118.1 (d, C-P), 120.5, 122.4 (d, C-P), 121.0, 124.0, 126.3 (Ar-CH), 127.4 (C=*C*H_2), 129.4, 134.1, 134.6, 135.2 (Ar-CH), 135.5 (*C*=CH_2), 152.1, 160.1 [C(Ar)-O], 163.6 ppm (C=O).

FT-IR (NaCl): 3500-2000 (OH), 2924 (C−H), 1725 (C=O), 1643 (C=C), 1594 (C=C, arom.), 1284 (P=O), 1090 cm^{-1} (C−O).

3.3.3. Synthesis of Monomer 3a

Diethyl (2-hydroxyphenyl) phosphonate (1.28 g, 5.57 mmol), glycidyl methacrylate (GMA) (0.72 g, 5.06 mmol) and triethyl amine (TEA) (0.031 g, 0.30 mmol %6 based on epoxy) are mixed at 85 ^{o}C under nitrogen for 1 day. The mixture was washed with cyclohexane to remove excess diethyl (2-hydroxyphenyl) phosphonate and TEA. The pure product was obtained as a yellow viscous liquid after column chromatography (silica gel 0.063-0.200 mm), with ethyl acetate as an elutant in 68 per cent yield.

^{1}H NMR ($CDCl_3$): δ= 1.26 (td, 6H, CH_2−C*H*$_3$), 1.86 (s, 3H, [C*H*$_3$−C]), 3.95 (m, 4H, C*H*$_2$−CH_3), 4.19 (s, 4H, CH_2−O), 4.24 (m, 2H, CH−O), 5.16 (s, 1H, −OH), 5.49, 6.05 (s, 2H, CH_2=C), 6.90 (t, 1H, Ar−CH), 6.97 (td, 1H, Ar−CH), 7.42 (t, 1H, Ar−CH), 7.60 ppm (qdt, 1H, Ar−CH).

^{13}C NMR ($CDCl_3$): δ= 16.4 (*C*H_3-CH_2), 18.7 [*C*H_3-C], 62.5, 72.8 (CH_2-O), 65.2 (CH_3-*C*H_2), 68.3 (CH-OH), 114.7 (Ar-CH), 117.0, 118.8 (d, C-P), 121.5 (Ar-CH), 126.0 (C=*C*H_2), 133.6, 134.8 (Ar-CH), 136.3 (*C*=CH_2), 161.2 [C(Ar)-O], 167.4 ppm (C=O).

^{31}P NMR ($CDCl_3$): δ= 18.5 ppm.

FT-IR (NaCl): 3349 (b, −OH), 2981 (m, C−H), 1715 (s, C=O), 1637 (m, C=C), 1593, 1480 (w, C=C, arom.), 1392, 1250 (w, C−O, arom.), 1283 (vs, P=O), 1093 (s, C−O), 1163, 969 cm^{-1} (vs, P−O−Et).

3.3.4. Synthesis of Monomer 4a

A mixture of bisphenol A diglycidyl ether 0.22 g (0.7 mmol), 0.5 g (2.2 mmol) of diethyl (2-hydroxyphenyl) phosphonate and 0.054 g of triethylamine were stirred at 100^{o}C for 18 h under nitrogen atmosphere. After cooling the reaction mixture, the excess of diethyl (2-hydroxyphenyl) phosphonate was removed by washing with petroleum ether. The diol intermediate which was a brown residue was purified by chromatography on a silica gel column, starting with a mixture of hexane: CH_2Cl_2 (30:70 by volume), changing to 100 per cent CH_2Cl_2 gradually and finally CH_2Cl_2:MeOH (99:1).

^{1}H NMR ($CDCl_3$): δ= 1.18 (m, 12H, CH_2-CH_3), 1.51 (s, 6H, [(CH_3)$_2$-C]), 4.01 (m, 8H, CH_2-CH_3), 4.31 (m, 8H, CH_2-O), 5.44 (t, 2H, CH-O), 6.76 (d, 4H, Ar-CH), 6.90 (t, 2H, Ar-CH), 6.97 (m, 2H, Ar-CH), 7.03 (d, 4H, Ar-CH), 7.42 (t, 2H, Ar-CH), 7.78 ppm (dd, 2H, Ar-CH).

^{13}C NMR ($CDCl_3$): δ= 16.4 (CH_3-CH_2), 31.0 [(CH_3)$_2$-C], 41.7 [C-(CH_3)$_2$], 62.4 (CH_3-CH_2), 68.3, 68.7 (CH_2-O), 72.4 (CH-O), 113.9, 114.5 (Ar-CH), 116.7, 118.6 (d, C-P), 121.3 (Ar-CH), 127.7, 133.7, 134.4 (Ar-CH), 143.6 (Ar-C), 156.4, 161.3 ppm [C(Ar)-O].

FT-IR (NaCl): 2964 (m, C−H), 1599, 1475 (w, C=C, arom.), 1391, 1200 (w, C−O, arom.), 1250 (vs, P=O), 1048 (s, C−O), 1150, 972 cm^{-1} (vs, P−O−Et).

The diol intermediate (0.60 g, 0.75 mmol) was dissolved in 6 ml of freshly dried dichloromethane along with 0.15 g (1.49 mmol) of triethylamine and 0.0023 g (0.018 mmol) of dimethyl aminopyridine (DMAP). Under nitrogen atmosphere, the mixture was cooled at 0^{o}C and 0.19 g (1.87 mmol) of methacrloyl chloride mixed with 4 ml dichloromethane was added dropwise and the reaction mixture was stirred at room temperature overnight. The mixture was extracted with HCl (1 M solution) 3x3 ml, satd. $NaHCO_3$ 3x3 ml and then with 2x 2 ml distilled water. The organic layer was dried with

anhydrous Na_2SO_4, filtered and the solvent was removed under vacuum. The pure product was obtained as a light yellow viscous liquid after column chromatography (silica gel 0.063-0.200 mm), starting with ethylacetate:hexane (50:50) elutant and changing to EtAc:MeOH (99:1) in 35 per cent yield.

^{1}H NMR ($CDCl_3$): δ= 1.16 (m, 12H, CH_2-C*H*$_3$), 1.51 (s, 6H, [(C*H*$_3$)$_2$-C]), 1.85 (s, 6H, CH_3-C), 4.01 (m, 8H, C*H*$_2$-CH_3), 4.31 (m, 8H, CH_2-O), 5.44 (t, 2H, CH-O), 5.53, 6.05 (s, 4H, CH_2=C), 6.76 (d, 4H, Ar-CH), 6.90 (t, 2H, Ar-CH), 6.97 (m, 2H, Ar-CH), 7.03 (d, 4H, Ar-CH), 7.42 (t, 2H, Ar-CH), 7.78 ppm (dd, 2H, Ar-CH).

^{13}C NMR ($CDCl_3$): δ= 16.5 (*C*H_3-CH_2), 18.4 (*C*H_3-C=O), 31.3 [(*C*H_3)$_2$-C], 42.1 [*C*-(CH_3)$_2$], 63.3 (CH_3-*C*H_2), 66.0, 66.5 (CH_2-O), 71.0 (CH-O), 112.2, 114.5 (Ar-CH), 115.9, 117.8 (d, C-P), 121.1 (Ar-CH), 126.7 (C=*C*H_2), 128.1, 134.8, 135.8 (Ar-CH), 136.1 (*C*=CH_2), 143.8 (Ar-C), 156.5, 160.1 [C(Ar)-O], 166.9 ppm (C=O).

FT-IR (NaCl): 2976 (m, C−H), 1719 (s, C=O), 1636 (m, C=C), 1593 (w, C=C, arom.), 1247 (vs, P=O), 1092 (s, C−O), 1026 cm^{-1} (vs, P−O−Et).

3.3.5. Synthesis of Monomers 5a and 5b

3.3.5.1. Synthesis of Monomer 5a. To a mixture of diethyl (2-hydroxyphenyl) phosphonate (0.55 g, 2.4 mmol), K_2CO_3 (3.44 g, 24.9 mmol), and acetone (5 mL), TBBr (0.58 g, 2.6 mmol) was added dropwise under N_2. After 2 days of stirring at 60^{o}C, the solvent was evaporated. The residue was diluted with 20 mL of CH_2Cl_2, and the solution was extracted with 3x5 mL of water. After the drying of the CH_2Cl_2 phase with anhydrous Na_2SO_4 and the evaporation of the solvent, the crude product was purified by column chromatography (with 98:2 CH_2Cl_2:isopropyl alcohol as the eluent) to give a yellow solid with a melting point of 36^{o}C in 43 per cent yield.

^{1}H-NMR ($CDCl_3$): δ= 1.26 (t, 6H, CH_2-*C*H_3), 1.44 (s, 9H, (*C*H_3)$_3$-C) 4.14 (m, 4H, CH_2-O), 4.76 (s, 2H, CH_2-O), 6.21, 6.37 (s, 2H, CH_2═), 6.98, 7.45, 7.82 (m, 4H, CH═) ppm.

^{13}C NMR ($CDCl_3$): δ= 16.2 (*C*H_3-CH_2), 28.1 [(*C*H_3)$_3$-C], 62.2 (CH_3-*C*H_2), 66.3 (CH_2-O), 81.2 [*C*-(CH_3)$_3$], 112.5 (Ar-CH), 115.8, 117.6 [d, C-P], 121.8 (Ar-CH), 126.2 (*C*H_2=C), 134.8, 135.0 (Ar-CH), 136.2 (CH_2=*C*), 158.8 [C(Ar)-O], 164.3 (C=O) ppm.

FT-IR (NaCl): 2979 (C-H), 1705 (C=O), 1639 (C=C), 1253 (P=O) and 1026 (P-O-Et) cm^{-1}.

3.3.5.2. Synthesis of Monomer 5b. TMSBr (1.03 g, 6.71 mmol) was added dropwise to a solution of monomer 5a (1.13 g, 3.05 mmol) in 3 ml freshly dried CH_2Cl_2 in an ice bath under nitrogen, and then the solution was refluxed for 2 h. After the evaporation of the solvent, 6 ml of MeOH was added and the mixture was stirred at room temperature overnight. Then MeOH was evaporated and CF_3COOH (1.0 ml, 12.98 mmol) was added dropwise in an ice bath and the mixture was stirred at room temperature for one day. After evaporation of excess CF_3COOH the product was precipitated into diethyl ether as a light brown solid in 42 per cent yield. Melting point of pure substance is 182^{o}C.

^{1}H NMR (MeOD): δ= 4.83 (s, 2H, CH_2-O), 6.25, 6.30 (s, 2H, CH_2=C), 7.02 (m, 2H, Ar-CH), 7.47 (t, 1H, Ar-CH), 7.69 ppm (dd, 1H, Ar-CH).

^{13}C NMR (D_2O): δ= 66.7 (CH_2-O), 113.2 (Ar-CH), 118.2, 119.9 (d, C-P), 121.5 (Ar-CH), 128.7 (*C*H_2=C), 133.5, 134.8 (Ar-CH), 135.6 (CH_2=*C*), 159.6 [C(Ar)-O], 169.8 ppm (C=O).

^{31}P NMR (MeOD): δ= +15.10 ppm

FT-IR (KBr): 3500-2000 (OH), 2934 (C−H), 1700 (C=O), 1628 (C=C), 1598, 1443 (C=C, arom.), 1400, 1147 (C−O, arom.), 1284 (P=O), 1095 cm^{-1}.

3.4. Synthesis of Monomers from Tetraethyl 2,5-Dihydroxy-1,4-Phenylene Diphosphonate

3.4.1. Synthesis of Monomers 6a and 6b

3.4.1.1. Synthesis of Monomer 6a. To a mixture of tetraethyl (2,5-dihydroxy-1,4-phenylene) bisphosphonate (2.2 g, 5.8 mmol), K_2CO_3 (15.9 g, 115 mmol) and acetone (16 ml), TBBr (2.8 g, 12.7 mmol) was added dropwise under N_2. After 2 d of stirring at 60 °C, the solvent was evaporated. The residue was diluted with 25 ml of CH_2Cl_2 and the solution was extracted with water (4x5 ml). The organic phase was dried with Na_2SO_4. Evaporation of CH_2Cl_2, the residue was recrystallized from ether and white solid was obtained with a melting point of 110 ºC in 92 per cent yield.

^{1}H NMR ($CDCl_3$): δ= 1.3 (t, 12H, C*H*$_3$-CH_2), 1.5 [s, 18H, $(CH_3)_3$-C], 4.13 (q, 8H, CH_3-C*H*$_2$), 4.76 (CH_2-O), 6.2 (s, 2H, CH=C), 6.3 (s, 2H, CH=C), 7.4-7.5 [m, 2H, CH (Ar)] ppm.

^{13}C NMR ($CDCl_3$): δ= 16.0 (*C*H_3-CH_2), 27.7 [(*C*H_3)$_3$-C], 62.1 (CH_3-*C*H_2), 67.1 (CH_2-O), 81.0 [*C*-$(CH_3)_3$], 118.7 (Ar-CH), 121.4, 123.2 [d, C-P], 125.2 (*C*H_2=C), 136.4 (CH_2=*C*), 153.3 [C(Ar)-O], 164.1 (C=O) ppm.

FT-IR (NaCl): 2973 (C-H), 1700 (C=O), 1636 (C=C), 1231 (P=O) and 1025 (P-OEt) cm^{-1}.

3.4.1.2. Synthesis of Monomer 6b. TMSBr (1.24 g, 8.11 mmol) was added dropwise to a solution of monomer 6a (1.17 g, 1.85 mmol) in 2 ml freshly dried CH_2Cl_2 in an ice bath under nitrogen, and then the solution was refluxed for 2 h. After the evaporation of the solvent, 4 ml of MeOH was added and the mixture was stirred at room temperature overnight. Then MeOH was evaporated and CF_3COOH (1.0 ml, 12.98 mmol) was added dropwise in an ice bath and the mixture was stirred at room temperature for one day. After evaporation of excess CF_3COOH, the product was precipitated into diethyl ether and a pure light brown solid product was obtained in 56 per cent yield. It decomposed at 200 ºC before melting.

^{1}H NMR (MeOD): δ= 4.83 (s, 4H, CH_2-O), 6.13, 6.28 (s, 4H, CH_2=C), 7.37 ppm (dd, 2H, Ar-CH).

^{13}C NMR (D_2O): δ= 67.2 (CH_2-O), 118.0 (Ar-CH), 125.9, 127.7 (d, C-P), 127.2 (*C*H_2=C), 136.8 (CH_2=*C*), 153.1 [C(Ar)-O], 167.1 ppm (C=O).

^{31}P NMR (MeOD): δ= +12.69 ppm

FT-IR (KBr): 3500-2000 (OH), 2956 (C−H), 1715 (C=O), 1636 (C=C), 1442 (C=C, arom.), 1403 (C−O, arom.), 1284 (P=O), 1084 cm^{-1} (C−O).

3.5. Synthesis of Monomers from Dimethyl 2-Hydroxyethyl Phosphonate

3.5.1. Synthesis of Monomer 7a

To a stirring mixture of dimethyl 2-hydroxyethyl phosphonate (1.50 g, 9.73 mmol) and TEA (1.23 g, 12.15 mmol) in 10 ml dry THF in an ice bath CMAC (0.56 g, 4.05 mmol) was slowly added in an ice bath. After 24 h of stirring at 55^{o}C, THF was evaporated. The solution was diluted with THF and TEA salts were filtered. After removal of solvent yellow liquid was left, the pure product was obtained as a light yellow liquid after reverse phase column chromatography (C18), starting 100 % H_2O eluent and changing to 100% MeOH gradually in 45 per cent yield.

^{1}H-NMR ($CDCl_3$): δ= 2.17 (m, 4H, C*H*$_2$-P), 3.75 (m, 14H, O-C*H*$_2$, O-C*H*$_3$), 4.21 (s, 2H, CH_2-O), 4.41 (2H, t, C*H*$_2$-O), 5.93, 6.33 (s, 2H, CH_2=C).

^{13}C NMR ($CDCl_3$): δ= 24.4, 25.5 (d, C-P), 25.8, 26.9 (d, C-P), 52.7 (O-CH_3), 58.9, 64.7, 69.1 (CH_2-O), 126.8 (C=*C*H_2), 136.7 (*C*=CH_2), 165.4 ppm (C=O).

FT-IR (NaCl): 2957 (m, C-H), 1721 (s, C=O), 1640 (m, C=C), 1184 (s, P=O), 1028 (s, C-O), 1249, 818 cm^{-1} (vs, P-O-Me).

3.6. Photopolymerizations

3.6.1. Polymerization Procedure

All the photopolymerizations were carried out by TA Instruments Q 100 Photo-DSC using Irgacure 651 as the photoinitiator (Figure 3.1).

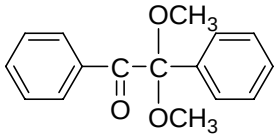

Figure 3.1. 2,2-Dimethoxy-2-phenyl acetophenone (Irgacure 651)

3-4 mg of sample was placed in an uncovered aluminum DSC pan. Then, the photoinitiator which was disolved in CH_2Cl_2 was added with a micro-syringe to give a final concentration in the monomer of 2.0 mol per cent after evaporation of the solvent. After placing the sample and reference pans to sample compartment, the DSC chamber was purged with nitrogen for 10 min to remove air and CH_2Cl_2 before polymerization and purging was continued during polymerization. The samples were irradiated for 10 minutes at 40 °C with an incident light intensity of 20 mW/cm^2. The heat flux as a function of time was monitored using DSC under isothermal conditions and both the rates of polymerization (R_p) and conversions were calculated as a function of time. The heat of reaction values, ΔH_p= 64.5, 54.5, 57.5, 50 and 55 kJ/mol, were used as the theoretical heat evolved for methacrylic acid, t-butyl ester, ethyl ester, 2-hydroxyethyl ester and methyl ester of methacrylic acid double bonds respectively. The rates of polymerizations were calculated according to the following formula:

$$R_p = \frac{(Q/s)M}{n\Delta H_p m}$$

Figure 3.2. Equation of the rate of polymerization

where Q/s is the heat flow per second during reaction, M is the molar mass of the monomer, n is the number of double bonds per monomer molecule, ΔH_p is the heat released per mole of double bonds reacted and m is the mass of the monomer in the sample.

3.7. Solution Polymerizations

3.7.1. Polymerization Procedure

For the solution polymerization, the monomers, solvent and the initiator were added in a septum sealed tube. Then the sealed tubes were degassed by means of freeze-thaw cycles before they were placed in a constant temperature bath. After a selected period of time, the viscous polymer solutions were precipitated into nonsolvents. The polymers were filtered and dried under vacuum.

3.7.2. Copolymerization of Monomers with Acrylamide

Monomers **5b, 6b** were copolymerized with acrylamide in H_2O at 65 ºC with 0.5 wt per cent V-50. Both linear and crosslinked polymers formed were swelled in H_2O and precipitated into acetone to remove the residual monomers.

3.8. Interactions of Phosphonic Acid containing Monomers with the Calcium in the Hydroxyapatite

The interaction of the acidic monomers with hydroxyapatite, a model compound for dentin and enamel, was evaluated using the ^{13}C-NMR and FT-IR techniques.

3.8.1. ^{13}C-NMR technique

Acidic monomer was dissolved into deuterium oxide aqueous solution. Deutoriated DMSO was used as an external standard. The pH value of the solution was measured and ^{13}C-NMR spectrum was obtained. The hydroxyapatite with different amounts was then added to this solution. After the suspensions were kept at an ultrasonic bath at 37 $^{\circ}$C for one hour, the pH values were measured and the ^{13}C NMR spectra were obtained. The chemical shift values of the α-methylene carbon assigned to the phosphonic acid and carbonyl carbon assigned to carboxylic acid were determined. The interactions of the carboxylic acid and phosphonic acid with the calcium in the HAP were determined by the chemical shift differences before and after mixing with HAP.

3.8.2. FT-IR technique

FT-IR spectra of the monomers with and without HAP were obtained using KBr pellets. HAP added NMR samples were used after dried under sublimation.

4. RESULTS AND DISCUSSION

Novel mono- and di(phosphonate) phosphonic and carboxylic acid containing monomers for use in dental materials were synthesized starting from o-hydroxyaryl phosphonates and dimethyl 2-hydroxyethyl phosphonate.

4.1. Synthesis of Novel Dental Monomers from o-Hydroxyaryl Phosphonates and from Dimethyl (2-Hydroxyethyl) Phosphonate

4.1.1. Synthesis of Monomers 1a-5b from Diethyl (2-Hydroxyphenyl) Phosphonate

Monomers **1a-3b** were synthesized within a project for Ivaclor Vivadent.

4.1.1.1. Synthesis of diethyl (2-hydroxyphenyl) phosphonate. Diethyl (2-hydroxyphenyl) phosphonate was mostly used as a starting compound for preparation of our dental monomers. Synthesis of this compound involved two steps (Figure 4.1) [89, 90].

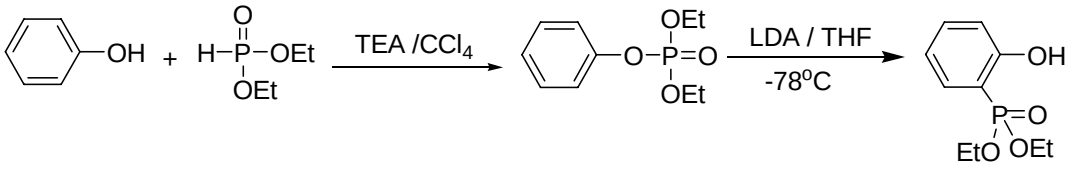

Figure 4.1. Synthesis of diethyl (2-hydroxyphenyl) phosphonate

In the first step, phenol and diethylphosphite were reacted in the presence of TEA as a catalyst in CCl_4 for 1 day. After removing of TEA salts with water, pure product was obtained in 86 per cent yield as yellow liquid. It should be dried very well for the rearrangement step.

The ^{13}C-NMR spectrum of diethyl phenyl phosphate showed characteristic peaks for ethyl carbons at 16.4 and 64.7 ppm, aromatic carbon attached to oxygen at 151.1 ppm and other aromatic carbons at 120.1, 125.3, 129.9 ppm (Figure 4.3).

In the ^{1}H-NMR spectrum, ethyl protons at 1.31 and 4.17 ppm and aromatic protons at 7.12, 7.18 and 7.29 ppm were characterized (Figure 4.4).

Treatment of dialkyl aryl phosphates with lithium diisoproylamide (LDA) generates an anion which undergoes a migration of phosphorus from oxygen to carbon. Although O→C migrations of phosphorus are not without precedent, C→O migrations of phosphorus moieties are much more commonly encountered (Figure 4.2).

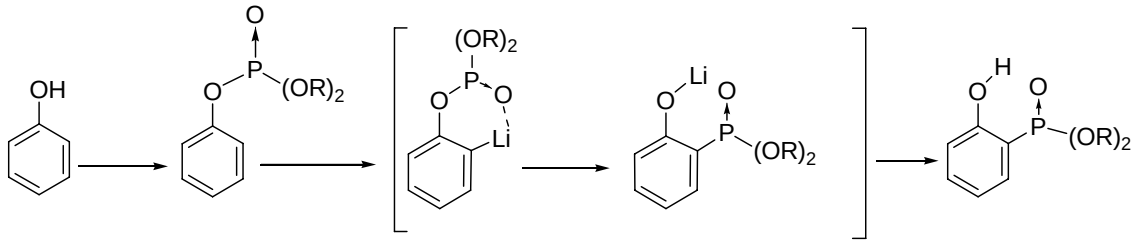

Figure 4.2. Rearrangement mechanism of phosphate-phosphonate

In the second step, diethyl phenyl phosphate was treated with LDA in dry THF at -78 ^{o}C. The product was purified by column chromatography using silica gel (0.0063-0.200 mm) treated with 1 % TEA and dichloromethane as eluent. The pure product, diethyl (2-hydroxyphenyl) phosphonate, was obtained as a yellow liquid in 86 per cent yield. It was soluble in acetone, methanol, ethanol, ether, dichloromethane, THF, CCl_4, cyclohexane and petroleum ether whereas insoluble in water and hexane.

The ^{13}C-NMR spectrum of this compound showed characteristic peaks for ethyl carbons at 16.6 and 63.1 ppm, aromatic carbon attached to phosphorus atom at 107.9, 109.8 ppm (doublet), aromatic carbon attached to hydroxyl at 162.4 ppm and other aromatic carbons at 118.0, 119.8, 131.9, 135.4 ppm (Figure 4.3).

^{1}H-NMR spectrum showed ethyl protons at 1.26 and 4.04 ppm, aromatic protons at 6.84, 6.89, 7.29, 7.38 ppm and hydroxyl proton at 10.19 ppm (Figure 4.4).

The FT-IR spectrum showed characteristic peaks for –OH, C-H, aromatic C=C, P=O and P-O-Et at 3075, 2984, 1598, 1250, 1163 cm^{-1} respectively (Figure 4.5).

The ^{31}P NMR spectrum showed a singlet at 23.4 ppm.

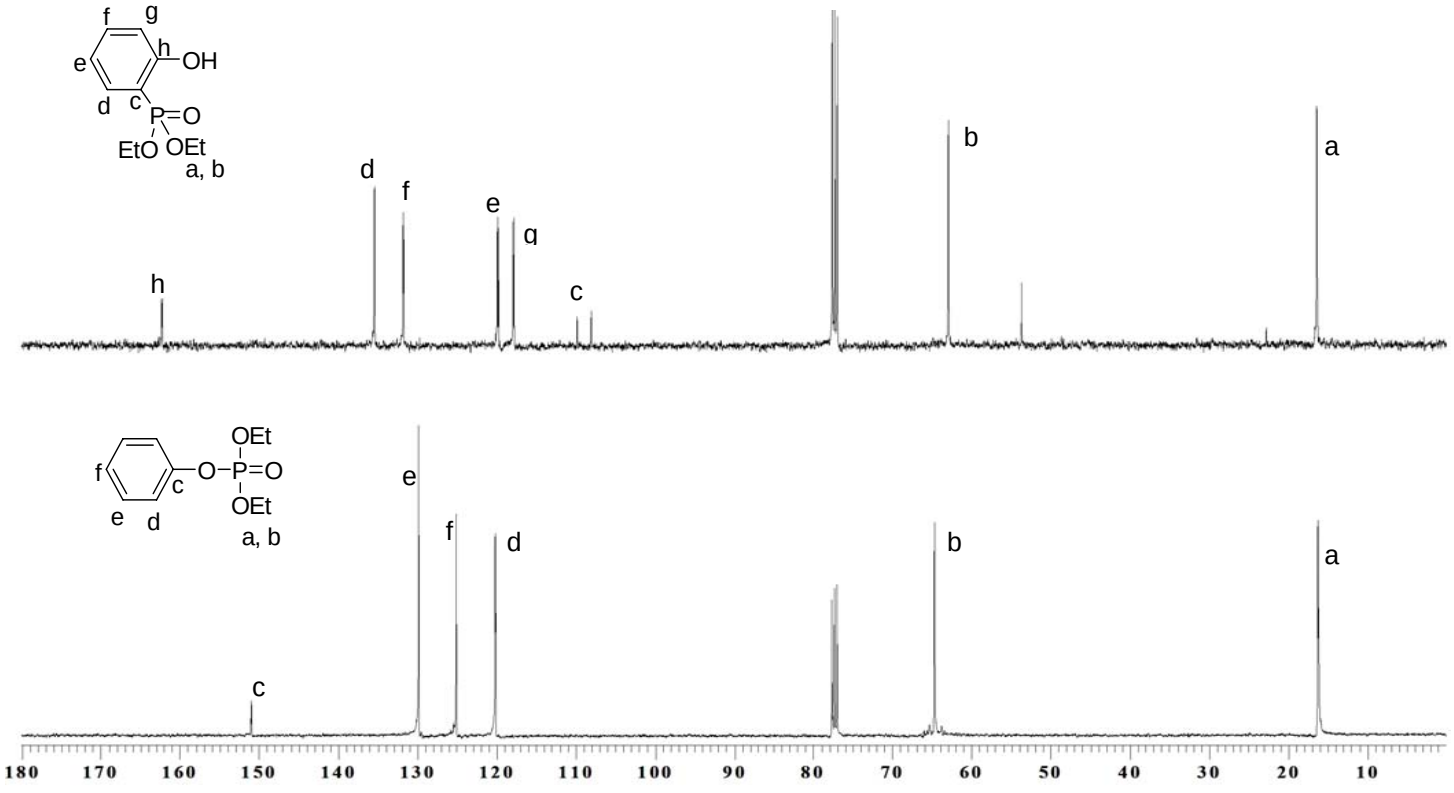

Figure 4.3. ^{13}C-NMR spectra of diethyl phenyl phosphate and diethyl (2-hydroxyphenyl) phosphonate

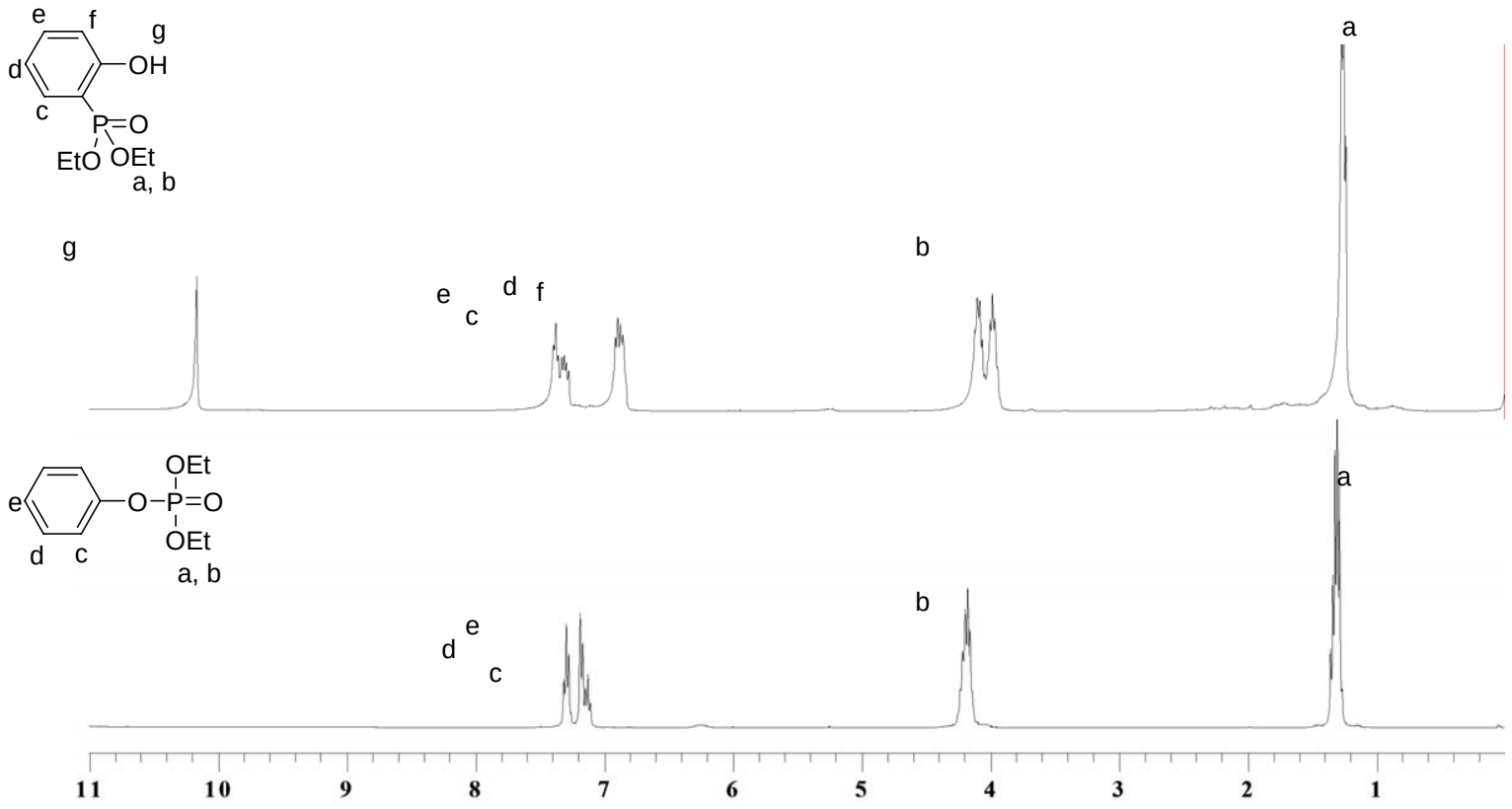

Figure 4.4. ^{1}H-NMR spectra of diethyl phenyl phosphate and diethyl (2-hydroxyphenyl) phosphonate

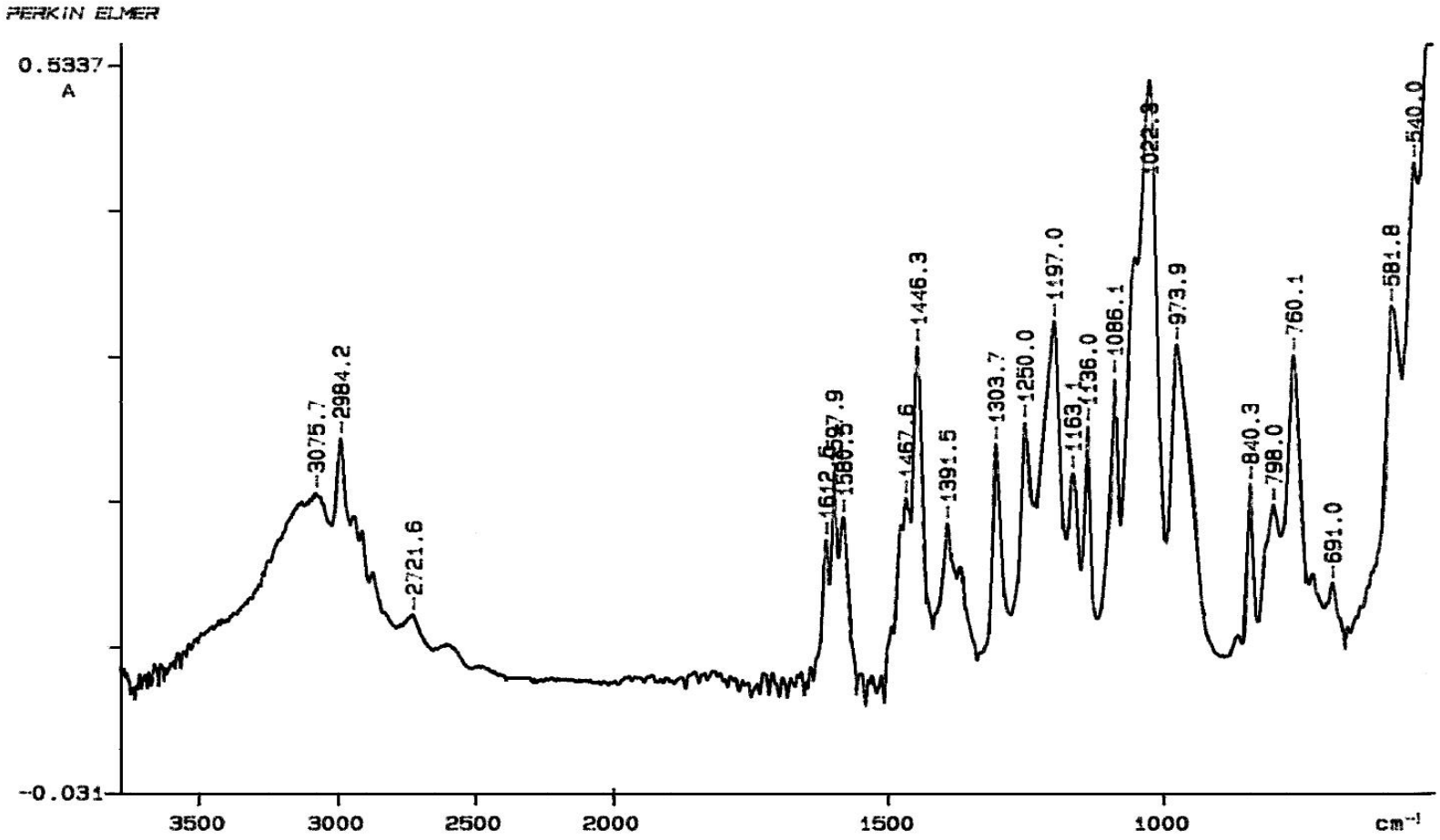

Figure 4.5. FT-IR spectrum of diethyl (2-hydroxyphenyl) phosphonate

4.1.1.2. Synthesis of Monomers **1a** and **1b**. The first pair of monomers **1a** and **1b** contain both Bisphenol A and phenolic structures and phosphonates or phosphonic acids incorporated in the phenolic ring (Figure 4.6).

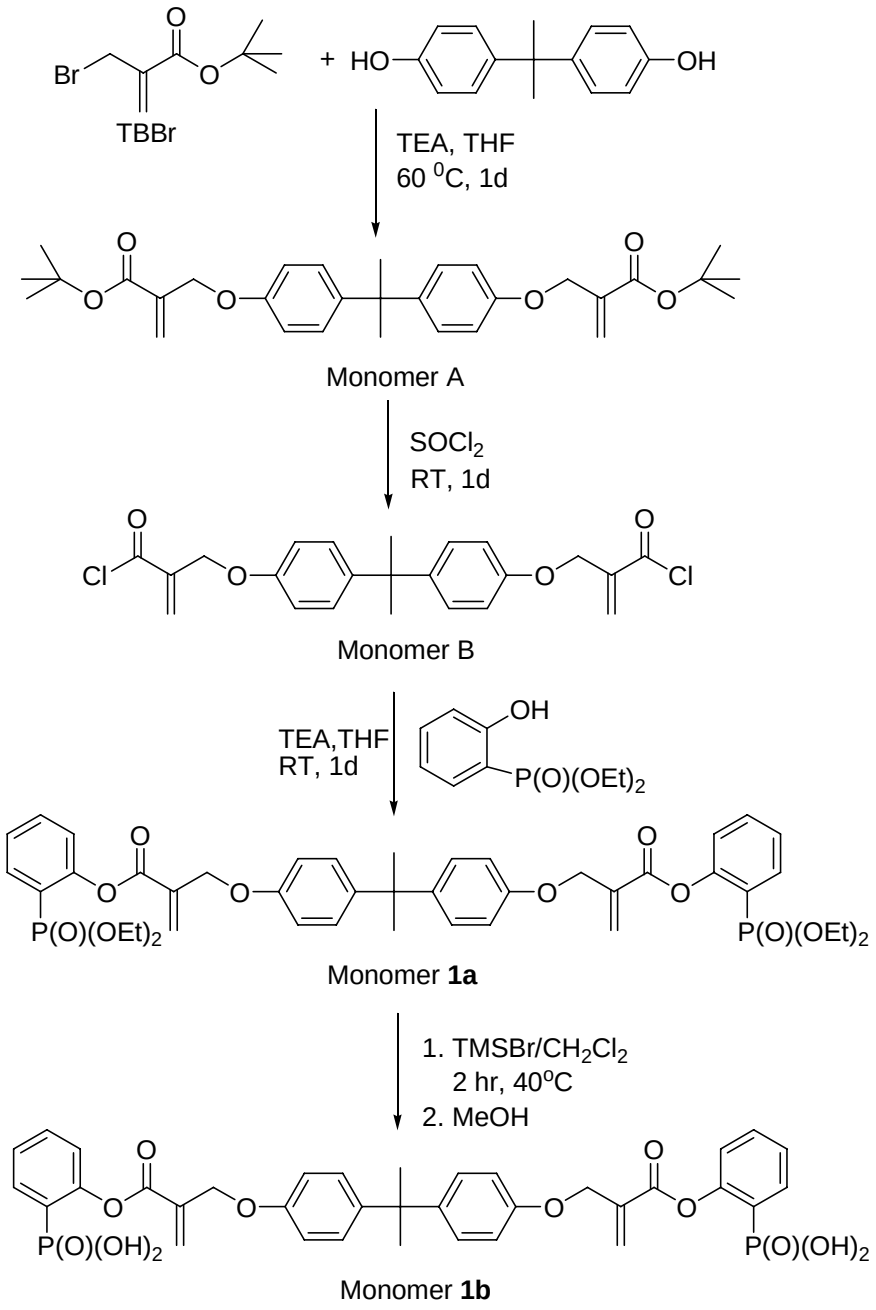

Figure 4.6. Synthesis of monomers A, B, **1a** and **1b**

The monomers are based on t-butyl α-bromomethacrylate (TBBr) which was synthesized using the literature procedure. The first step for the synthesis of TBBr involves Baylis-Hillman reaction which is the 1,4-diazobicyclo [2.2.2] octane (DABCO)

catalyzed insertion of paraformaldehyde at the α-position of tert-butyl acrylate to produce tert-butyl α-hydroxymethyl acrylate (TBHMA) [91]. In the second step, reaction of TBHMA with excess PBr_3 gives TBBr as colorless liquid in 72 per cent yield after distillation under reduced pressure (Figure 4.7).

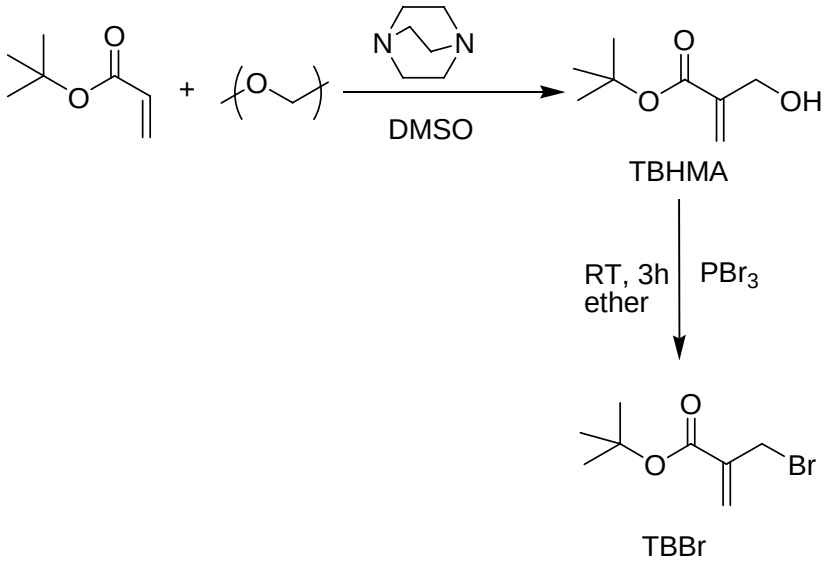

Figure 4.7. Synthesis of TBHMA and TBBr

Synthesis of monomer **1a** occurs in three steps. The first step involves the reaction of Bisphenol A with TBBr in the presence of TEA at 60 ^{o}C to give an intermediate monomer (monomer A) which was a white solid (melting point at 66-67 ^{o}C) after recrystallization from methanol. It was soluble in THF, ether, and acetone, whereas insoluble in water, hexane, and methanol.

The ^{13}C-NMR spectrum of monomer A showed characteristic peaks for t-butyl group at 28.4 and 81.5 ppm, methyl carbons of Bisphenol A at 31.4 ppm, a quaternary carbon at 41.9 ppm, methylene carbon at 66.5 ppm, double bond carbons at 125.4 and 143.8 ppm, aromatic carbons at 114.4, 128.2, 137.9, 156.5 ppm and a carbonyl carbon at 165.2 ppm (Figure 4.8).

The ^{1}H-NMR spectrum of this monomer was characterized by t-butyl protons at 1.42 ppm, methyl protons of Bisphenol A at 1.54 ppm, methylene protons at 4.59 ppm,

double bond protons at 5.80 and 6.17 ppm and aromatic protons at 6.73 and 7.01 ppm (Figure 4.9).

The FT-IR spectrum of monomer A showed characteristic absorption of C-H, C=O, C=C and aromatic C=C, C-O groups at 2973, 1720, 1637, 1582, 1149 cm^{-1}, respectively.

In the second step, monomer A was converted to a diacid chloride intermediate (Monomer B) by thionyl chloride reaction under nitrogen purge to avoid side reactions of HCl. Light brown solid was obtained in 80 per cent yield after removing excess thionyl chloride.

The ^{13}C-NMR spectrum of monomer B showed a complete disappearance of t-butyl ester groups at 28.4 and 81.5 ppm (Figure 4.8).

In the ^{1}H-NMR spectrum of monomer B, disappearance of t-butyl protons were also confirmed (Figure 4.9).

The FT-IR spectrum of monomer A showed characteristic absorption of C-H, C=O, C=C and aromatic C=C, C-O groups at 2967, 1745, 1636, 1582, 1182 cm^{-1}, respectively.

In the third step, reaction of the diacid chloride (monomer B) with diethyl (2-hydroxyphenyl) phosphonate using TEA as catalyst in dry THF at room temperature gave monomer **1a** with diphosphonate groups. The pure product was obtained as a light yellow viscous liquid after column chromatography, starting ethylacetate:hexane (50:50) elutant and changing to EtAc:MeOH (99:1), in 45 per cent yield. This monomer was soluble in THF, ether, dicholomethane, ethyl acetate, DMSO and acetone, whereas insoluble in water, petroleum ether and hexane.

The ^{13}C-NMR spectrum of this monomer was characterized by methyl carbons of phosphonate ester and Bisphenol A at 15.2 ppm and 30.0 ppm, a quaternary carbon at 40.7 ppm, methylene carbons at 61.2 and 64.8 ppm, double bond carbons at 127.6 and

142.6 ppm, aromatic carbons of phenol phosphonate at 119.4, 121.2, 122.8, 125.0, 132.8, 133.9, 151.0 ppm and aromatic carbons of Bisphenol A at 113.1, 126.7, 134.5, 155.2 ppm and carbonyl carbon at 162.6 ppm (Figure 4.8).

The ^{1}H-NMR spectrum of this monomer was characterized by ethyl protons of phosphonate ester at 1.18 and 3.95 ppm, methyl protons of Bisphenol A at 1.56 ppm, methylene protons at 4.81 ppm, double bond protons at 6.15 and 6.62 ppm, aromatic protons of Bisphenol A at 6.81 and 7.08 ppm and aromatic protons of phenol phosphonate at 7.16, 7.27, 7.53 and 7.90 ppm (Figure 4.9).

The ^{31}P-NMR spectrum shows a singlet at 16.1 ppm. The FT-IR spectrum of this monomer showed the characteristic absorptions of C-H, C=O, C=C, P=O, P-OEt groups at 2964, 1745, 1641, 1257 and 1021 cm^{-1}, respectively (Figure 4.10).

In the last step, the silylation of monomer **1a** with TMSBr, followed by methanolysis of the silyl derivative, gave a new diphosphonic acid monomer. Monomer **1b** is very sensitive to water, therefore in order to reduce water content of the product; acetonitrile was added and evaporated immediately. This procedure was repeated four times, finally solid was washed with acetonitrile and pure product was obtained in 79 per cent yield. This monomer was soluble in polar solvents such as MeOH, EtOH and water, insoluble in most organic solvents such as THF, dichloromethane, acetone, ethyl acetate, ether and hexane.

The ^{13}C-NMR spectrum of monomer **1b** showed the disappearance of the ethyl ester peaks at 15.2 and 61.2 ppm that confirms the complete reaction (Figure 4.11).

In the ^{1}H-NMR spectrum of monomer **1b**, disappearance of the ethyl protons also confirmed the hydrolysis of phosphonate esters (Figure 4.12).

The FT-IR spectrum proved shows a broad peak between 3500 and 2000 cm^{-1} due to phosphonic acid groups (Figure 4.13).

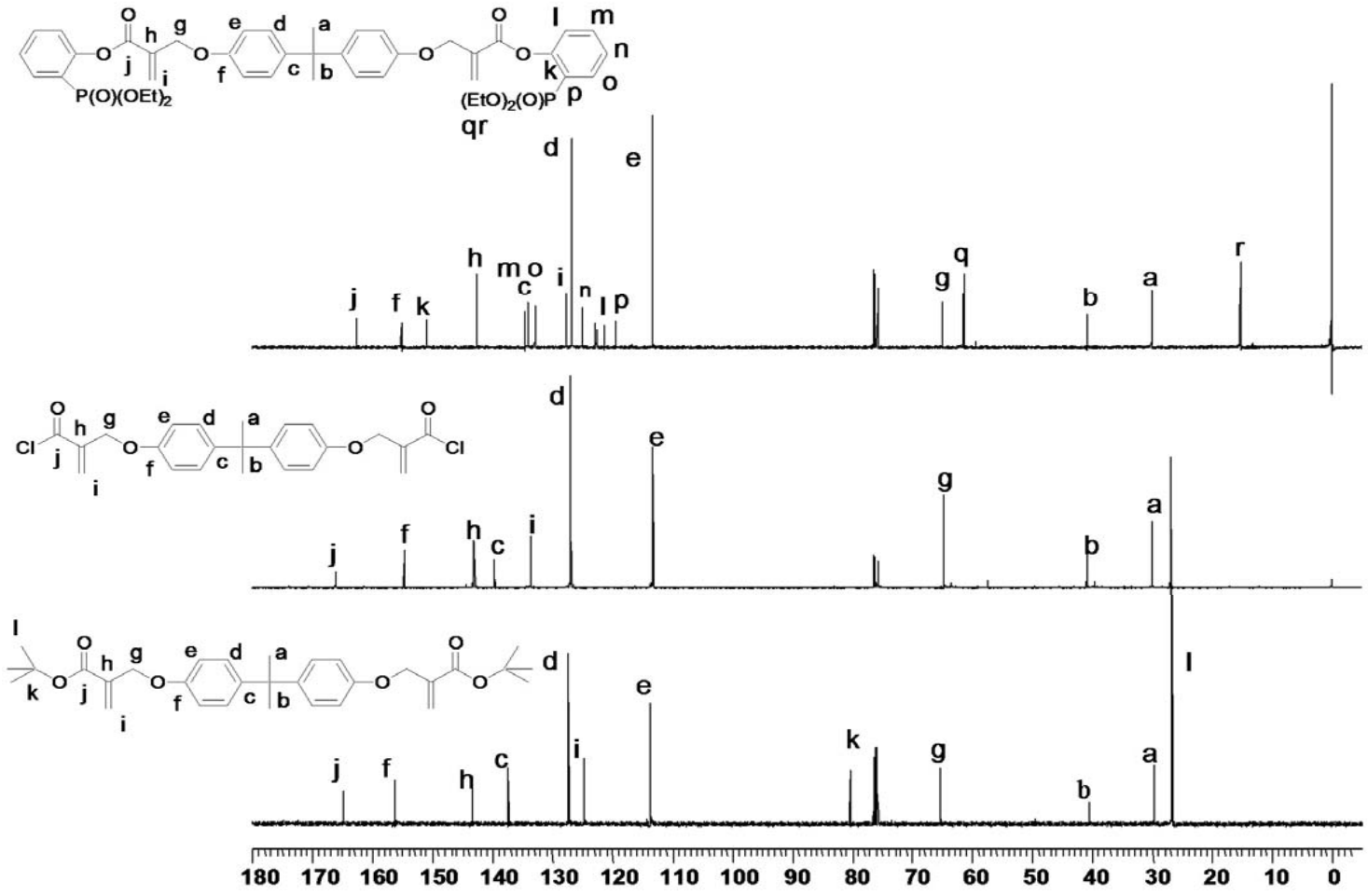

Figure 4.8. ^{13}C-NMR spectra of monomers A, B and **1a**

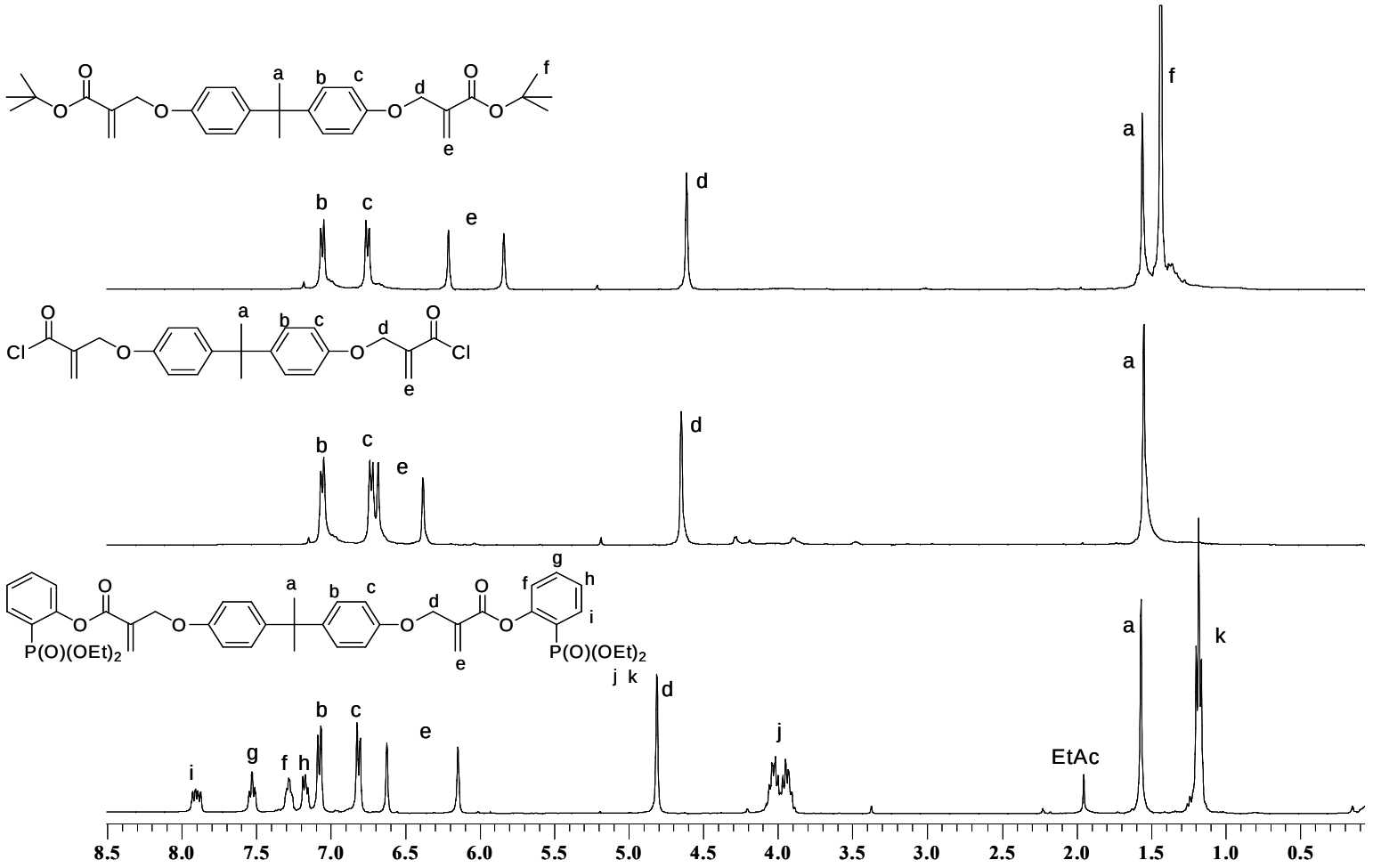

Figure 4.9. ^{1}H-NMR spectra of monomers A, B and **1a**

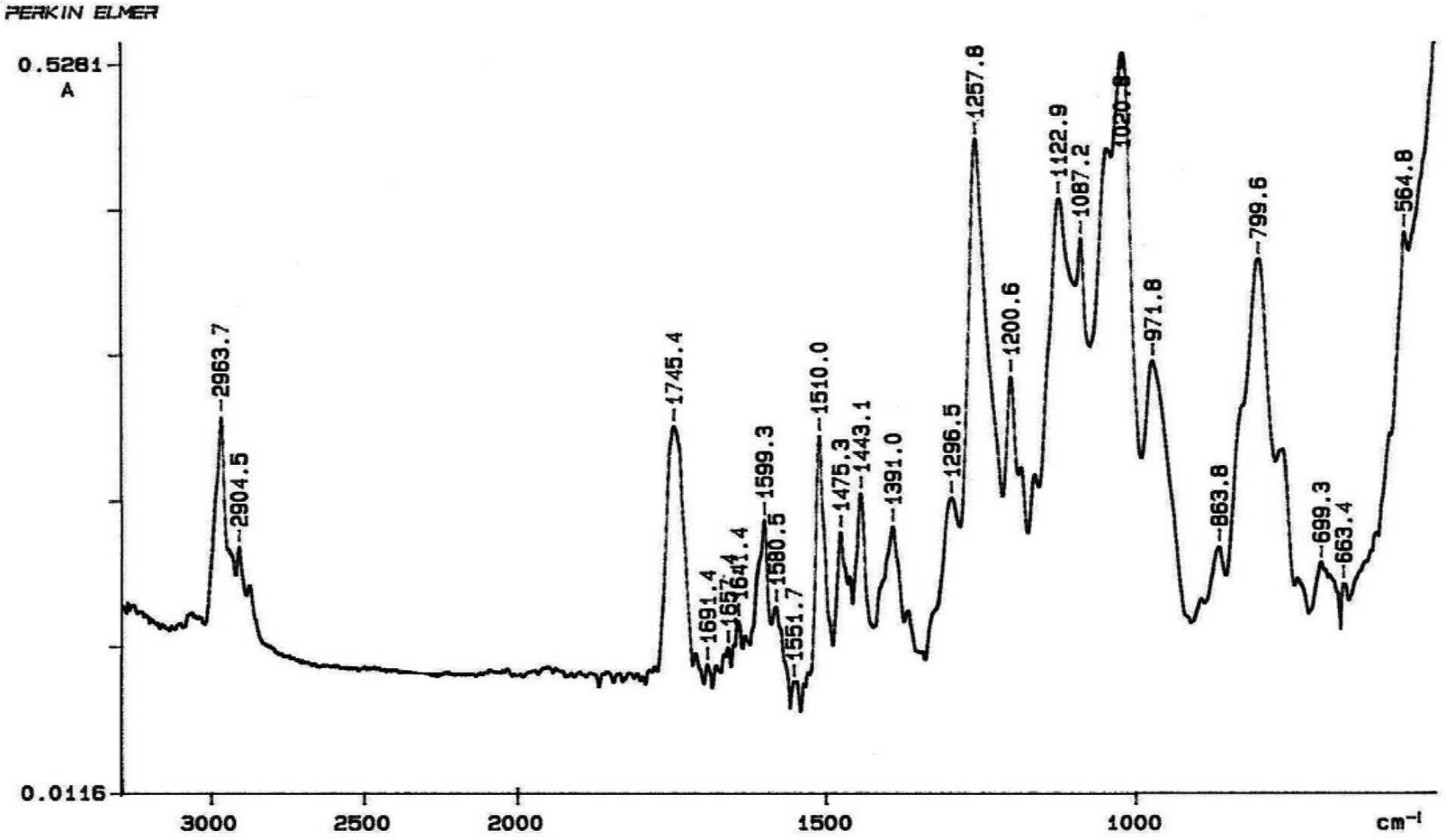

Figure 4.10. FT-IR spectrum of monomer **1a**

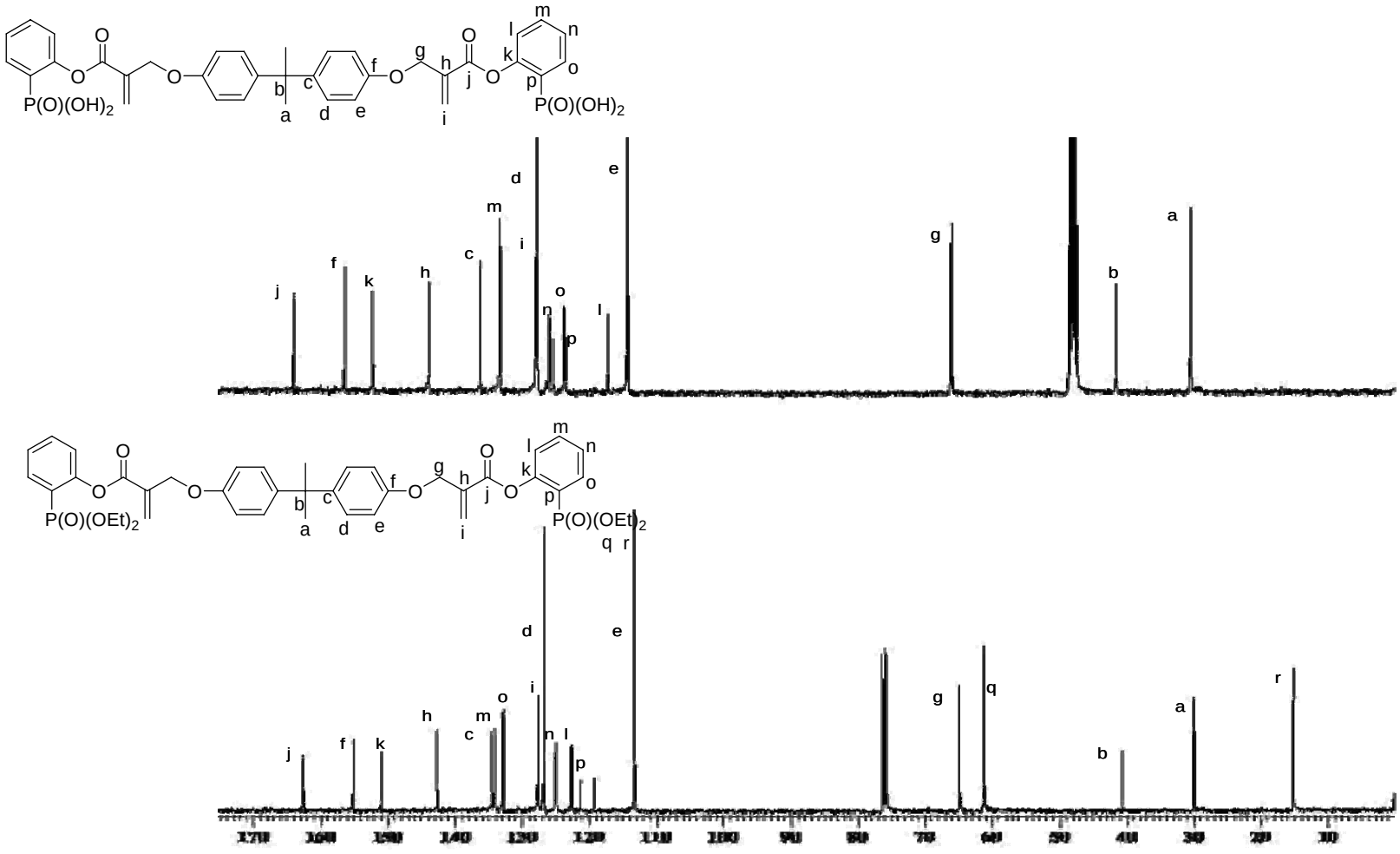

Figure 4.11. ^{13}C-NMR spectra of monomers **1a** and **1b**

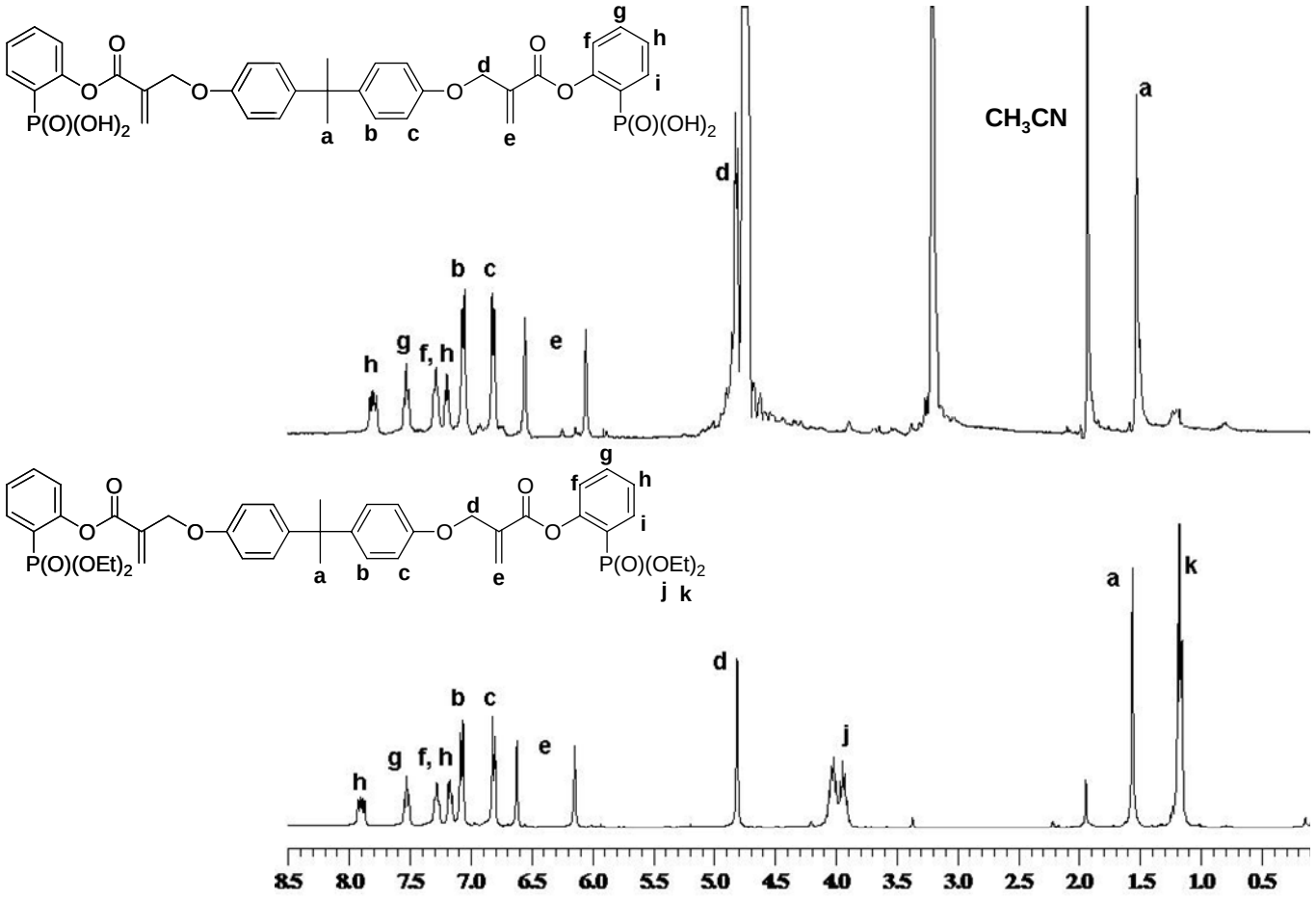

Figure 4.12. ^{1}H-NMR spectra of monomers **1a** and **1b**

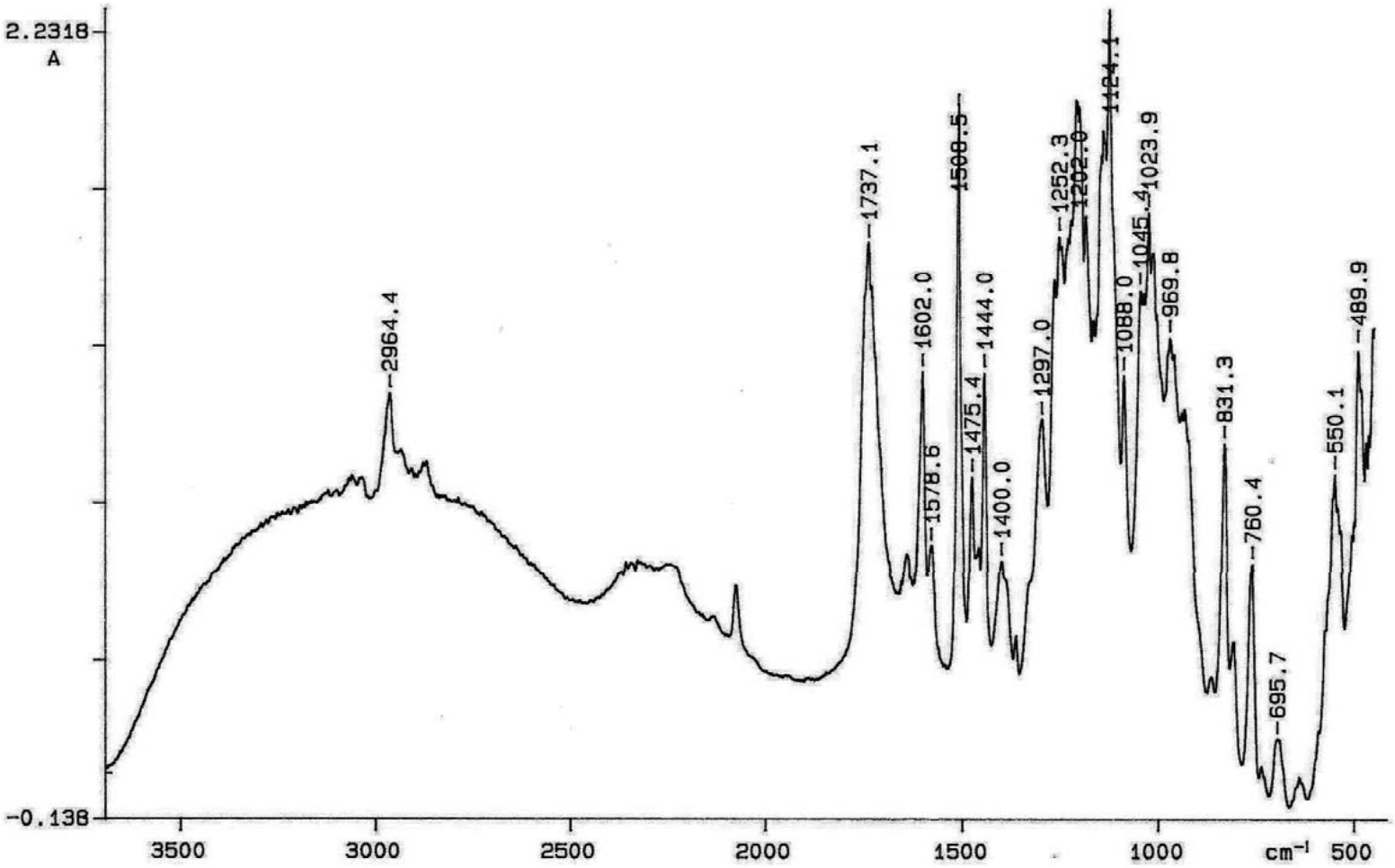

Figure 4.13. FT-IR spectrum of monomer **1b**

4.1.1.3. Synthesis of Monomers **2a** and **2b**. For the synthesis of the second pair of monomers, TBHMA was converted to CMAC in one step reaction with thionyl chloride [92]. CMAC was reacted with diethyl (2-hydroxyphenyl) phosphonate to obtain monomer **2a** with identical ester and ether groups (Figure 4.14).

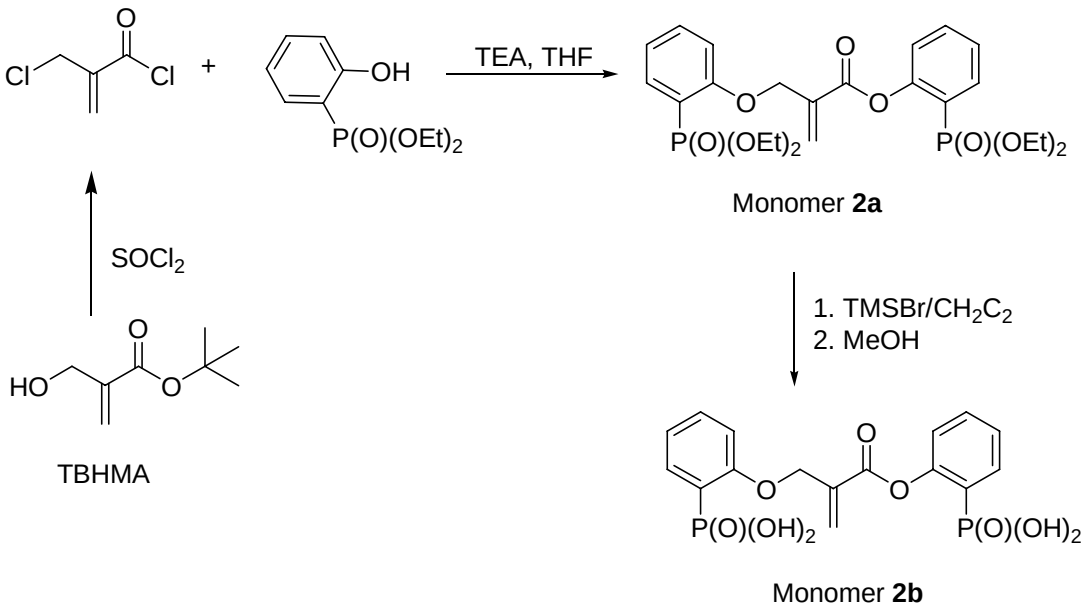

Figure 4.14. Synthesis of monomers **2a** and **2b**

The purification of this monomer with column chromatography using silica gel was not successful due to its high polarity. Therefore, reverse phase column chromatography (C18) with starting H_2O:MeOH (70:30) elutant and changing to 100% MeOH gradually was used and monomer **2a** was obtained in 45 per cent yield. This monomer was soluble in almost all organic solvents such as ethanol, methanol, THF, ether, acetone and dichloromethane whereas insoluble in water.

The ^{13}C-NMR spectrum of monomer **2a** showed characteristic peaks for ethyl groups at 14.1, 59.7 and 60.0 ppm, methylene carbon at 63.6 ppm, double bond carbons at 126.7 and 133.0 ppm, aromatic carbons attached to phosphorus atoms at 113.2, 115.0, 117.9, 119.7, other aromatic carbons at 109.8, 118.6, 121.3, 123.7, 131.7, 132.1, 132.2 and 132.7 ppm and a carbonyl carbon at 161.1 ppm (Figure 4.15).

The ^{1}H-NMR spectrum of this monomer was characterized by ethyl protons at 1.29 and 4.12 ppm, methylene protons at 5.01 ppm, double bond protons at 6.59, 6.76 ppm and aromatic protons at 7.07, 7.27, 7.37, 7.51, 7.61, 7.88 and 7.98 ppm (Figure 4.16).

The FT-IR spectrum of monomer **2a** showed characteristic absorption of C-H, C=O, C=C and aromatic C=C, P=O, C-O and P-O-Et groups at 2983, 1746, 1643, 1593, 1250, 1091 and 1023 cm^{-1}, respectively (Figure 4.17).

The synthesis of monomer **2b** involved the silylation reaction of monomer **2a** with TMSBr, followed by methanolysis of the silyl derivative. After reducing water content of the product with acetonitrile, pure product was obtained in 60 per cent yield. This monomer was soluble in THF, MeOH, EtOH and water, insoluble in most organic solvents such as dichloromethane, acetone, ethyl acetate, ether and hexane.

The ^{13}C-NMR spectrum of monomer **2b** showed the disappearance of the ethyl ester peaks at 14.1 and 60.0 ppm that confirms the complete reaction (Figure 4.15).

In the ^{1}H-NMR spectrum of monomer **2b**, disappearance of ethyl protons also confirmed the hydrolysis of phosphonate esters (Figure 4.16).

The FT-IR spectrum showed a broad peak between 3500 and 2000 cm^{-1} due to phosphonic acid groups (Figure 4.18).

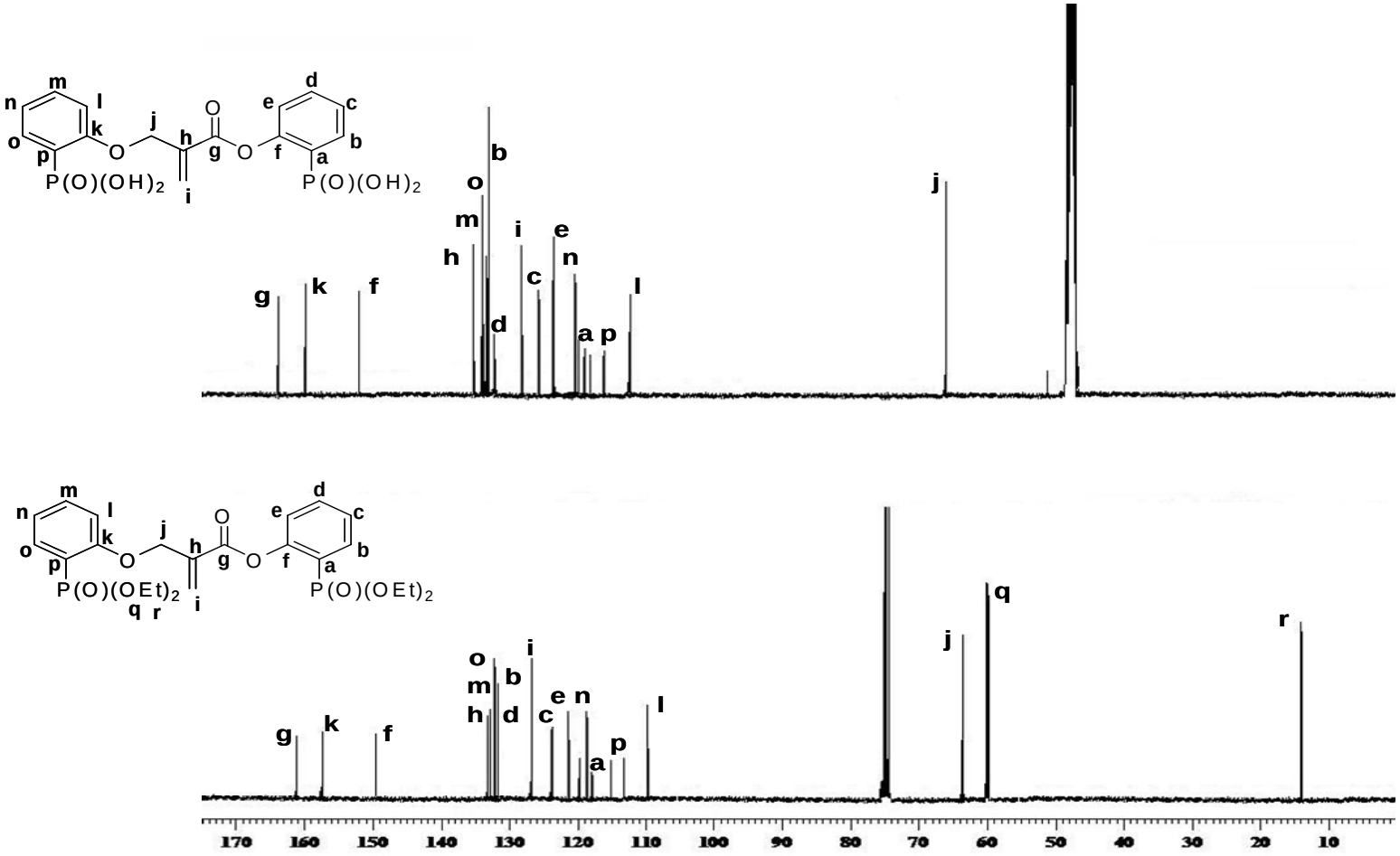

Figure 4.15. ^{13}C-NMR spectra of monomers **2a** and **2b**

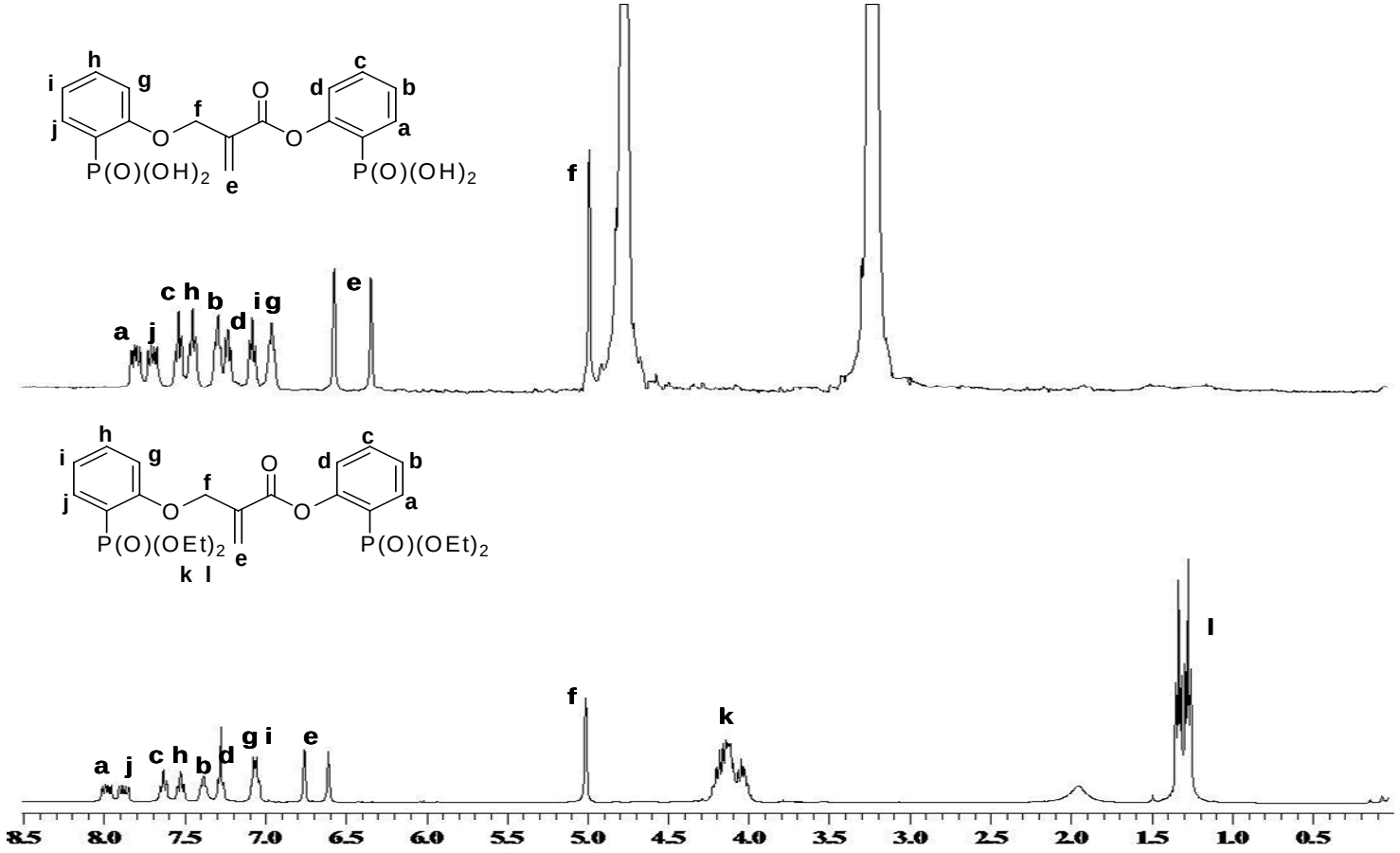

Figure 4.16. ^{1}H-NMR spectra of monomers **2a** and **2b**

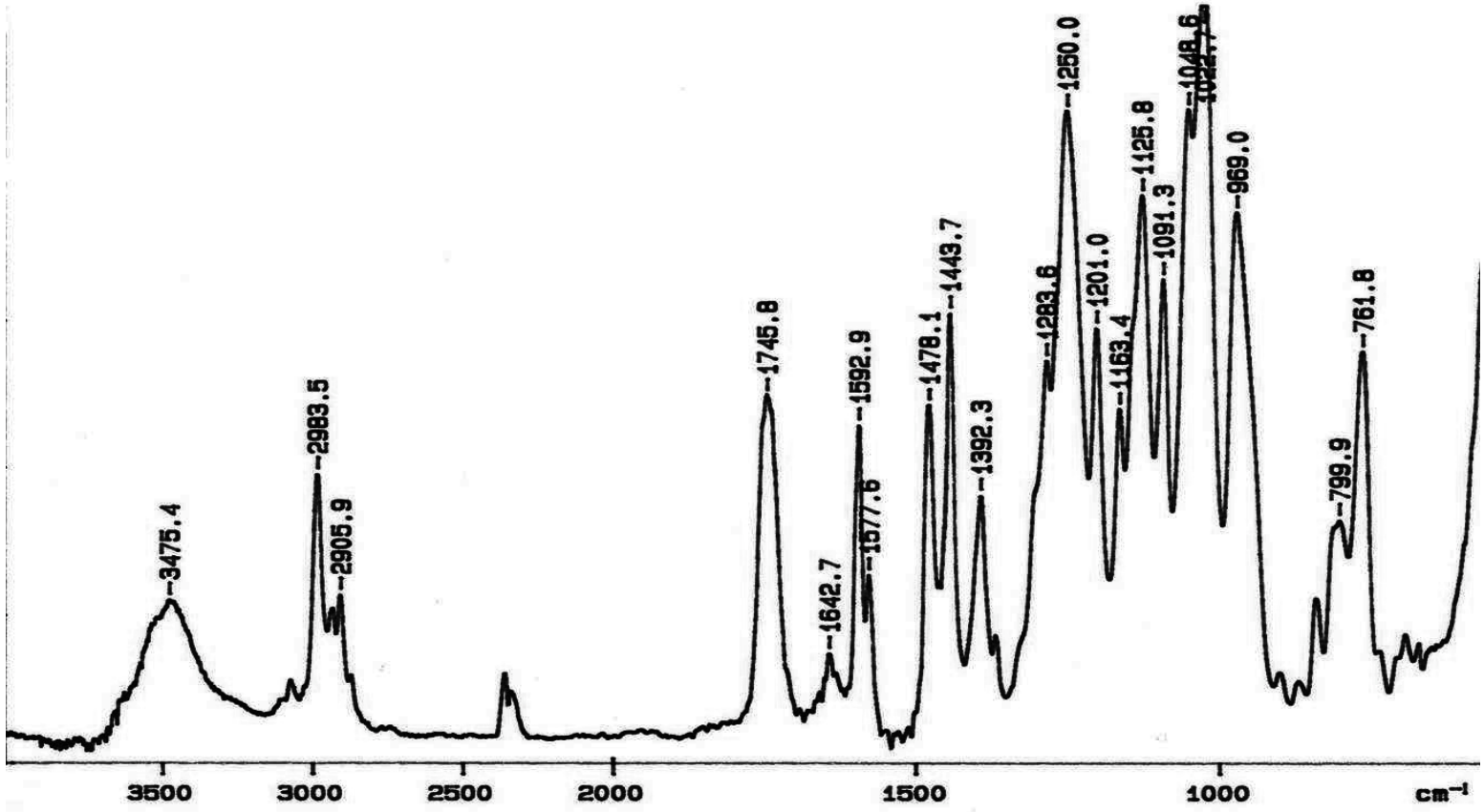

Figure 4.17. FT-IR spectrum of monomer **2a**

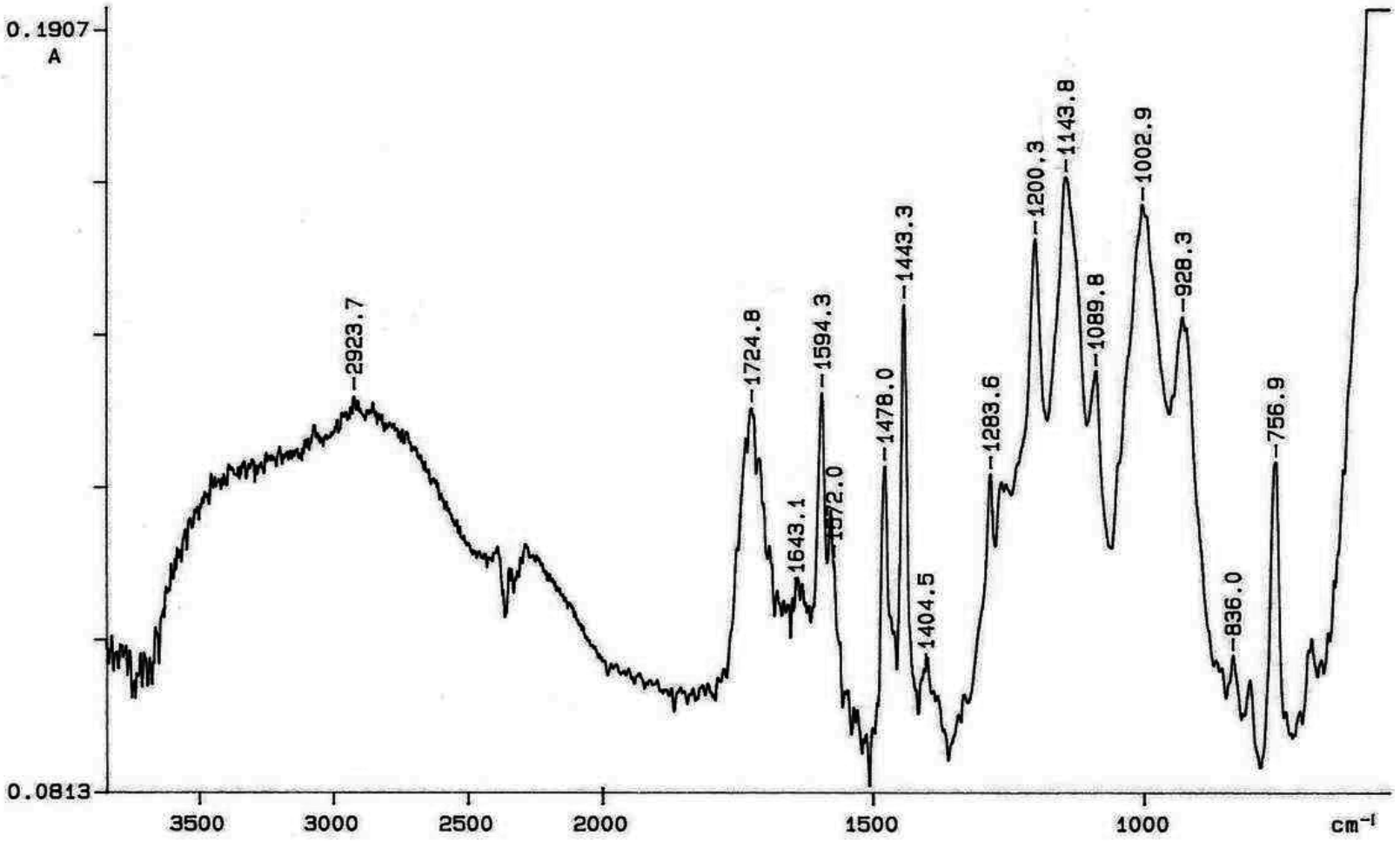

Figure 4.18. FT-IR spectrum of monomer **2b**

4.1.1.4. Synthesis of Monomer **3a**. The synthesis of monomer **3a** was begun by the reaction of diethyl (2-hydroxyphenyl) phosphonate with glycidyl methacrylate (GMA) (Figure 4.19). The reaction was carried out in the presence of two different catalysts, TEA and triphenyl phosphine under nitrogen at 70 ºC and 85 ºC. The reaction was monitored by ^{13}C-NMR and FTIR spectra. The disappearance of the characteristic epoxy peaks at 44.3 and 49.8 ppm in the ^{13}C-NMR spectra and around 840 and 908 cm^{-1} in the FT-IR spectra (Figure 4.20) were used to follow product formation. According to FT-IR indications, the reaction with TEA was almost complete after 16 hours, whereas the ^{13}C-NMR indications showed only 85 per cent completion. Therefore, reaction time was chosen 1 day. When, triphenyl phsophine was used as a catalyst at 85 ^{o}C, there was no reaction at the end of 6 days.

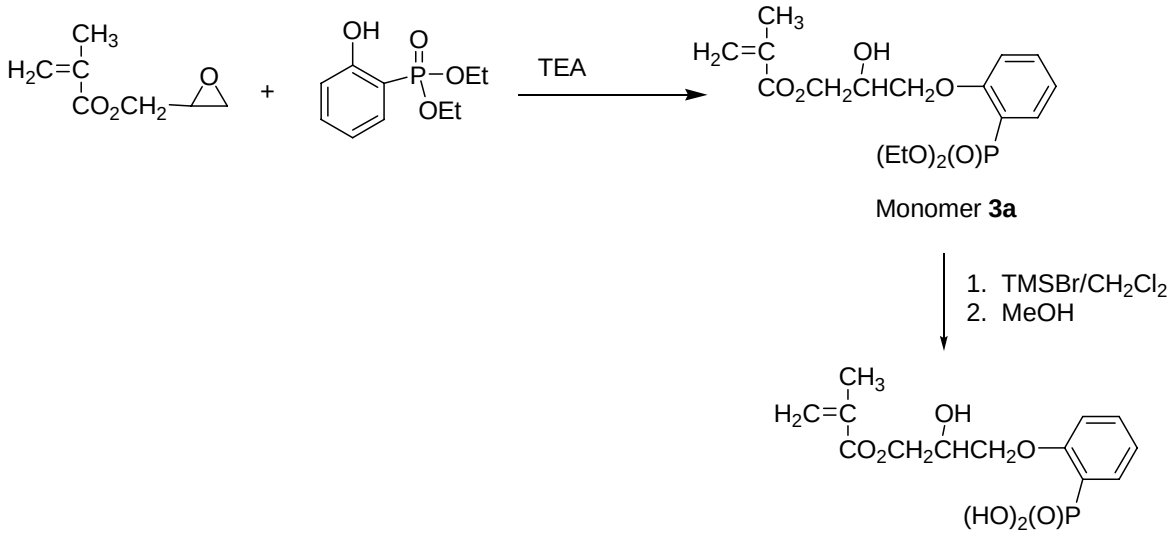

Figure 4.19. Synthesis of monomer **3a**

There are two possible sites for the attack of alcohols, acids and anhydrides. If the attack occurs from the less hindered side the linear isomer is obtained otherwise the branched isomer or both isomers are produced. The crude product yield of our reaction was 87 %, containing mostly linear monomer with a very small amount of the branched isomer. When this mixture was subjected to a chromatographic separation on silica gel, fractions containing mixture of isomers at different ratios were obtained.

The ^{13}C-NMR spectrum of one of the fractions showed methyl carbons of phosphonate ester and GMA at 16.4 ppm and 18.7 ppm, methylene carbons at 62.5, 65.2 and 72.8 ppm, a tertiary carbon at 68.3 ppm, aromatic carbon attached to phosphorus atom at 117.0, 118.8 ppm, other aromatic carbons at 114.7, 121.5, 133.6, 134.8 ppm, double bond carbons at 126.0, 136.3 ppm, aromatic carbon attached to oxygen atom at 161.2 ppm and carbonyl carbon at 167.4 ppm. The small peaks at 67.2 (CH_2), 66.3 (CH_2) and 70.2 (CH) ppm are due to branched isomer (Figure 4.21).

The ^{1}H-NMR spectrum of this monomer was characterized by ethyl protons of phosphonate ester at 1.36 and 3.95 ppm, methyl protons of GMA at 1.86 ppm, methylene protons at 4.19, 4.24 ppm, hydroxyl proton at 5.16 ppm, double bond protons at 5.49, 6.05 ppm and aromatic protons at 6.90, 6.97, 7.42 and 7.60 ppm (Figure 4.22).

The ^{31}P-NMR spectrum showed a singlet at 18.5 ppm. The FT-IR spectrum of this monomer showed the characteristic absorptions of –OH, C-H, C=O, C=C, P=O, P-OEt groups at 3349, 2981, 1715, 1637, 1283 and 1163 cm^{-1}, respectively (Figure 4.23).

The attempted hydrolysis of monomer **3a** with TMSBr under different conditions was unsuccessful. NMR spectrum of the product was too complicated to identify product(s) but did not show formation of the expected acid monomers. The ethyl peaks of the phosphonate esters remained intact after the attempted reaction.

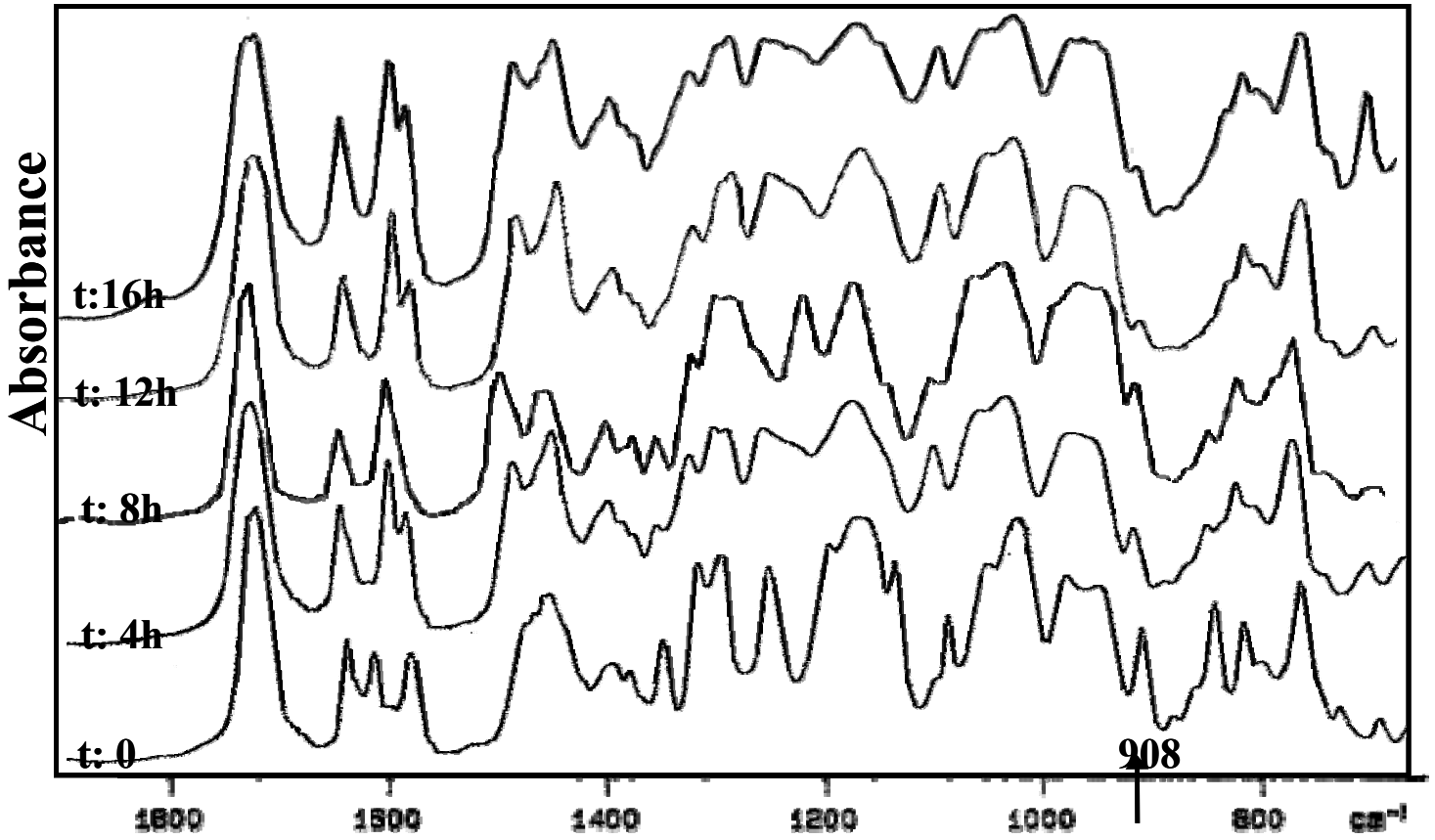

Figure 4.20. Monitoring of monomer **3a** synthesis as a function of time

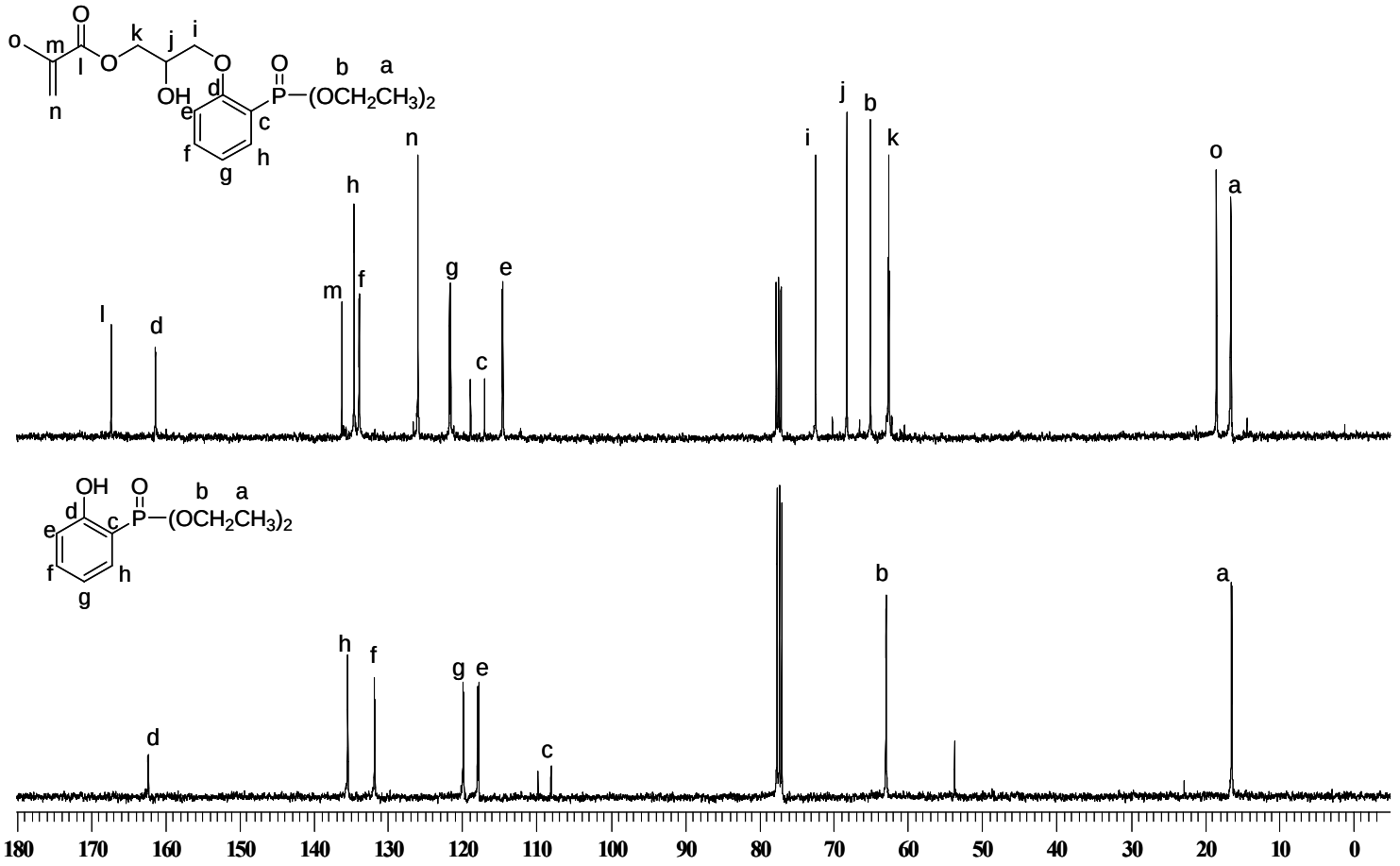

Figure 4.21. ^{13}C-NMR spectra of diethyl (2-hydroxyphenyl) phosphonate and monomer **3a**

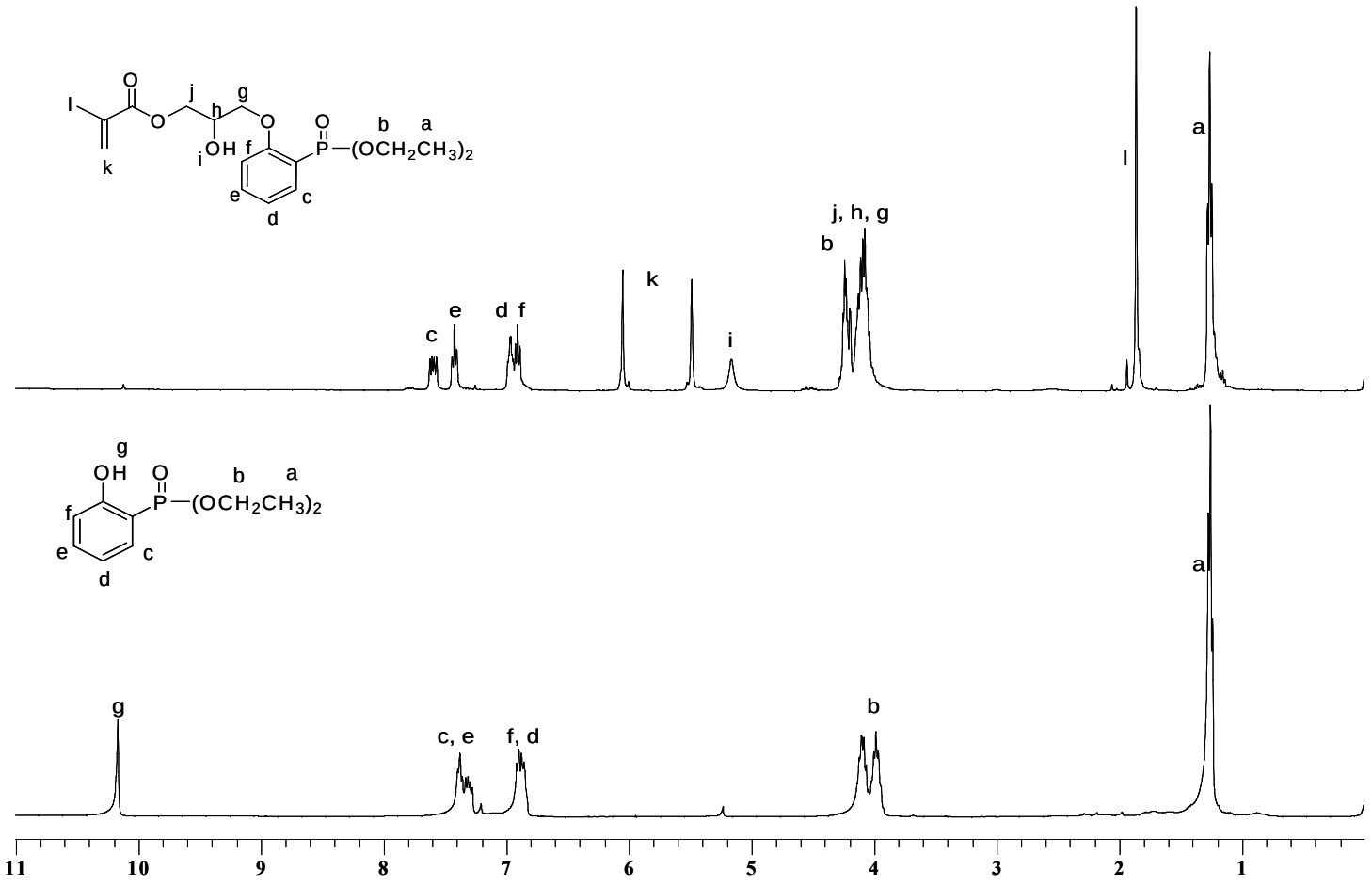

Figure 4.22. ^{1}H-NMR spectra of diethyl (2-hydroxyphenyl) phosphonate and monomer **3a**

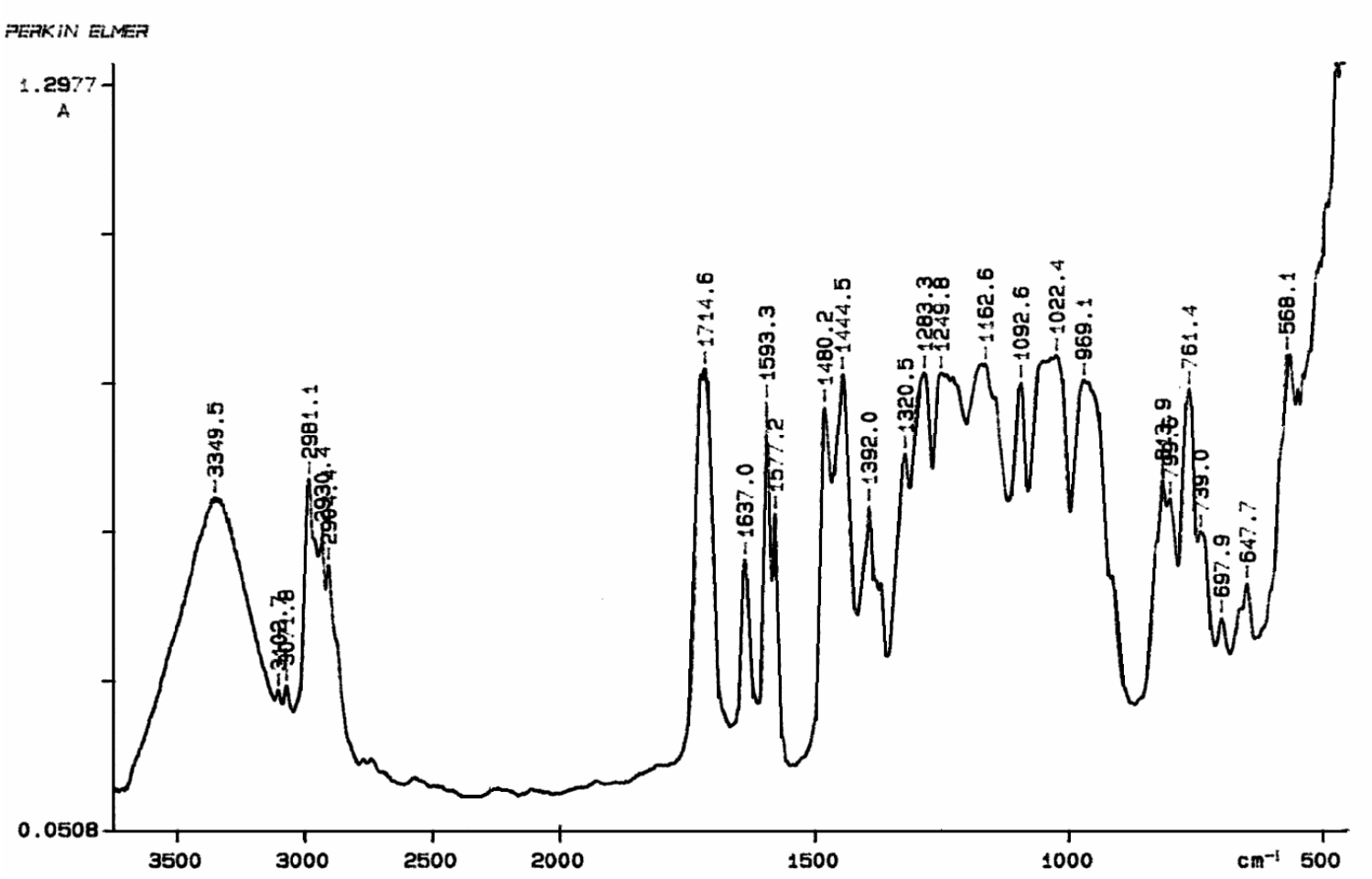

Figure 4.23. FT-IR spectrum of monomer **3a**

4.1.1.5. Synthesis of Monomer **4a**. The synthesis of monomer **4a** was begun by the reaction of diethyl (2-hydroxyphenyl) phosphonate with an aromatic diepoxide (DER) (Figure 4.24).

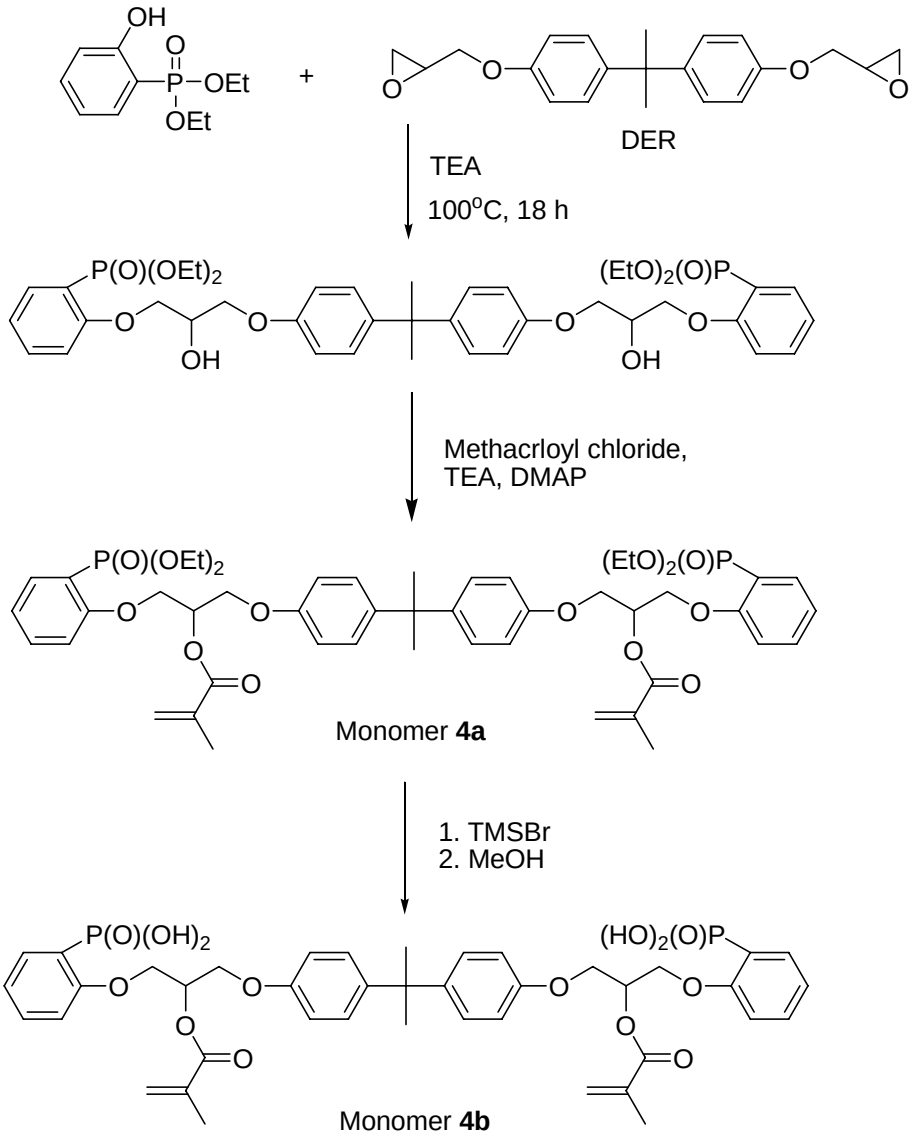

Figure 4.24. Synthesis of monomer **4a**

In the first step, the ring opening reaction of bisphenol A diglycidyl ether (DER) with diethyl (2-hydroxyphenyl) phosphonate was used to obtain diol intermediate.

The ^{13}C-NMR spectrum of diol intermediate was characterized by methyl carbons of phosphonate ester and Bisphenol A at 16.4 ppm and 31.0 ppm respectively, a

quaternary carbon at 41.7 ppm, methylene carbons at 62.4, 68.3 and 68.7 ppm, methylene carbon attached to hydroxyl at 72.4 ppm, aromatic carbon attached to phosphorus atom at 116.7, 118.6 ppm, other aromatic carbons of phenol phosphonate at 114.5, 121.3, 133.7, 134.4 ppm and aromatic carbons of Bisphenol A at 113.9, 127.7, 143.6 ppm and aromatic carbons attached to oxygen atom at 156.4, 161.3 ppm.

The ^{1}H-NMR spectrum also confirmed structure of the diol.

The FT-IR spectrum of this monomer showed the characteristic absorptions of -OH, C-H, P=O, P-OEt groups at 3339, 2964, 1257 and 1123, 972 cm^{-1}, respectively.

In the second step, reaction of the diol intermediate with methacrloyl chloride using TEA and DMAP as catalyst in freshly dried CH_2Cl_2 at room temperature gave monomer **4a**. The pure product was obtained as a light yellow viscous liquid after column chromatography, starting with ethylacetate:hexane (50:50) elutant and changing to EtAc:MeOH (99:1). This monomer was soluble in methanol, THF, dichlormethane, but insoluble in acetone, ether and water.

The ^{13}C-NMR spectrum of this monomer showed characteristic peaks for methyl carbons of phosphonate ester, methacrylate and Bisphenol A at 16.5, 18.4 and 31.3 ppm respectively, a quaternary carbon at 42.1 ppm, methylene carbons at 63.3, 66.0 and 66.5 ppm, methylene carbon attached to hydroxyl at 71.0 ppm, double bond carbons at 126.7 and 136.1 ppm, aromatic carbons attached to phosphorus atom at 115.9, 117.8 ppm, aromatic carbons of phenol phosphonate at 114.5, 121.1, 128.1, 134.8 ppm and aromatic carbons of Bisphenol A at 112.2, 128.1, 135.8 ppm, aromatic carbons attached to oxygen atom at 156.5, 160.1 ppm and carbonyl carbon at 166.9 ppm (Figure 4.25).

The ^{1}H-NMR spectrum of this monomer was characterized by ethyl protons of phosphonate ester at 1.16 and 4.01 ppm, methyl protons of Bisphenol A and methacrylate at 1.51 and 1.85 ppm respectively, methylene protons at 4.31 and 5.44 ppm, double bond protons at 5.53 and 6.05 ppm, aromatic protons of Bisphenol A at 6.76 and 6.90 ppm and aromatic protons of phenol phosphonate at 6.97, 7.03, 7.42 and 7.78 ppm (Figure 4.26).

The FT-IR spectrum of this monomer showed the characteristic absorptions of C-H, C=O, C=C, P=O, P-OEt groups at 2976, 1719, 1636, 1247 and 1026 cm^{-1}, respectively (Figure 4.27).

Hydrolysis of phosphonate groups of monomer **4a** will give a new diphosphonic acid-containing monomer which may have applications in dental adhesive systems. We expect to perform synthesis of this monomer in future work.

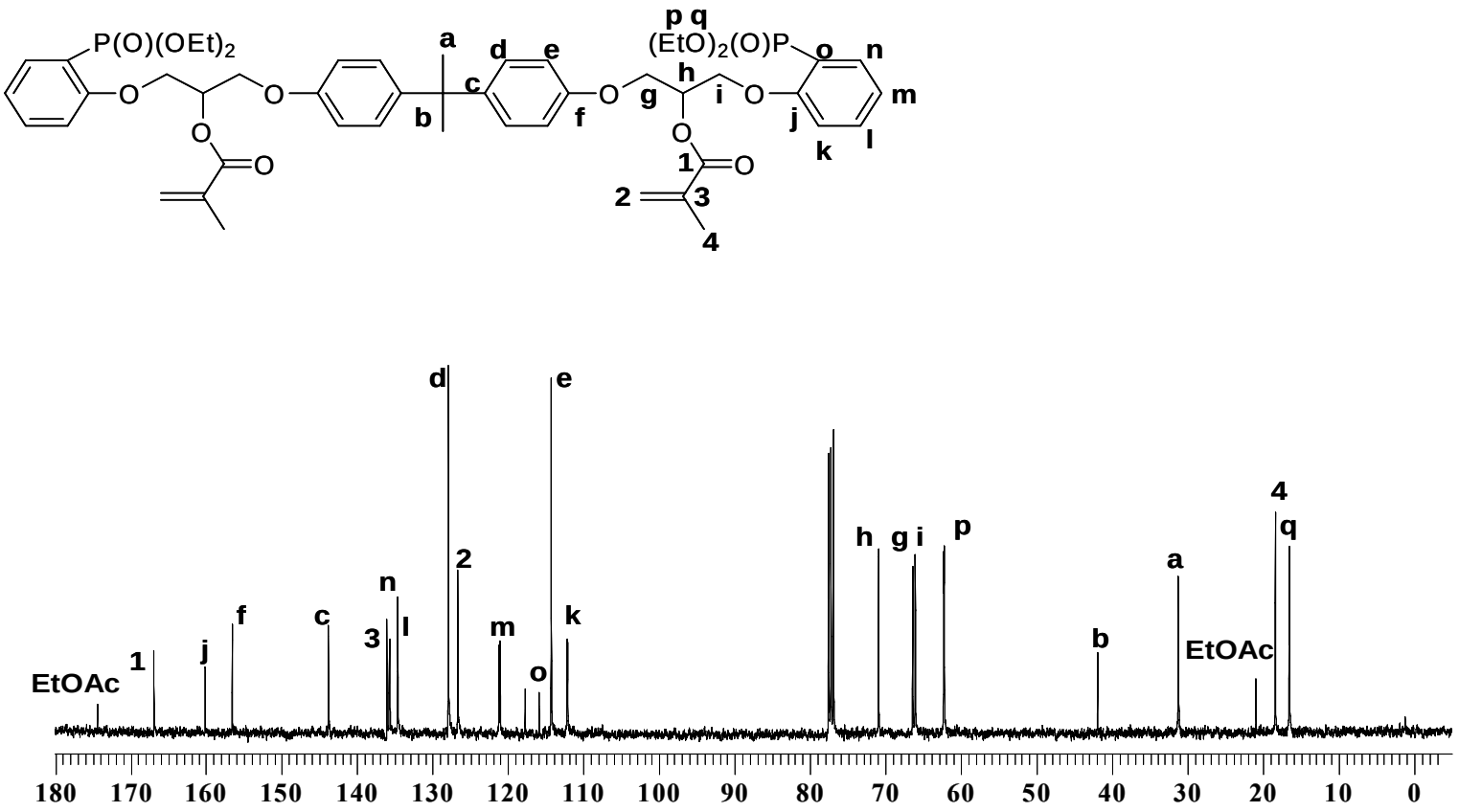

Figure 4.25. ^{13}C-NMR spectrum of monomer **4a**

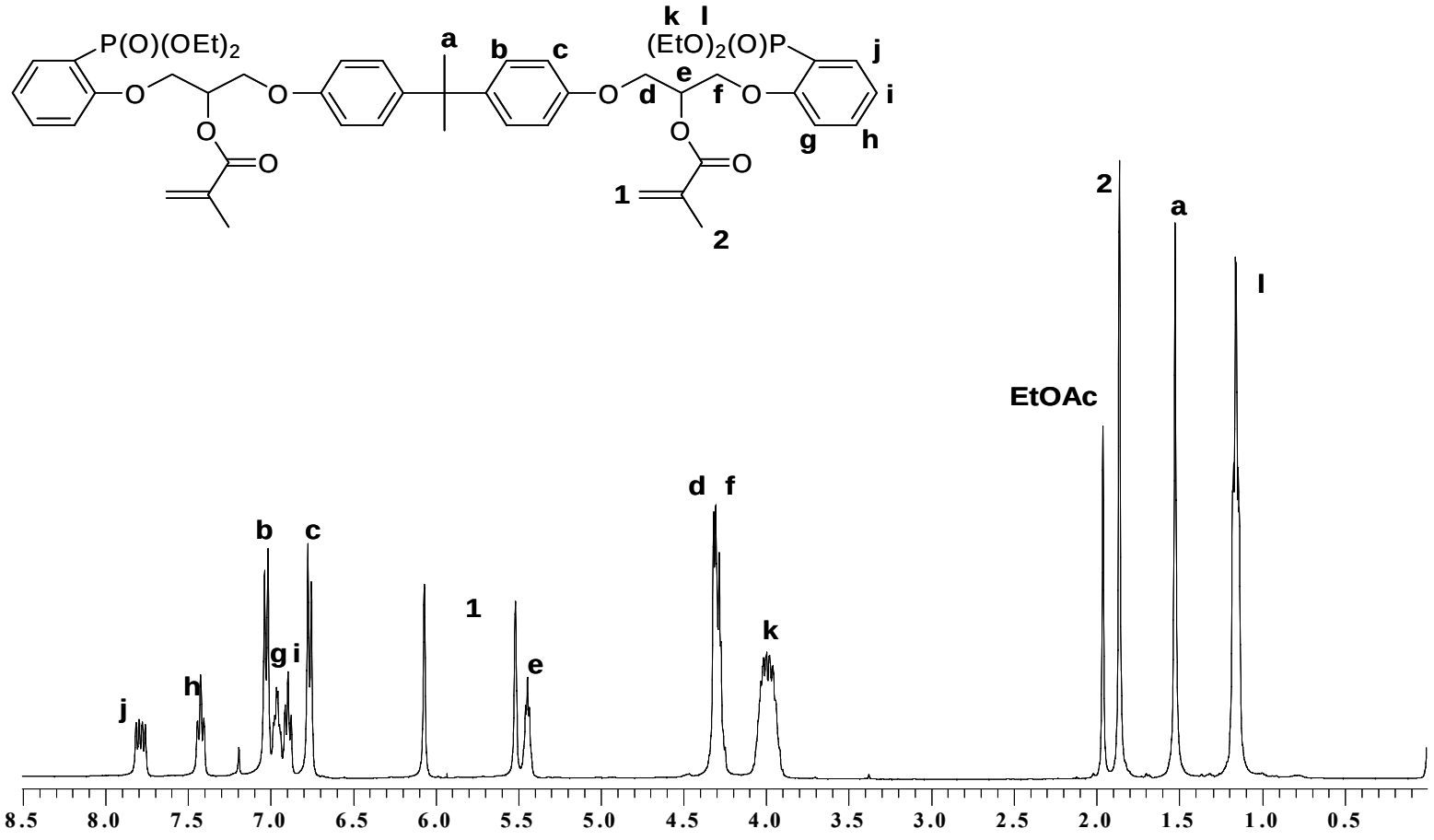

Figure 4.26. ^{1}H-NMR spectrum of monomer **4a**

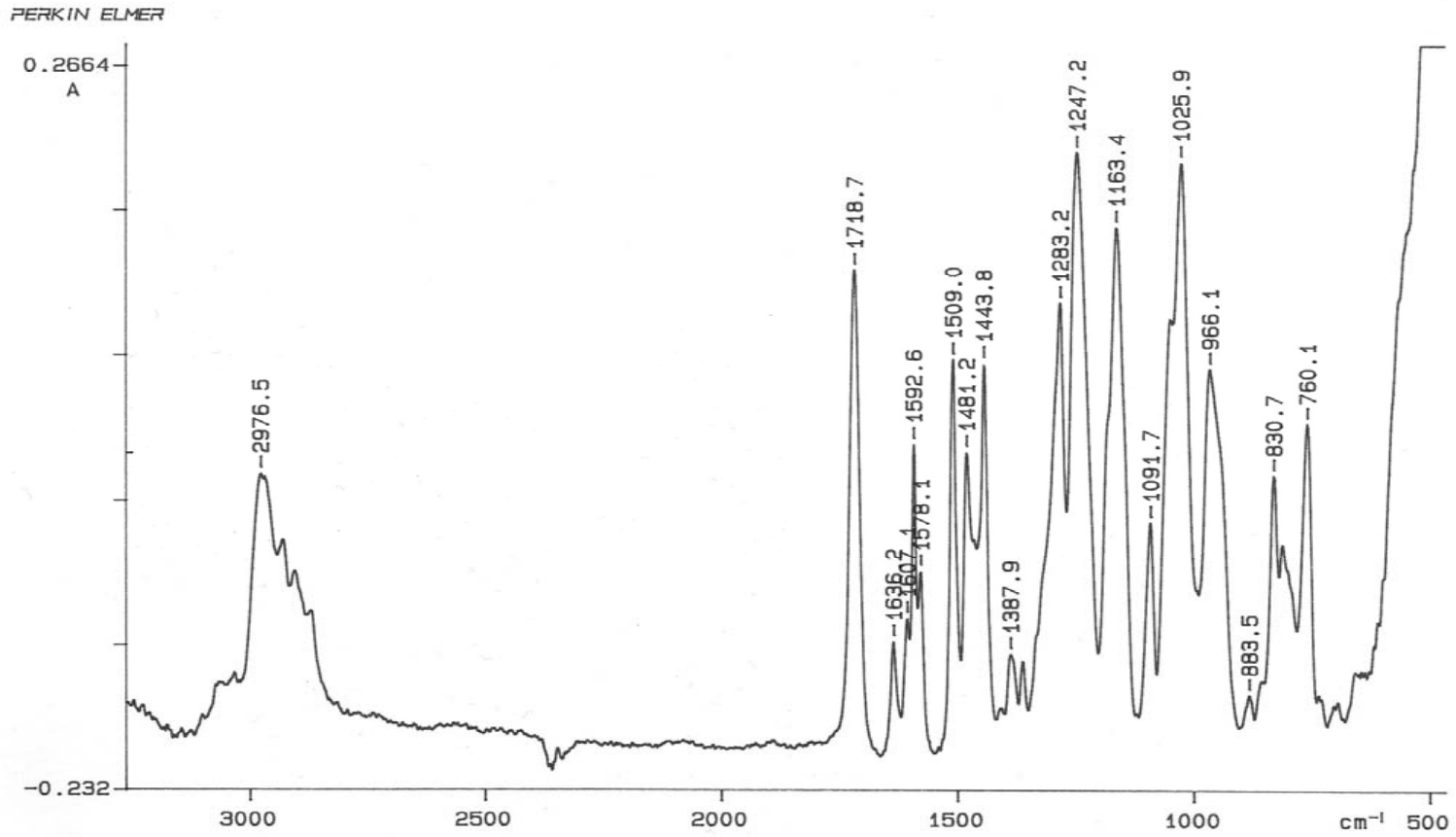

Figure 4.27. FT-IR spectrum of monomer **4a**

4.1.1.6. Synthesis of Monomers **5a** and **5b**. Synthesis of monomers **5a** and **5b** involved the reaction of diethyl (2-hydroxyphenyl) phosphonate with TBBr and hydrolysis of the t-butyl and phosphonate ester groups (Figure 4.28).

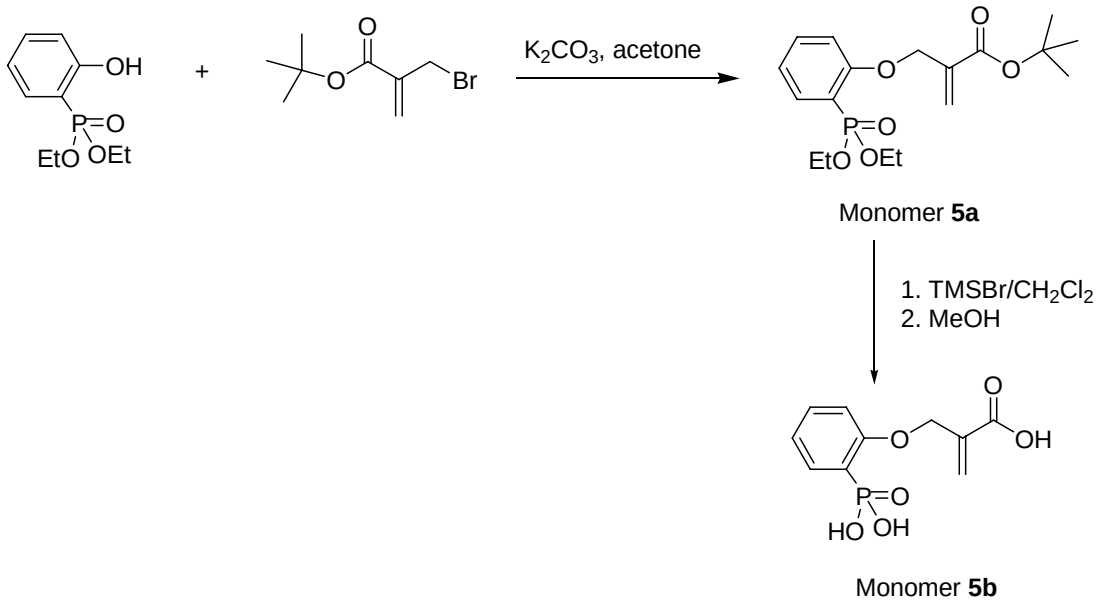

Figure 4.28. Synthesis of monomers **5a** and **5b**

The reaction of TBBr with diethyl (2-hydroxyphenyl) phosphonate in the presence of K_2CO_3 as catalyst in acetone gave monomer **5a** as a yellow solid with a melting point of 36 ^oC. The purification of the product required column chromatography with CH_2Cl_2/isopropyl alcohol as the eluent and pure monomer was obtained in 43 per cent yield. This monomer was soluble in almost all organic solvents such as ethanol, methanol, THF, ether, acetone and dichloromethane whereas insoluble in water.

The ^{13}C-NMR spectrum of monomer **5a** showed characteristic peaks for ethyl groups at 16.1 and 62.2 ppm, t-butyl carbons at 28.1 and 81.2 ppm, methylene carbon at 66.3 ppm, double bond carbons at 126.2 and 136.2 ppm, aromatic carbons attached to phosphorus atoms at 115.8, 117.6, other aromatic carbons at 112.5, 121.8, 134.8, 135.0 ppm and a carbonyl carbon at 164.3 ppm (Figure 4.29).

The ^1H-NMR spectrum of this monomer was characterized by ethyl protons at 1.26 and 4.14 ppm, t-butyl protons at 1.44 ppm, methylene protons at 4.76 ppm, double

bond protons at 6.21, 6.37 ppm and aromatic protons at 6.98, 7.45 and 7.82 ppm (Figure 4.30).

The FT-IR spectrum of monomer **5a** showed characteristic absorption of C-H, C=O, C=C, P=O, C-O and P-O-Et groups at 2979, 1705, 1639, 1253 and 1026 cm^{-1}, respectively (Figure 4.31).

The synthesis of monomer **5b** involved the silylation reaction of monomer **5a** with TMSBr, followed by methanolysis of the silyl derivative. The literature showed that this hydrolysis is selective to phosphonates that means carboxylic acid esters remain intact. However, partial hydrolysis of the t-butyl ester groups were observed during this reaction. Total hydrolysis of the t-butyl groups were carried out by mixing with excess trifluoroacetic acid. Monomer **5b** was obtained as a light brown solid in 42 per cent yield which had a melting point of 182 ^{o}C. The monomer was soluble in water, methanol and ethanol but insoluble in ether and methylene chloride.

The ^{13}C-NMR spectrum of monomer **5b** showed the disappearance of the ethyl and t-butyl ester peaks at 16.1, 62.2, 28.1 and 81.2 ppm that confirmed the complete reaction (Figure 4.29).

In the ^{1}H-NMR spectrum of monomer **5b**, disappearance of ethyl protons and t-butyl protons at 1.26, 4.14 and 1.44 ppm also confirmed the hydrolysis of phosphonate and t-butyl ester groups (Figure 4.30).

The FT-IR spectrum showed a broad peak between 3500 and 2000 cm^{-1} due to phosphonic acid groups (Figure 4.32).

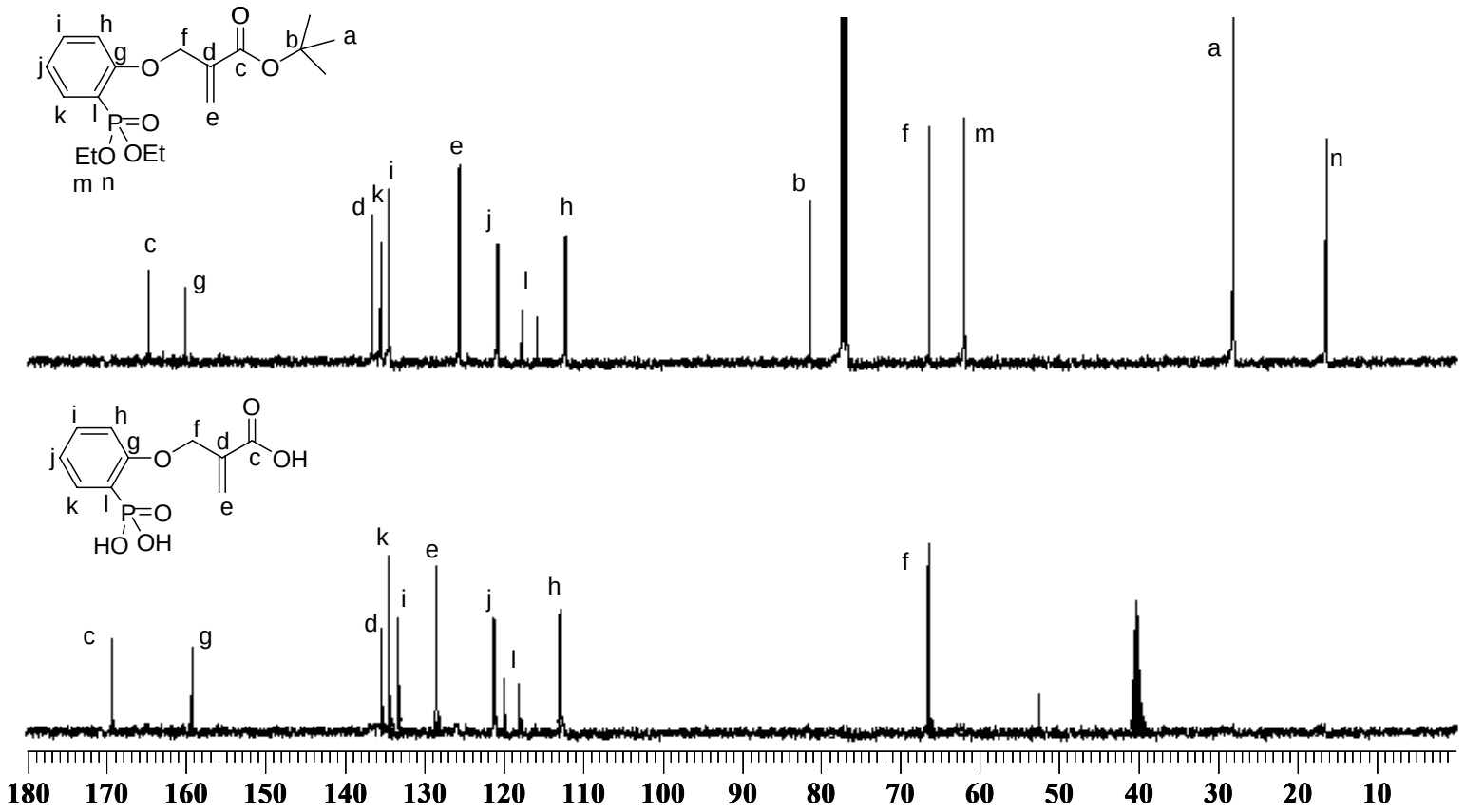

Figure 4.29. ^{13}C-NMR spectra of monomers **5a** and **5b**

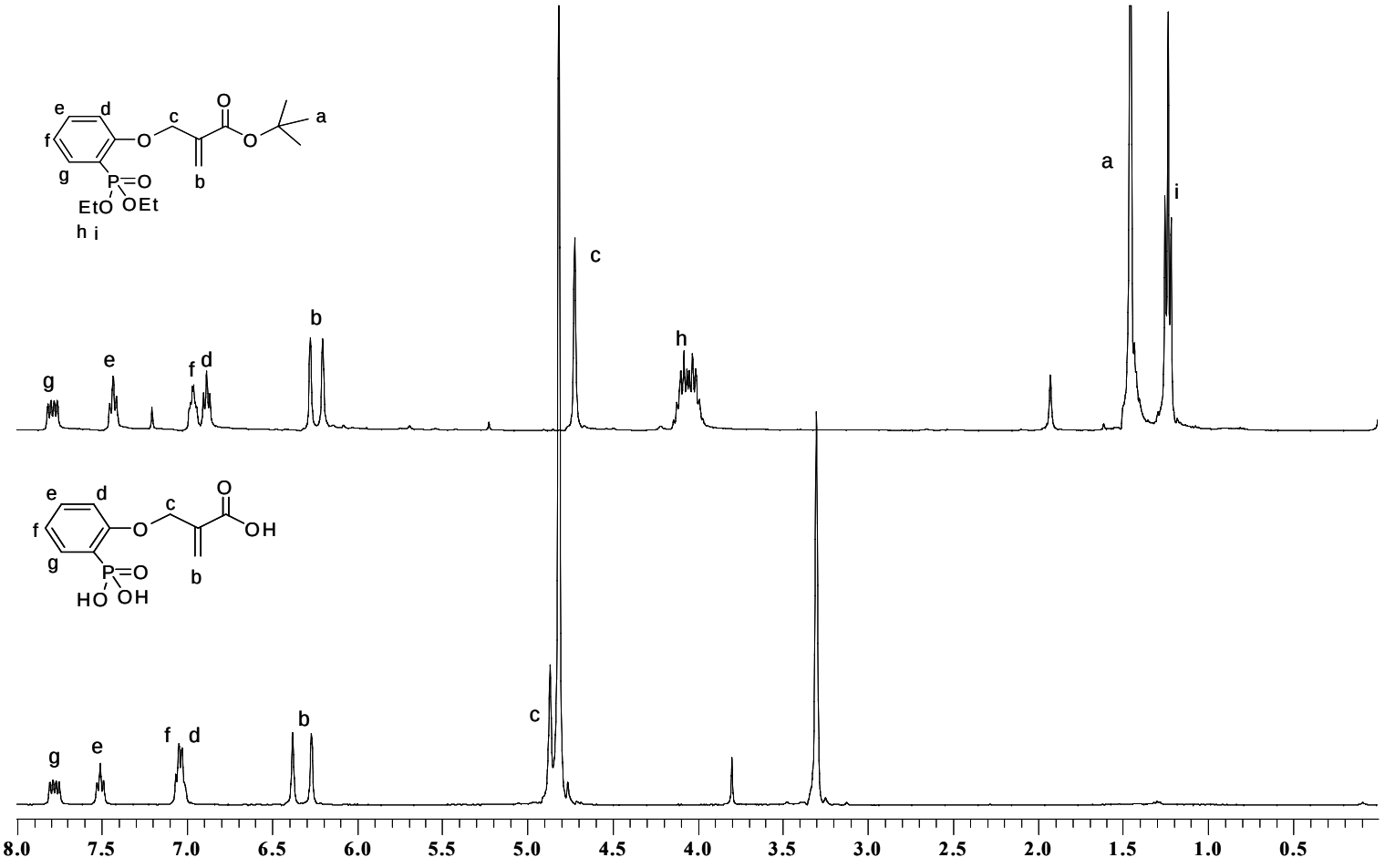

Figure 4.30. ^{1}H-NMR spectra of monomers **5a** and **5b**

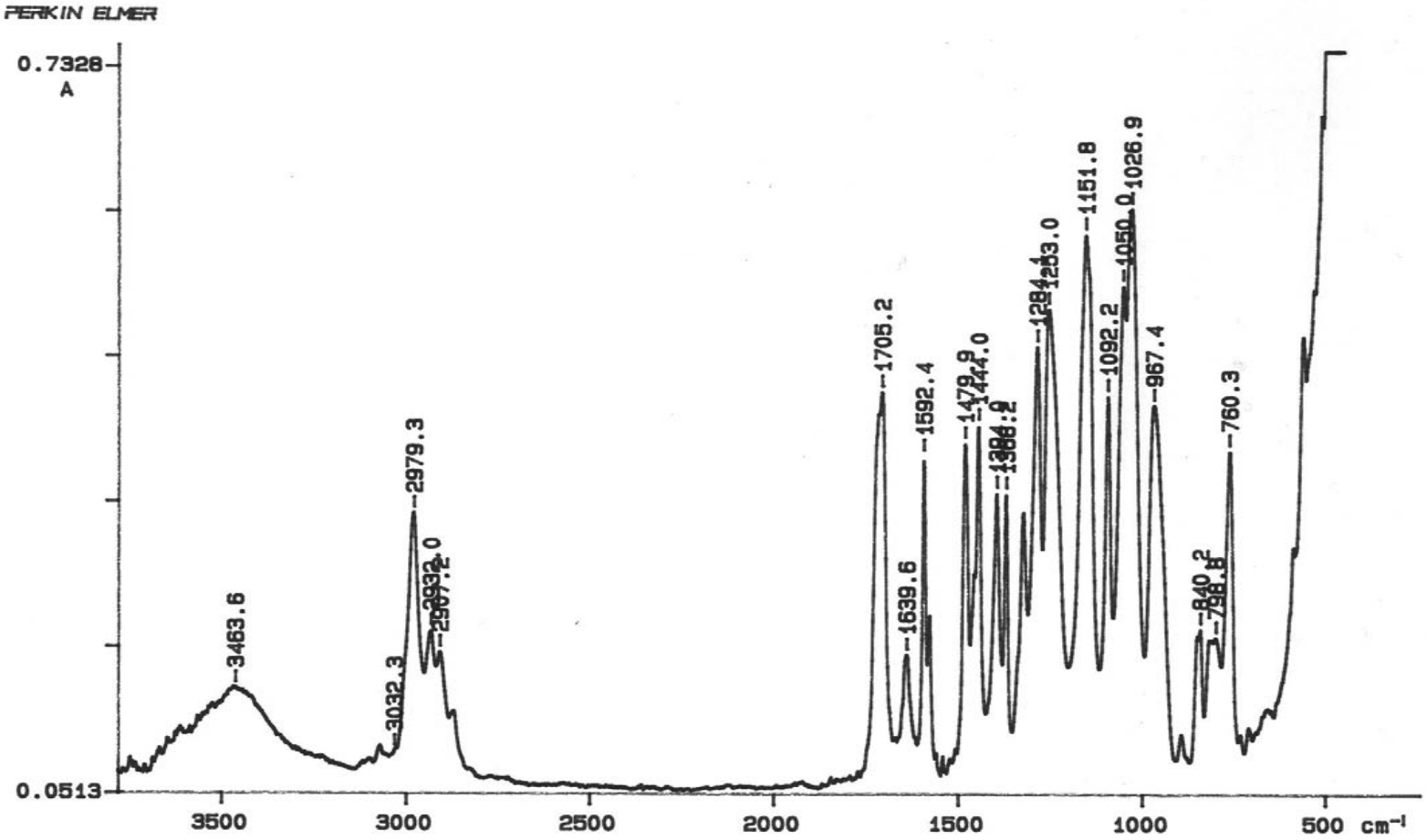

Figure 4.31. FT-IR spectrum of monomer **5a**

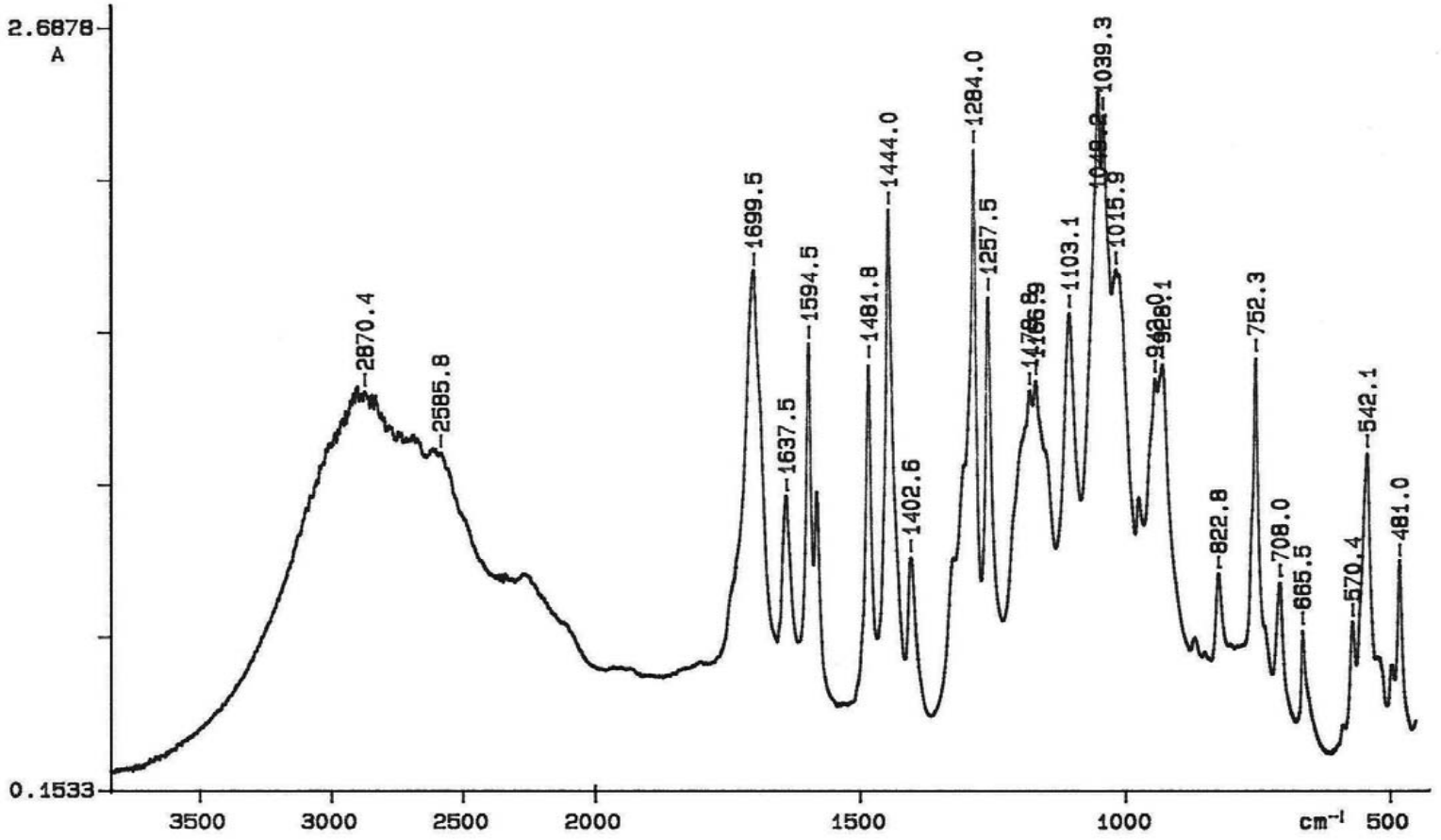

Figure 4.32. FT-IR spectrum of monomer **5b**

4.1.2. Synthesis of Monomers 6a-b from Tetraethyl 2,5-Dihydroxy-1,4-Phenylene Diphosphonate

4.1.2.1. Synthesis of Tetraethyl 2,5-Dihydroxy-1,4-Phenylene Diphosphonate. The second o-hydroxyaryl phosphonate used for the synthesis of new monomers was tetraethyl 2,5-dihydroxy-1,4-phenylene diphosphonate. It was synthesized using a similar procedure to diethyl (2-hydroxyphenyl) phosphonate (Figure 4.33).

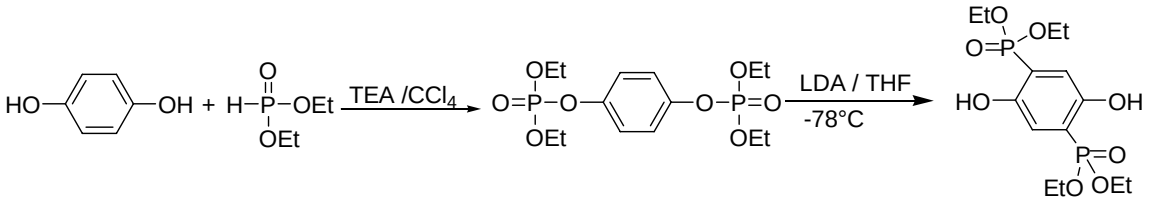

Figure 4.33. Synthesis of tetraethyl 2,5-dihydroxy-1,4-phenylene diphosphonate

In the first step, phosphate derivative of hydroquinone was obtained as colorless liquid in 72 per cent yield. This compound should be dried very well for the rearrangement step.

The ^{13}C-NMR spectrum of phosphate derivative showed characteristic peaks for ethyl carbons at 14.8 and 63.4 ppm, aromatic carbon attached to oxygen at 149.3 ppm and other aromatic carbon at 119.9 ppm (Figure 4.34).

In the ^{1}H-NMR spectrum, ethyl protons at 1.34 and 4.19 ppm, aromatic protons at 7.18 ppm were characterized (Figure 4.35).

In the second step, tetraethyl (1,4-phenylene) diphosphonate was treated with LDA in dry THF at -78^{o}C. The pure product, tetraethyl 2,5-dihydroxy-1,4-phenylene diphosphonate, was obtained as a light yellow solid after recrystalization with ethyl acetate in 86 per cent yield. It was soluble in acetone, methanol, ethanol, ether, dichloromethane, THF, CCl_4, cyclohexane and petroleum ether whereas insoluble in water and hexane.

The ^{13}C-NMR spectrum of the product showed characteristic peaks for ethyl carbons at 15.2 and 62.2 ppm, aromatic carbons attached to phosphorus atom at 114.1, 116.2 ppm (doublet), aromatic carbons attached to hydroxyl at 152.5 ppm and other aromatic carbons at 118.4 ppm (Figure 4.34).

^{1}H-NMR spectrum is characterized by ethyl protons at 1.34 and 4.19 ppm, aromatic protons at 7.10 ppm and hydroxyl protons at 9.62 ppm (Figure 4.35).

The FT-IR spectrum showed characteristic peaks for –OH, C-H, aromatic C=C, P=O and P-O-Et at 3076, 2986, 1523, 1284, 1162 cm^{-1} respectively (Figure 4.36)

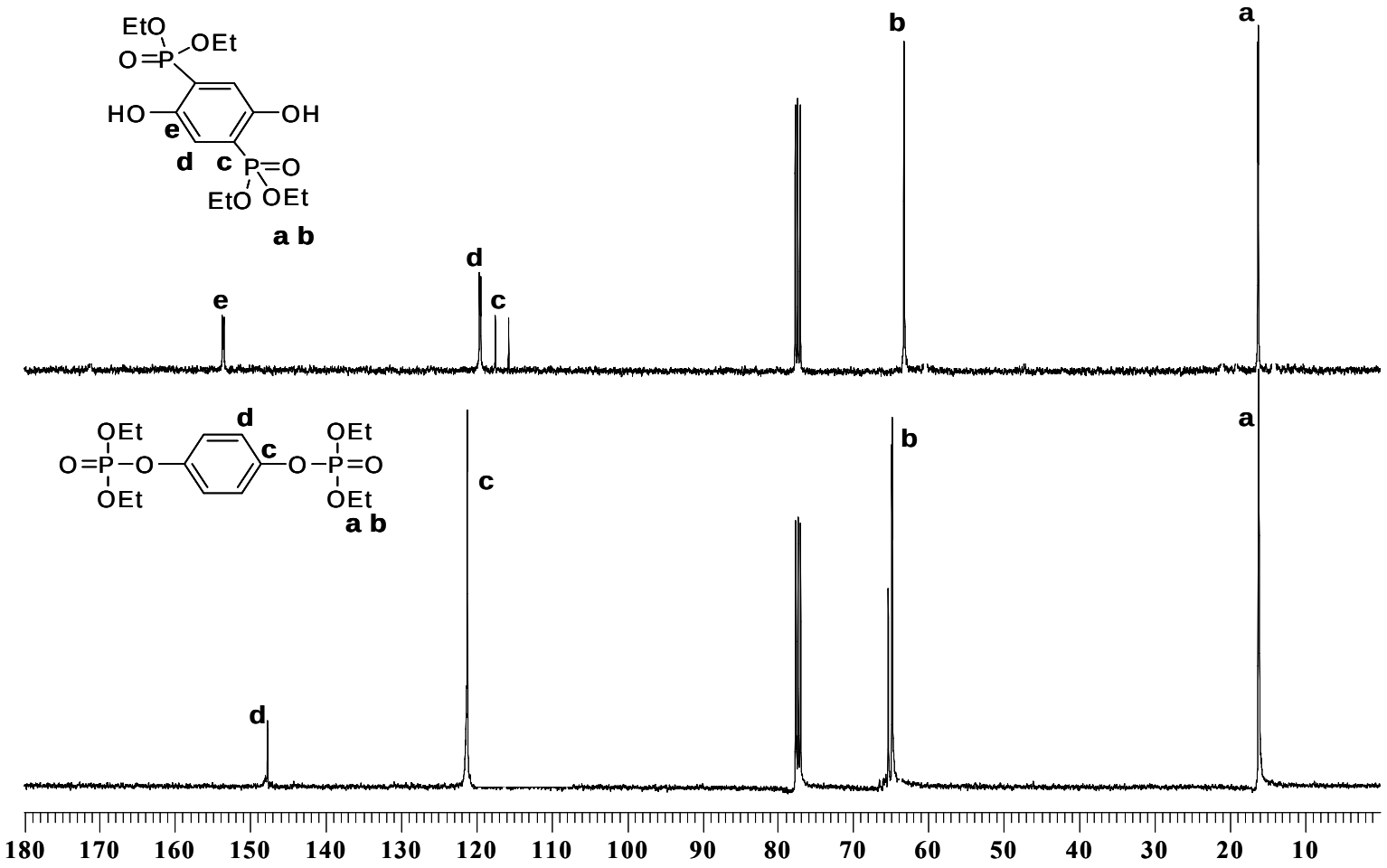

Figure 4.34. ^{13}C-NMR spectra of tetraethyl (1,4-phenylene) diphosphonate and tetraethyl 2,5-dihydroxy-1,4-phenylene diphosphonate

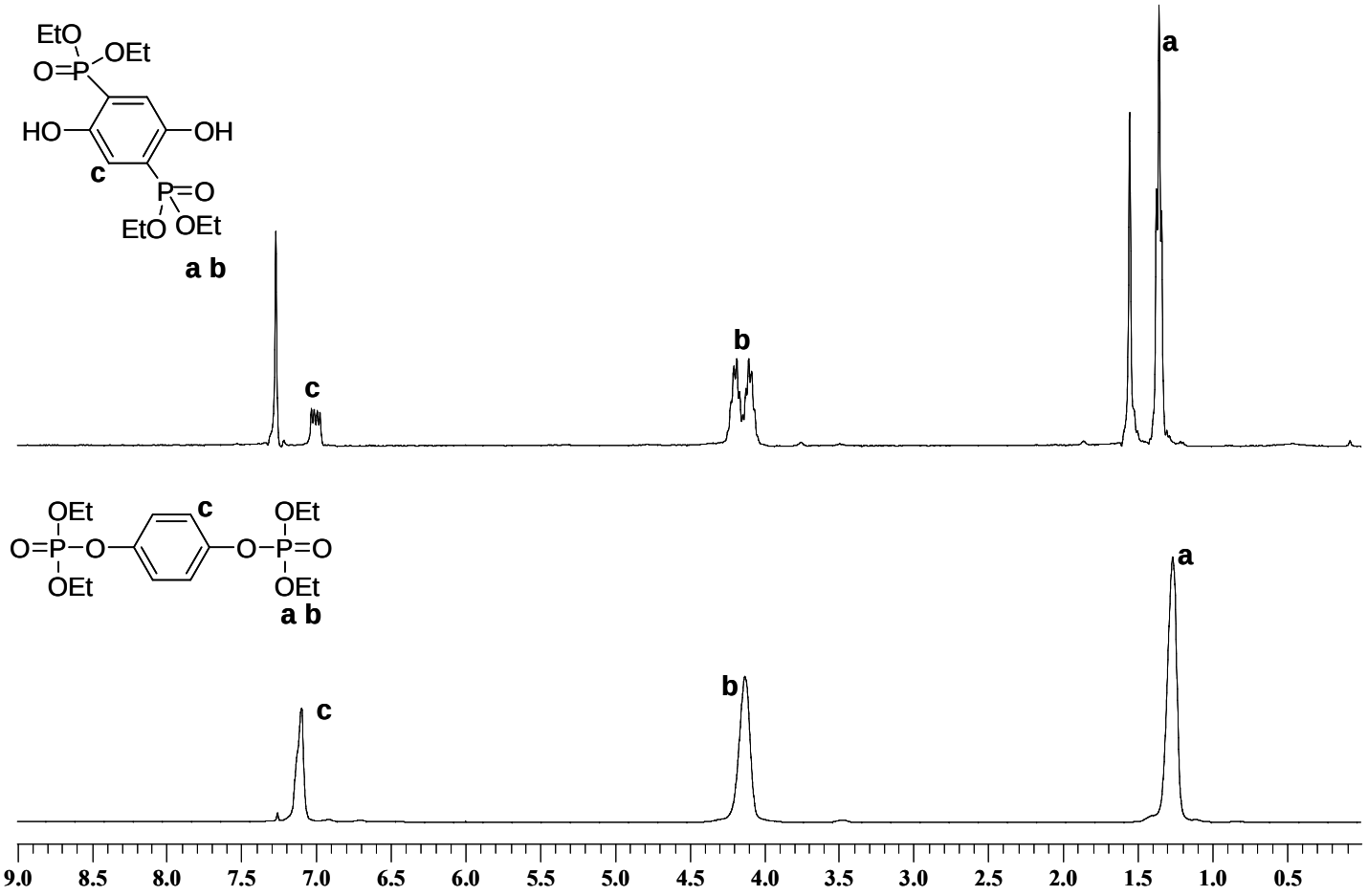

Figure 4.35. ^{1}H-NMR spectra of tetraethyl (1,4-phenylene) diphosphonate and tetraethyl 2,5-dihydroxy-1,4-phenylene diphosphonate

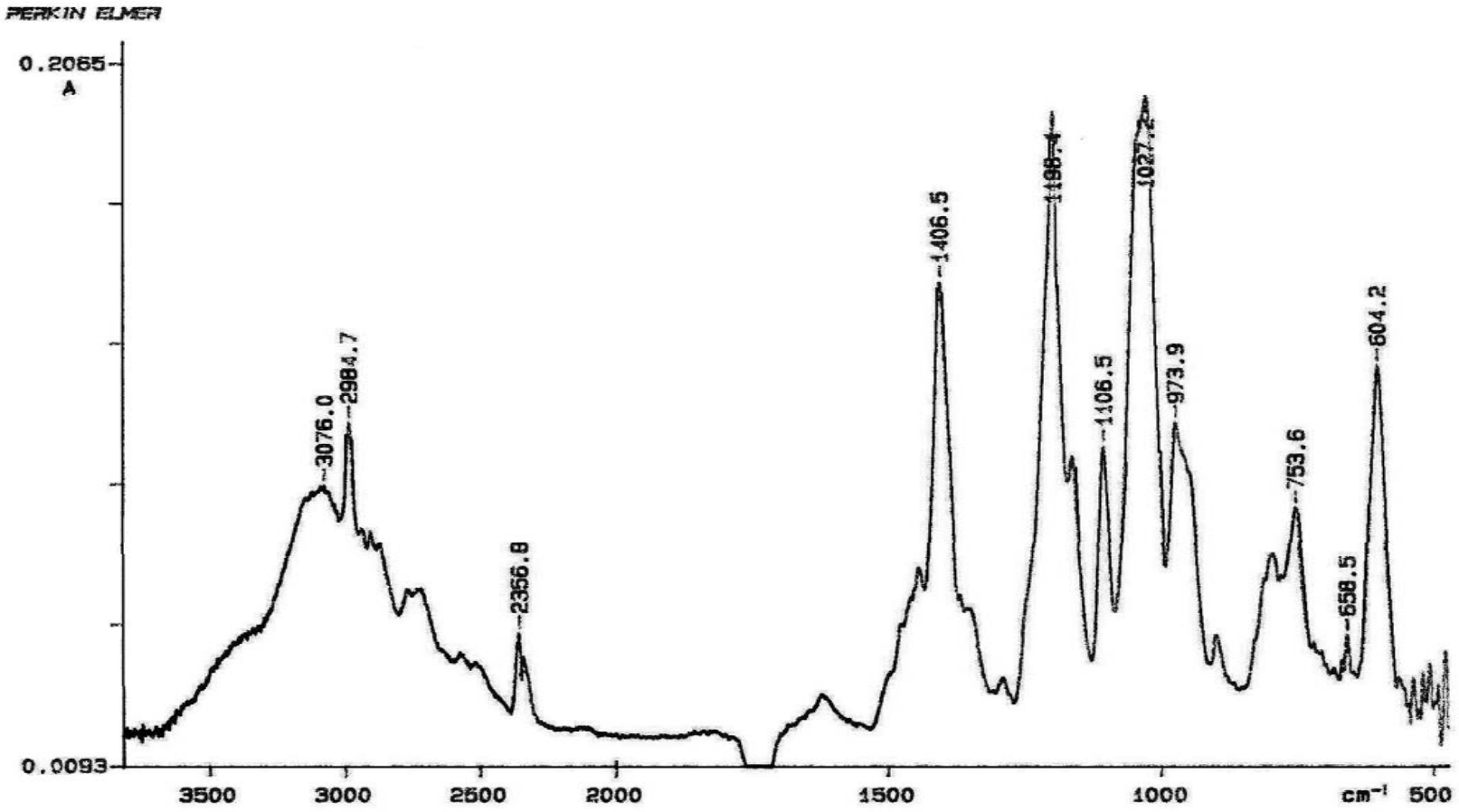

Figure 4.36. FT-IR spectrum of tetraethyl 2,5-dihydroxy-1,4-phenylene diphosphonate

4.1.2.2. Synthesis of Monomers 6a and 6b. Synthesis of monomers **6a** and **6b** involved the reaction of tetraethyl 2,5-dihydroxy-1,4-phenylene diphosphonate and TBBr and the hydrolysis of t-butyl and phosphonate ester groups (Figure 4.37).

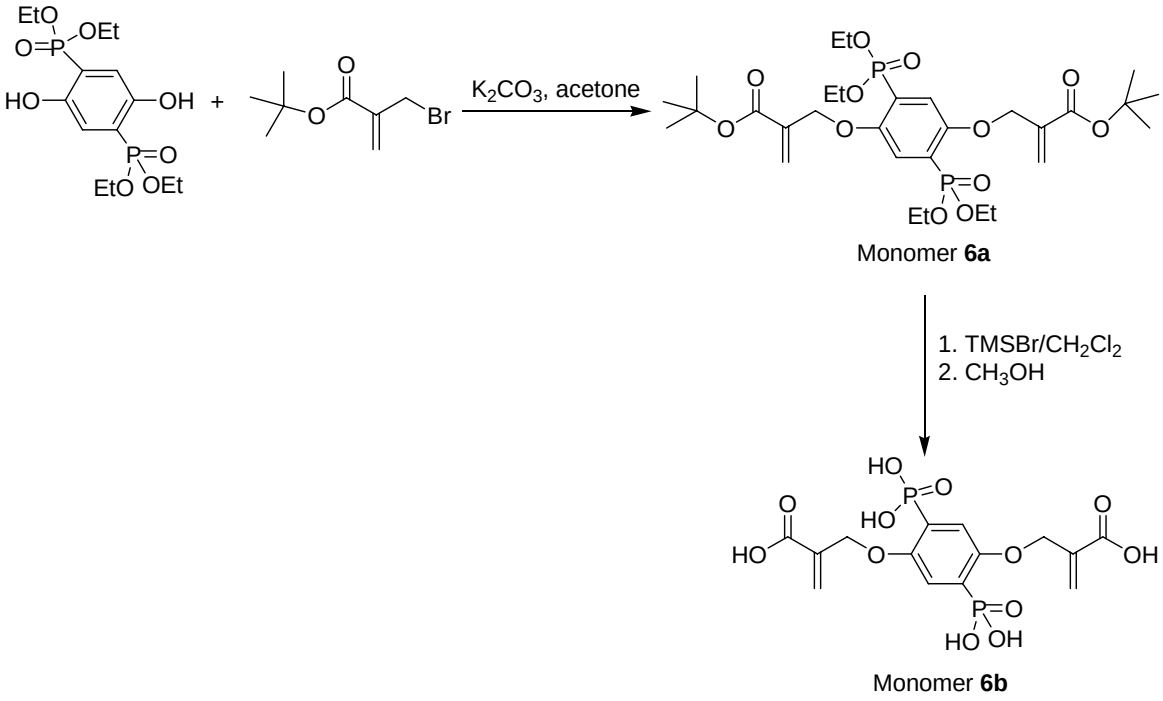

Figure 4.37. Synthesis of monomers **6a** and **6b**

The reaction of tetraethyl 2,5-dihydroxy-1,4-phenylene diphosphonate and TBBr in the presence of K_2CO_3 gave monomer **6a** which was purified by recrystallization from ether. This monomer was obtained as a white solid in 92 per cent yield with a melting point at 110 ^oC.

The ^{13}C-NMR spectrum of monomer **6a** showed characteristic peaks for ethyl carbons at 16.0 and 62.1 ppm, t-butyl carbons at 27.7 and 81.0 ppm, methylene carbon at 67.1 ppm, double bond carbons at 125.2 and 136.4 ppm, aromatic carbons attached to phosphorus atoms at 121.4, 123.2 , aromatic carbons 118.7 ppm and a carbonyl carbon at 164.1 ppm (Figure 4.38).

The ^{1}H-NMR spectrum of this monomer was characterized by ethyl protons at 1.32 and 4.13 ppm, t-butyl protons at 1.52 ppm, methylene protons at 4.76 ppm, double bond protons at 6.21 and 6.35 ppm and aromatic protons at 7.4-7.5 ppm (Figure 4.39).

The FT-IR spectrum of this monomer showed characteristic absorptions of C-H, C=O, C=C, C-O, P=O, P-O-Et groups at 2973, 1700, 1636, 1231, 1025 cm^{-1}, respectively (Figure 4.40).

The silylation of monomer **6a** with TMSBr, followed by methanolysis of the silyl derivative, gave a new diphosphonic acid monomer. Since some of t-butyl groups were also hydrolyzed, excess CF_3COOH was added dropwise in an ice bath for complete hydrolysis of carboxylic acid groups. After precipitation into ether, monomer **6b** which had both diphosphonic and dicarboxylic acid groups was obtained in 56 per cent yield. This monomer decomposed at 200 ^{o}C before melting. It was soluble in polar slovents such as water, methanol and ethanol but insoluble in ether and methylene chloride.

The ^{13}C-NMR spectrum of monomer **6b** showed the disappearance of the ethyl ester and t-butyl ester peaks at 16.0, 61.2 ppm and 27.7, 81.0 ppm that confirms the complete reaction (Figure 4.38).

In the ^{1}H-NMR spectrum of monomer **6b**, disappearance of ethyl and t-butyl protons also confirmed the hydrolysis of phosphonate and t-butyl esters (Figure 4.39).

The FT-IR spectrum showed a broad peak between 3500 and 2000 cm^{-1} due to phosphonic acid groups (Figure 4.41).

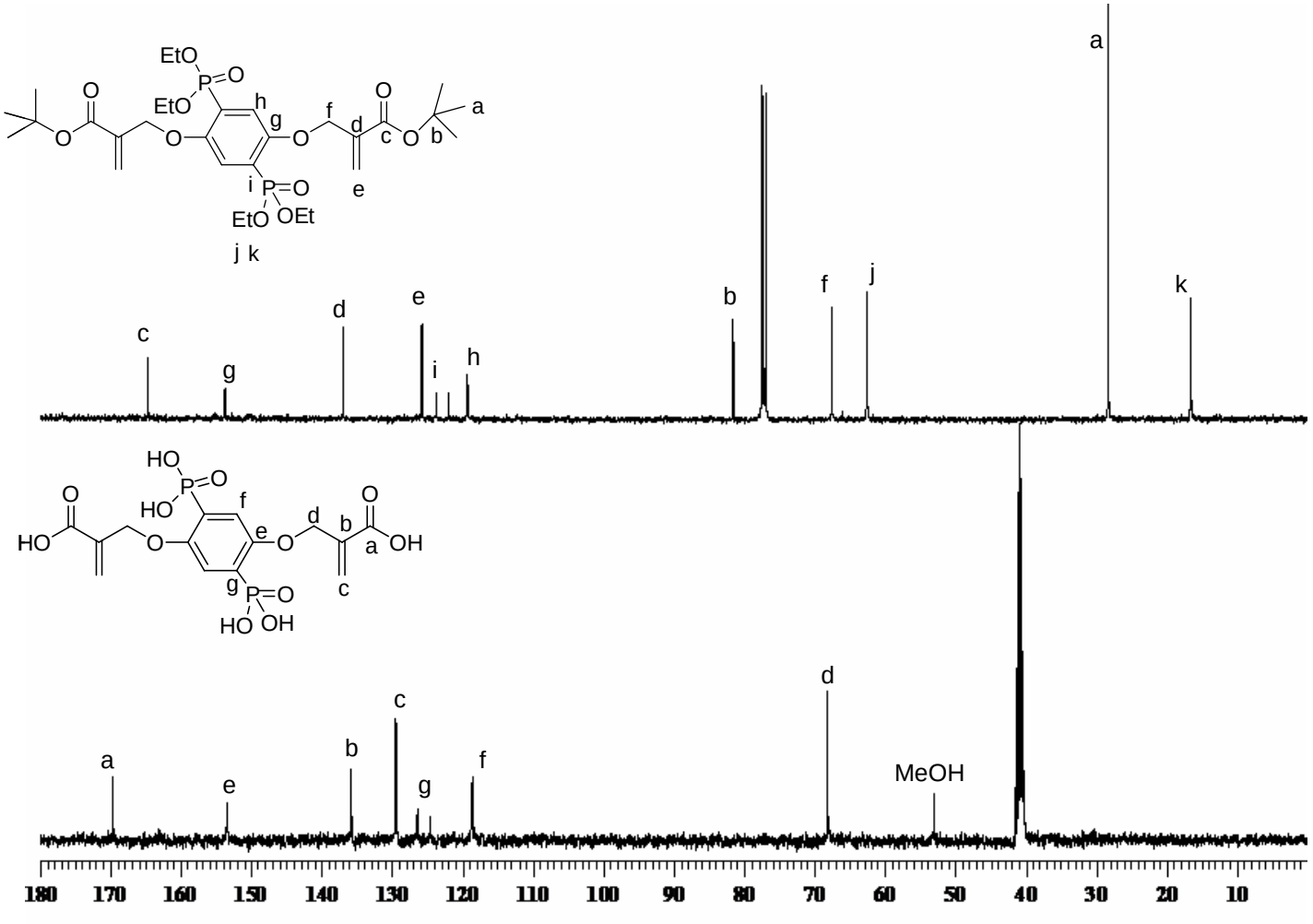

Figure 4.38. ^{13}C-NMR spectra of monomers **6a** and **6b**

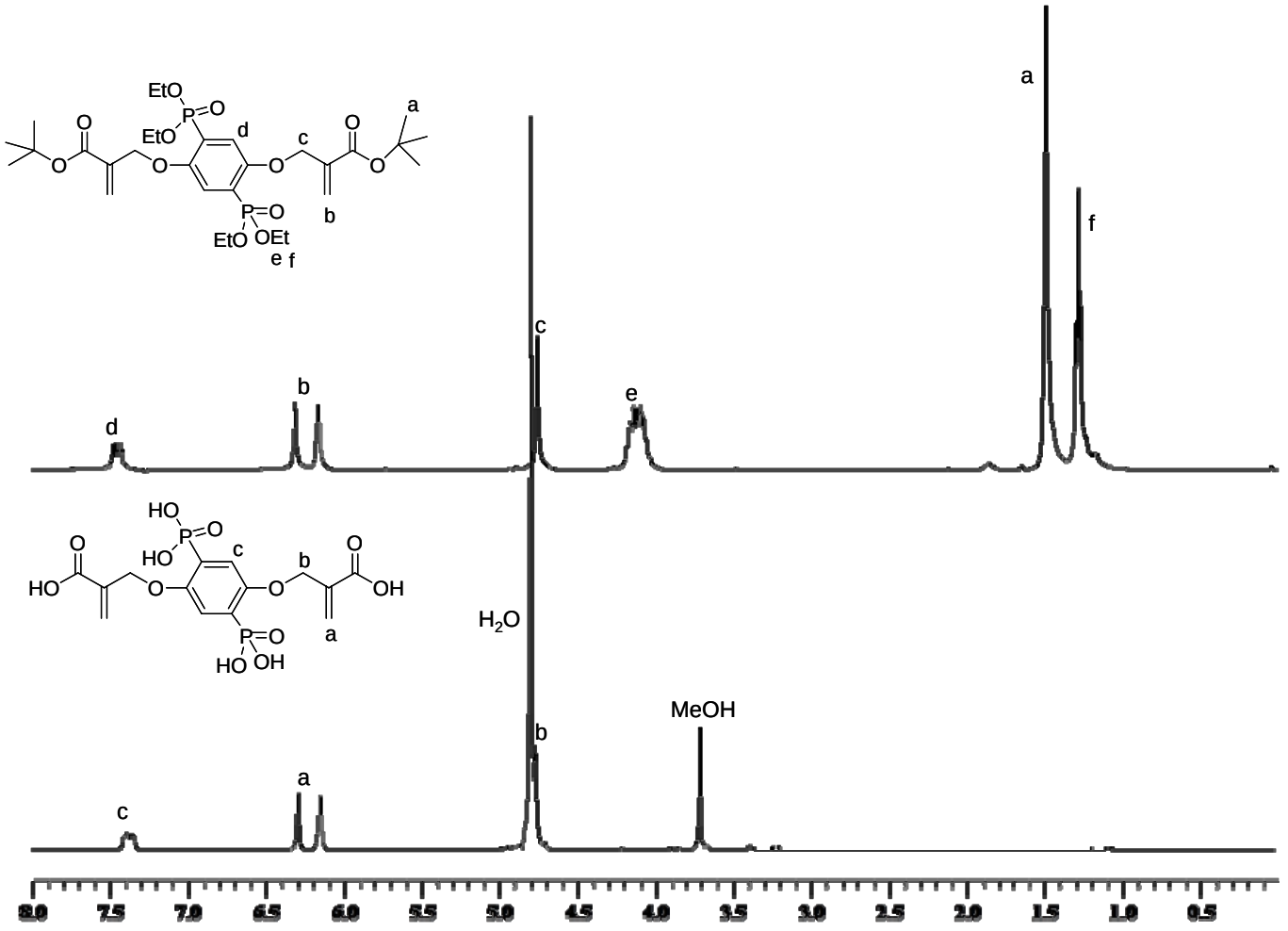

Figure 4.39. ^{1}H-NMR spectra of monomers **6a** and **6b**

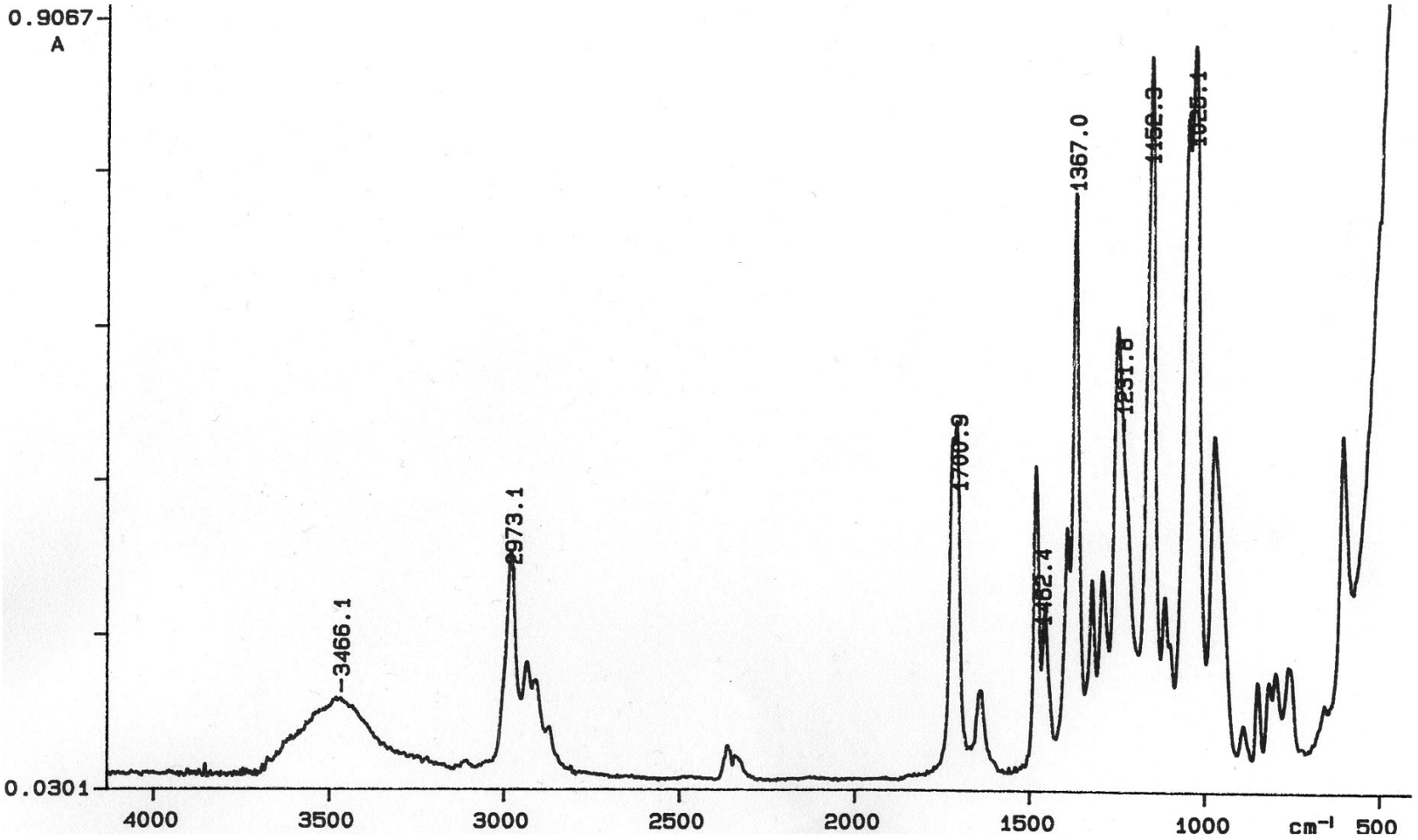

Figure 4.40. FT-IR spectrum of monomer **6a**

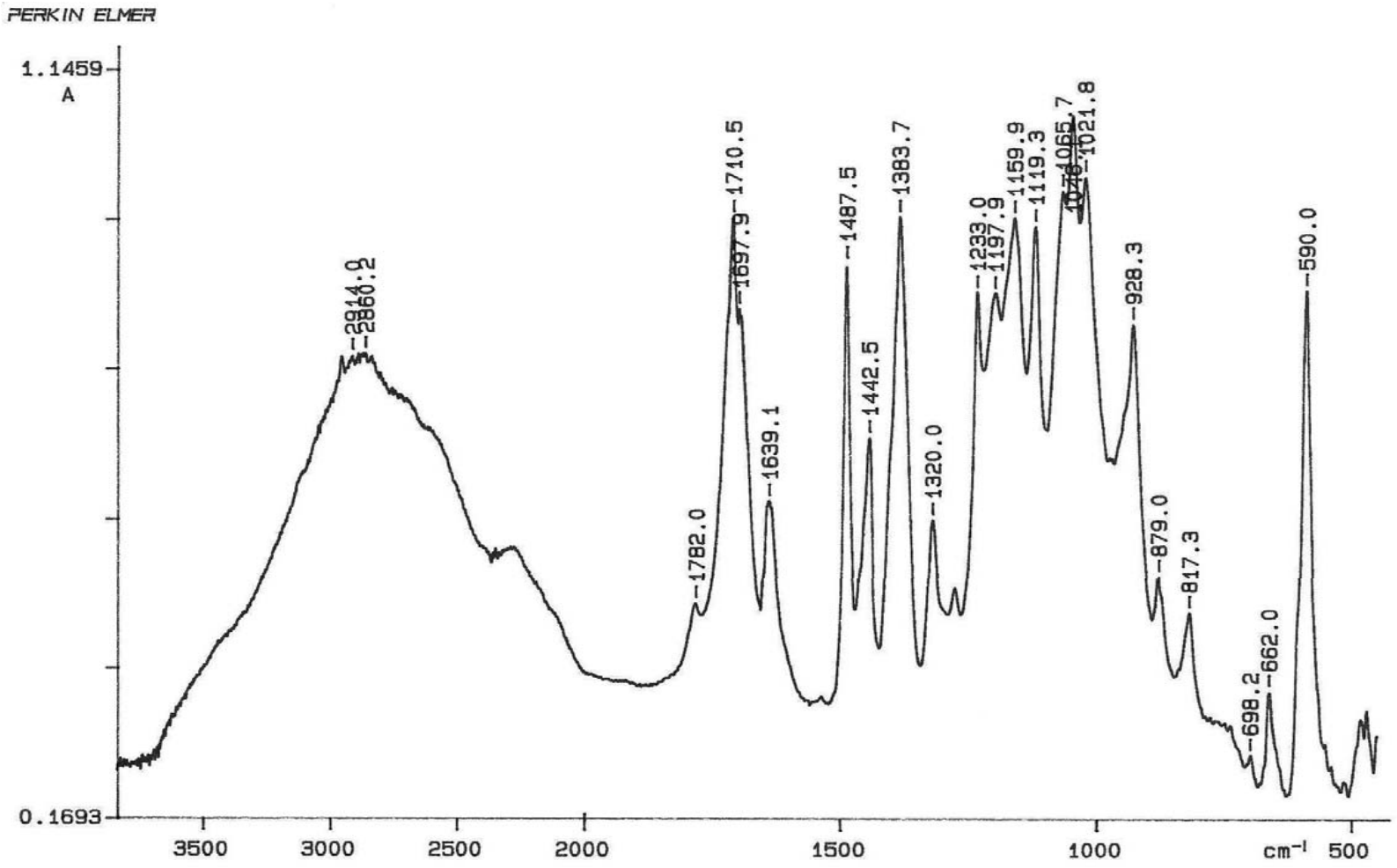

Figure 4.41. FT-IR spectrum of monomer **6b**

4.1.3. Synthesis of Monomer 7a from Dimethyl (2-hydroxyethyl) Phosphonate

A new phosphonated methacrylate (monomer **7a**) was synthesized starting from dimethyl 2-hydroxyethyl phosphonate (Figure 4.42).

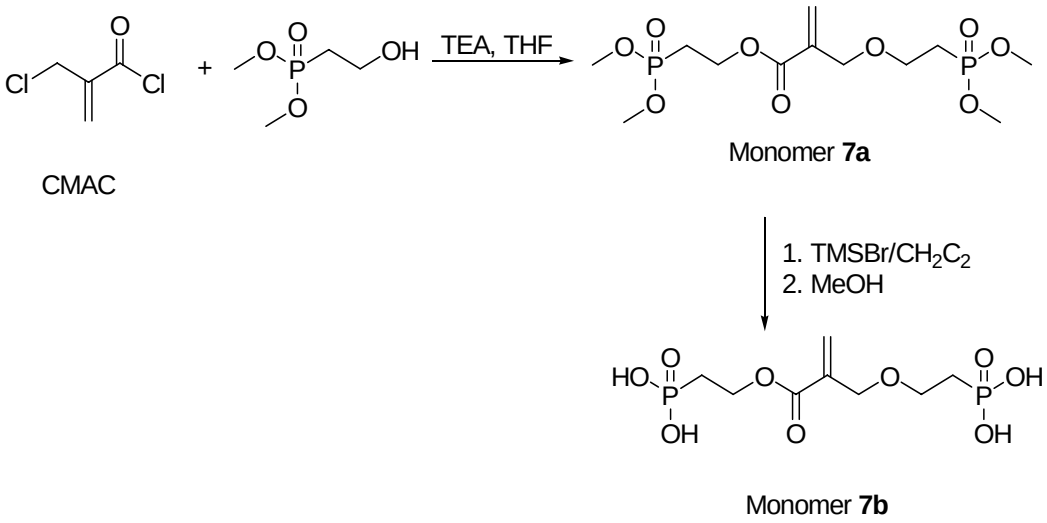

Figure 4.42. Synthesis of monomer **7a**

Synthesis of monomer **7a** was carried out by the reaction of CMAC and dimethyl (2-hydroxyethyl) phosphonate in the presence of TEA in dry THF at 55^{o}C.

The purification of this monomer with normal phase column chromatography was not successful due to its high polarity. Therefore, reverse phase column chromatography (C18) was used with starting 100 % H_2O as elutant and changing to 100% MeOH gradually. Yield after this procedure was 45 per cent.

Monomer was soluble in chloroform, acetone, THF and water, but insoluble in petroleum ether, cyclohexane and ether.

The ^{13}C-NMR spectrum of monomer **7a** showed characteristic peaks for carbons attached to phosphorus atoms at 24.4, 25.5 and 25.8, 26.9 methyl groups at 52.7, methylene carbon at ppm 58.9, 64.7, 69.1, double bond carbons at 126.8 and 136.7 ppm, and a carbonyl carbon at 165.4 ppm (Figure 4.43).

The ^{1}H-NMR spectrum of this monomer was characterized by methylene protons attached to phosphorus atoms at 2.17 ppm, methyl protons at 3.75 and 4.12 ppm, methylene protons at 4.21 and 4.41 ppm, double bond protons at 5.93, 6.33 ppm (Figure 4.44).

The FT-IR spectrum of monomer **7a** showed characteristic absorptions of C-H, C=O, C=C, P=O, C-O and P-O-Et groups at 2957, 1721, 1640, 1184, 1028 and 1249 cm^{-1}, respectively (Figure 4.45).

Hydrolysis of the phosphonate groups of monomer **7a** will give a new diphosphonic acid-containing monomer (**7b**) which may have applications in dental adhesive systems. We expect to perform synthesis of this monomer in future work.

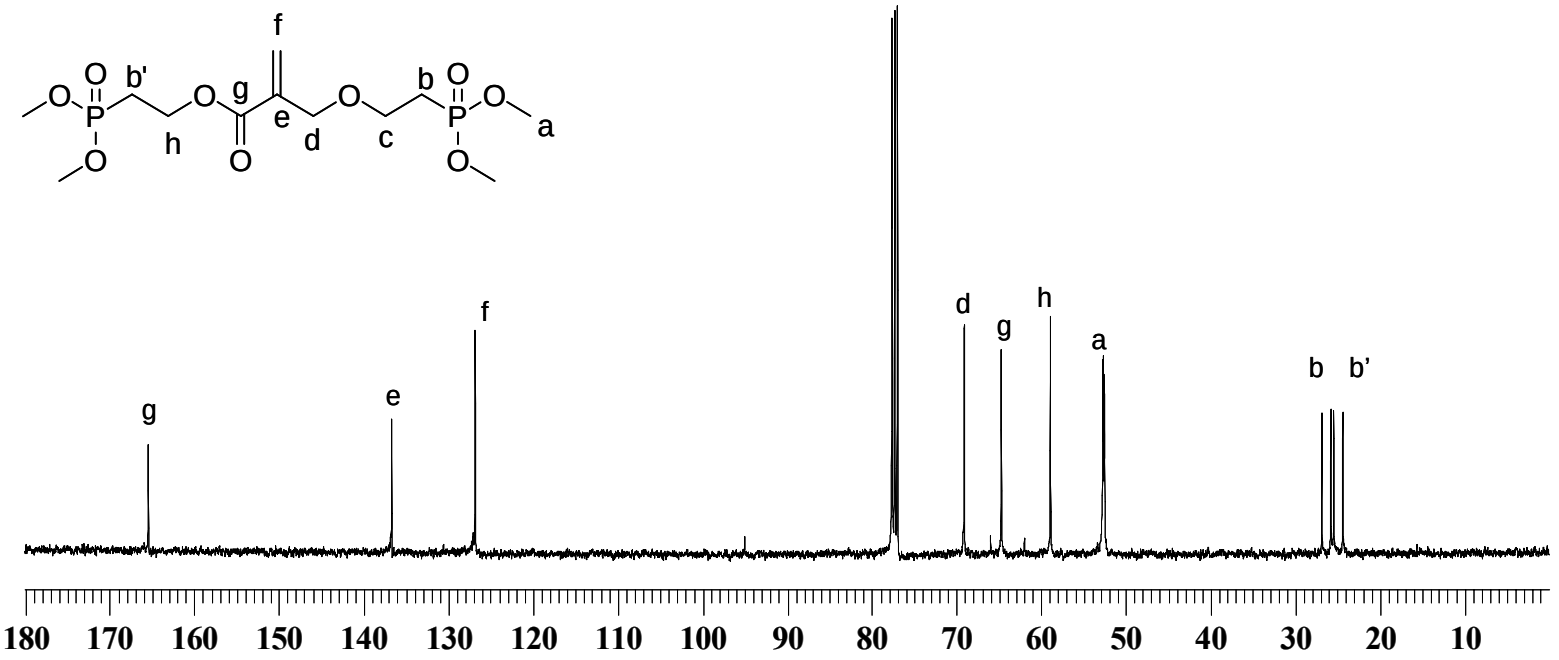

Figure 4.43. ^{13}C-NMR spectrum of monomer **7a**

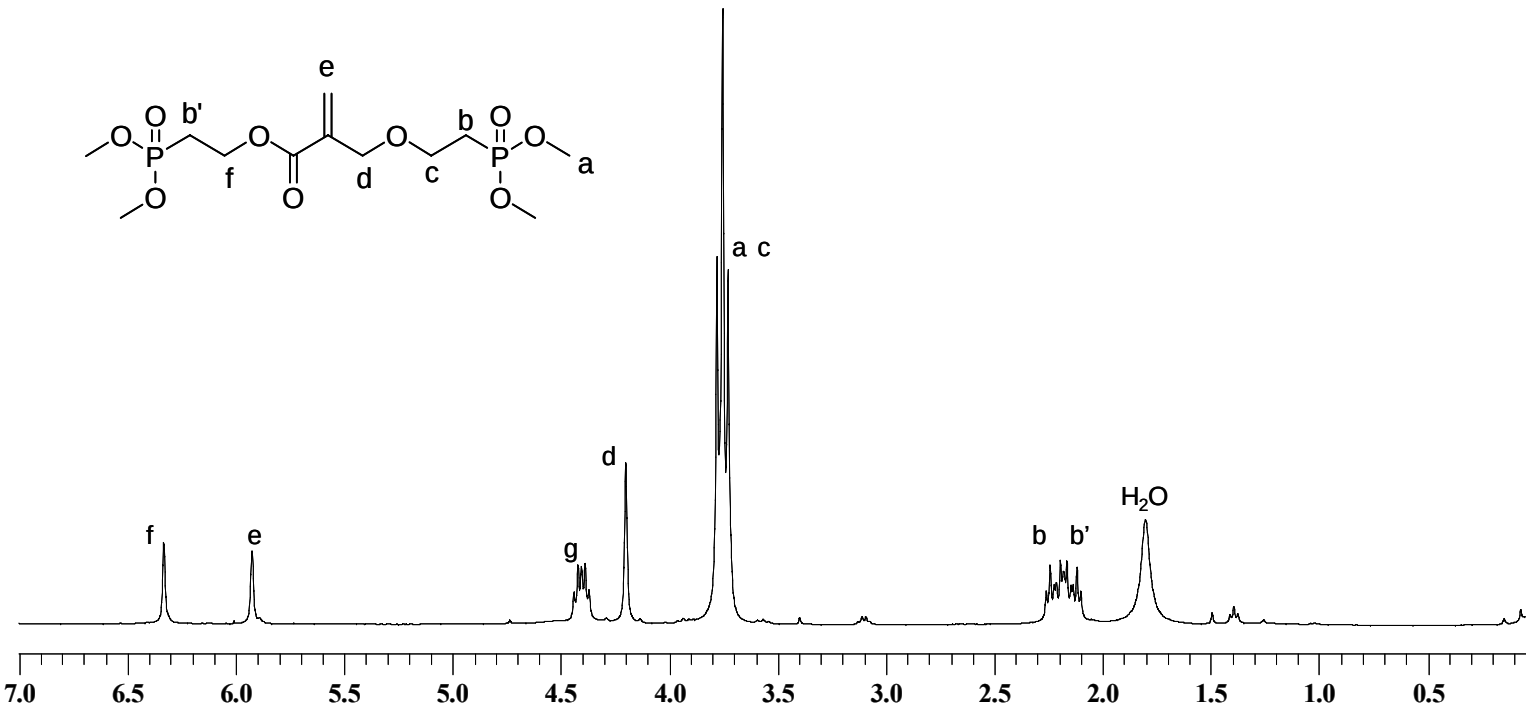

Figure 4.44. ^{1}H-NMR spectrum of monomer **7a**

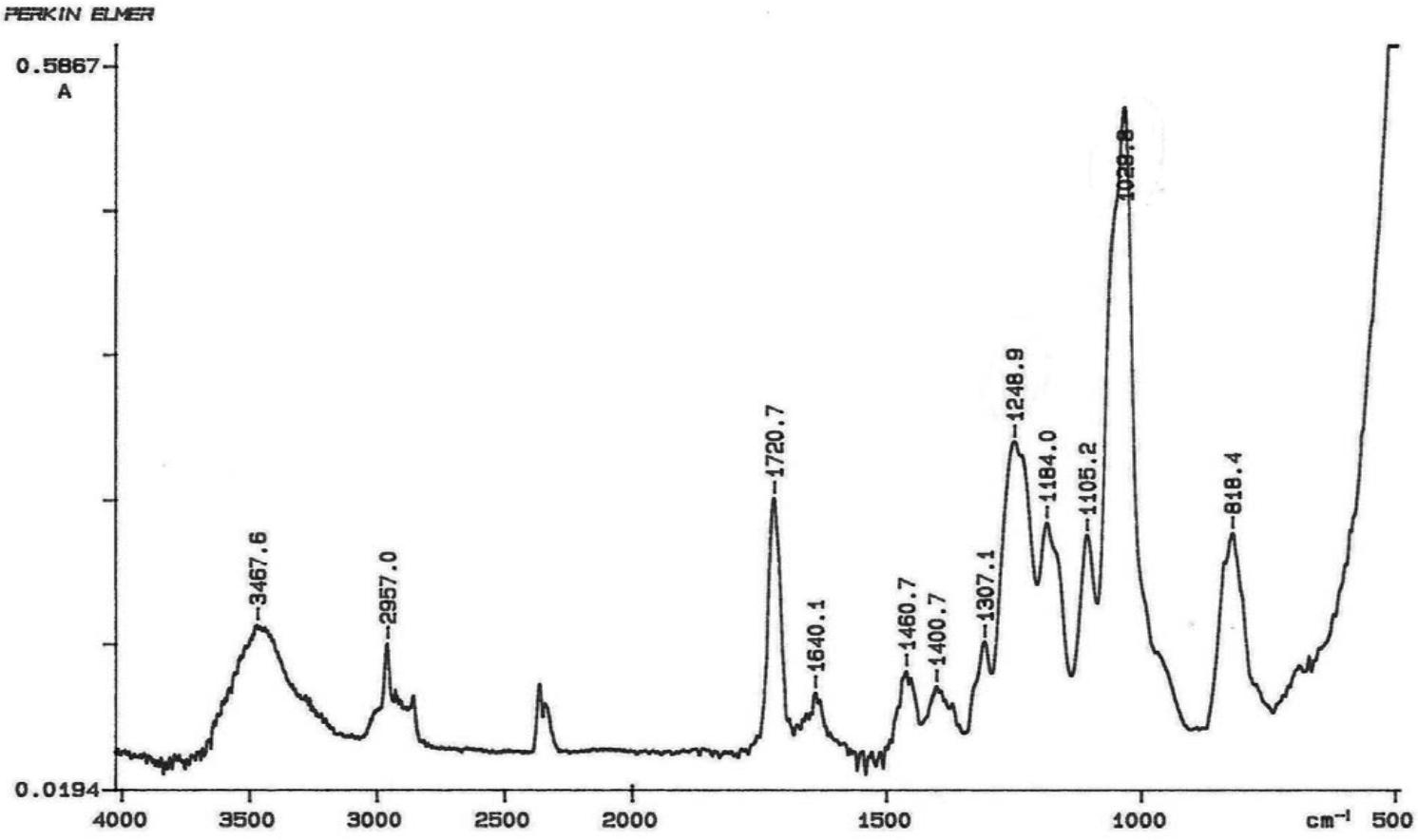

Figure 4.45. FT-IR spectrum of monomer **7a**

4.2. Evaluation of Synthesized Monomers

4.2.1. Polymerizations of Monomers 1a-3a

4.2.1.1.Photopolymerizations of Monomers **1a-3a**. The polymerization behaviors of the monomers were investigated using photo-DSC. All the polymerizations were performed under identical conditions of initiator concentration (2.0 mol%), UV light intensity (20 mW/cm^2) and temperature (40 ^oC).

First, the homopolymerization behavior of the synthesized monomers was investigated and compared with those of the commercial monomers such as GDMA (glycerol dimethacrylate), Bis-GMA (2,2-bis[4-(2-hydroxy-3-methacryloxyprop-1-oxy)phenyl]propane) and HEMA (2-hydroxyethyl methacrylate). The rate versus time and conversion versus time curves are shown in Figures 4.46 and 4.47.

Monomer **1a** showed very low maximum rate of polymerization (0.00073 s^{-1}) and conversion (10.3 %). Monomer **2a** was more reactive than monomer **1a** with a maximum rate of polymerization of 0.0051 s^{-1} but it also gave very low conversion (11.8 %). These monomers were less reactive than Bis-GMA (0.044 s^{-1}), HEMA (0.028 s^{-1}) and GDMA (0.043 s^{-1}) polymerized under the same conditions. We attributed this behavior to the presence of a bulky Bisphenol A and phenolic groups close to the double bond. Hydrolysis of the ethyl groups of these monomers (to produce monomers **1b** and **2b**) was expected to result in increased reactivity. However monomers **1b** and **2b** did not polymerize at all. This may be due to residual (2-hydroxyphenyl) phosphonic acid present due to ester cleavage reaction during TMSBr hydrolysis, which may act as a polymerization inhibitor. Monomer **3a** showed much higher maximum rate of polymerization (0.084 s^{-1}) and conversion (87.2 %) than monomers **1a** and **2a**. Unexpectedly, this monomer which is a monomethacrylate is more reactive than the dimethacrylate monomers, Bis-GMA (51.6 %) and GDMA (57.2 %). The reason for the high rate of polymerization is not clear but may be attributed to hydrogen bonding capability and flexibility of this monomer. Although this monomer has a rigid phenolic structure, this is far from the double bond. In order to see crosslinking tendency of monomer **3a** we studied its bulk and solution polymerization.

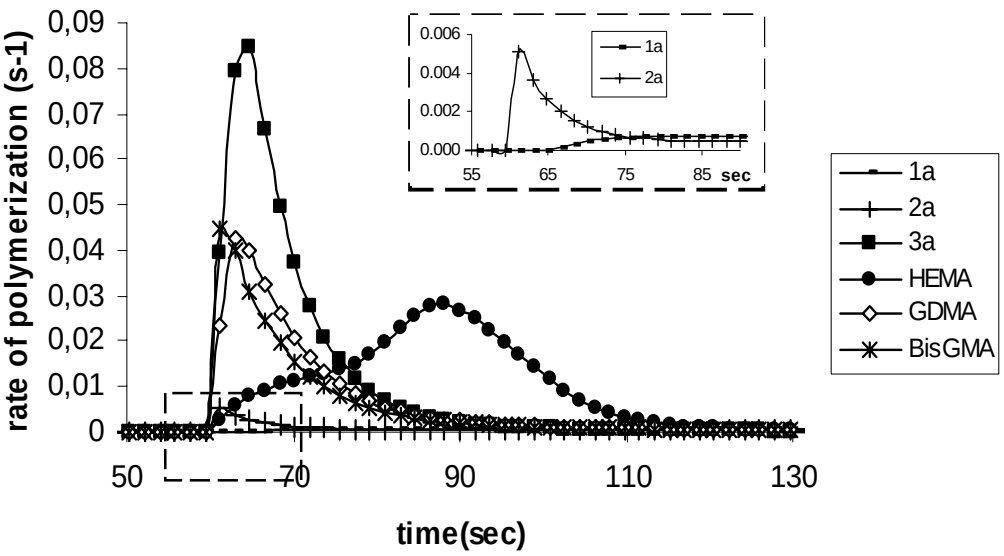

Figure 4.46. Rate of polymerization versus time graph of monomers **1a**, **2a**, **3a**, HEMA, GDMA and BisGMA

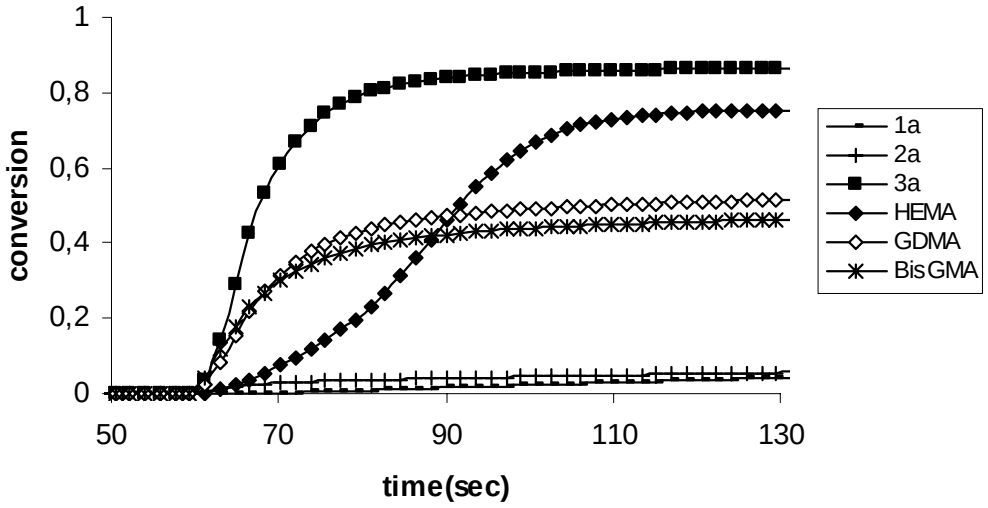

Figure 4.47. Conversion versus time graph of monomers 1a, 2a, 3a, HEMA, GDMA and BisGMA

Copolymerization behaviors of synthesized monomers (of 10 mol %) with BisGMA were investigated. Figure 4.48 shows the rate versus time graph for BisGMA:monomer (90:10) mixtures. It was observed that the addition of monomer **3a** has significant effect on the rate of polymerization (0.068 s^{-1}) value of rigid, very viscous, H-bonding BisGMA (0.044 s^{-1}). The incorporation of phosphorus containing monomers **1a**, **1b**, **2a** and **2b** resulted in a decrease of polymerization rate (0.035 s^{-1}, 0.014 s^{-1}, 0.033 s^{-1} and 0.028 s^{-1}). This may be due to steric effects of phosphorus groups in the propagation reaction.

Conversion versus time graph of copolymerizations is shown in Figure 4.49. Similarly, the addition of 10 mol % monomer **3a** (80.5 %) increased the conversion of BisGMA (51.6 %). However, significant increases in BisGMA:monomer **1a**, **2a** and **2b** (69.2 %, 69.4 % and 62.5 %) mixtures and similar conversion in BisGMA:monomer **1b** (51.5 %) were observed when compared to conversion of BisGMA. The higher conversions were probably due to a decrease in viscosity of Bis-GMA by the addition of monomers **1a**, **2a** and **2b**.

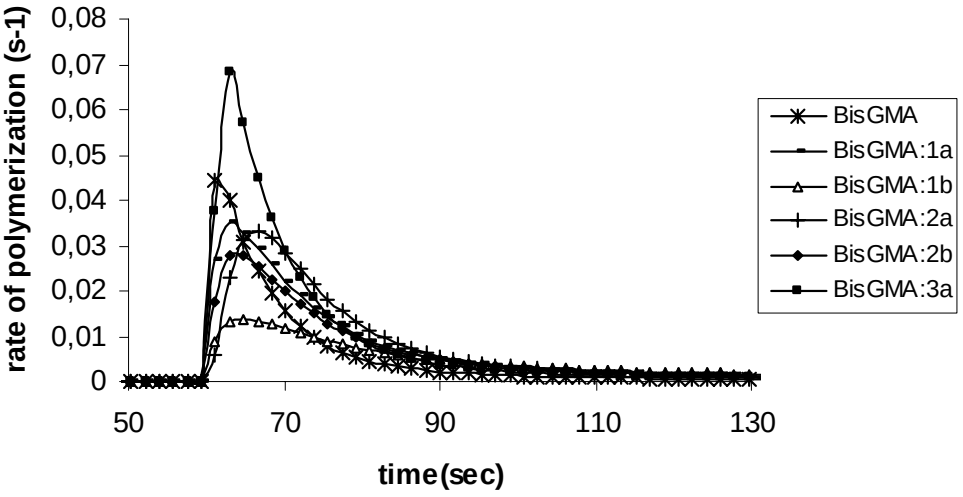

Figure 4.48. Rate of polymerization versus time graph for the mixtures of Bis-GMA containing 10 mol % monomer (**1a**-**3a**)

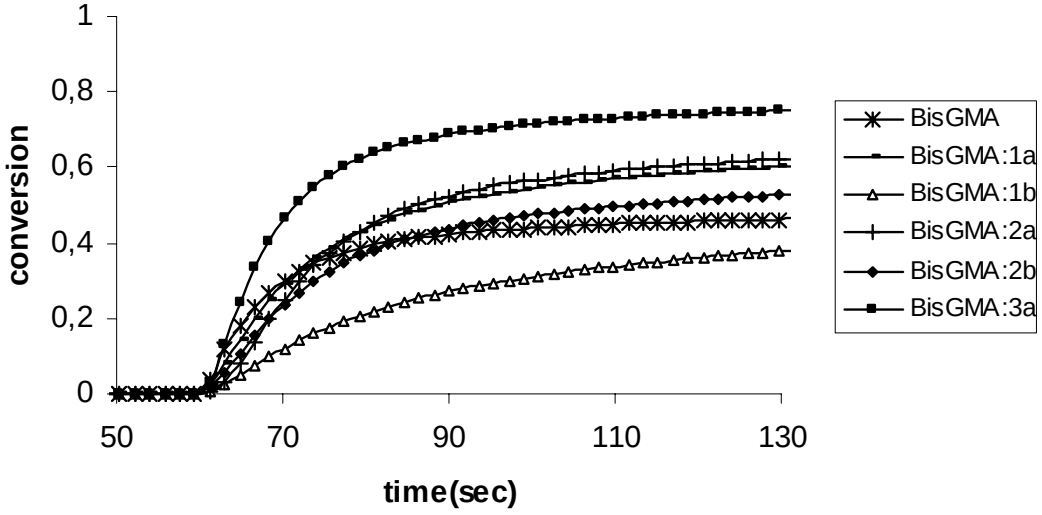

Figure 4.49. Conversion versus time graph for the mixtures of Bis-GMA containing 10 mol % monomer (**1a**-**3a**)

4.2.1.2. Polymerization of Monomer 3a. Bulk and solution polymerizations of monomer **3a** were carried out with AIBN and V-50 at 60 ^{o}C (Table 4.1). This monomer polymerized very fast to give crosslinked polymers.

Table 4.1. Bulk and solution polymerization results of monomer **3a**

[M]	[I] (10^{-2})	Solvent	Time (min)	Mw/Mn
3.0	1.0[a]	water	15	crosslinked
1.0	1.0[a]	water	40	crosslinked
b	c	-	< 25	crosslinked

a: V-50, b: bulk polymerization, c: amount of initiator (AIBN) was 3.0 wt% of the monomer

To remove the residual monomers, the polymers were swelled in CH_2Cl_2 and excess CH_2Cl_2 was decanted After repeating this procedure 3 times the polymer was dried. In the FTIR spectrum of the crosslinked polymer **3a**, the disappearance of band at 1635 cm^{-1} (assigned to the C=C stretching) was observed (Figure 4.50). The DSC spectrum showed no glass transition temperature in the temperature range of 25-160 ^{o}C.

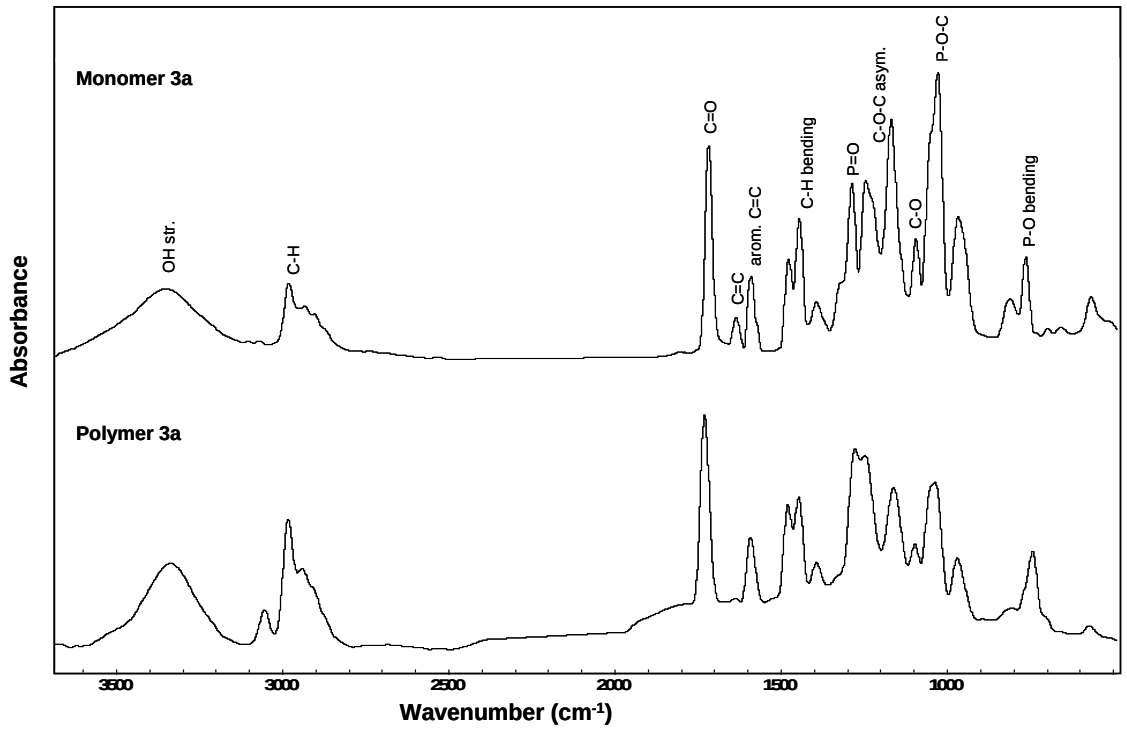

Figure 4.50. FT-IR spectra of monomer **3a** and its polymer

The thermal stability and thermal degradation behavior of the crosslinked polymer **3a** were investigated by thermogravimetric analysis (TGA) under nitrogen (Figure 4.51). The TGA spectrum of the crosslinked poly-**3a** showed degradation starting around 275 ^{o}C, with char yield of 30 % at 550 ^{o}C.

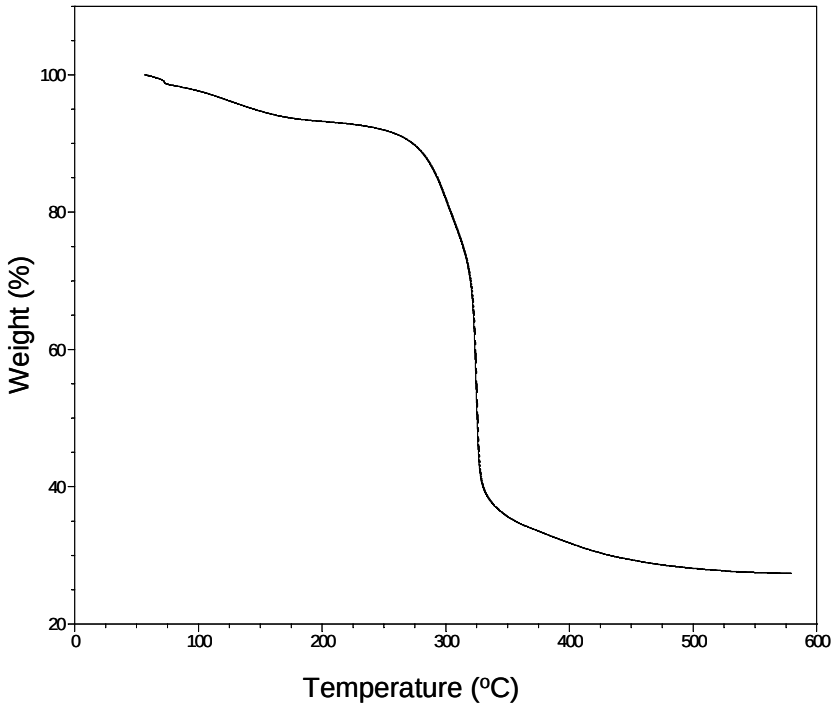

Figure 4.51. TGA curve of polymer **3a**

4.2.2. Acidity and Interactions of Monomers 1b and 2b with Hydroxyapatite

The aqueous solutions of monomers **1b** and **2b** (1 wt% in water) were acidic with pH values of 2.37 and 1.40, respectively. These values were higher than pH of 1 wt % aqueous phosphoric acid solution (pH=1.17) but in the range of acidity expected from a mild self-etching dental adhesive monomer (pH around 2.0). The addition of 30 mg hydroxyapatite (HAP), a model compound for dentin and enamel, to the solutions of monomers **1b** and **2b** resulted in an increase in the pH value from 2.37 to 4.59 for monomer **1b** and from 1.40 to 4.13 for monomer **2b**, respectively. The phosphonic acid groups of monomers can remove the smear layer, demineralize the dentin and enamel, and diffuses into collagen fibrils.

The interaction of monomers **1b** and **2b** with HAP was investigated using FTIR spectrometer. Pure monomers showed the OH peak of POOH at around 2500–2000 cm^{-1}. The C=O and P=O stretching vibrations are at ~ 1720 and ~ 1200 cm^{-1} respectively,

whereas P-O stretching bands are at ~ 1000 and ~ 925 cm^{-1} and finally the peaks around 650-450 cm^{-1} are due to P-O bending modes of POOH.

In HAP, symmetric and antisymmetric P-O stretching modes appear between 1020 and 960 cm^{-1} and antisymmetric P-O bending modes as two distinct peaks are in the 700 - 500 cm^{-1} region [93].

D'Andrea and Fadeev proposed that the reduction in the sharp peak at 3570 cm^{-1} (OH from the lattice of HAP) was due to changes in the crystalline structure and bulk modification of the HAP matrix [94]. In the monomer **1b** – HAP mixture, the same band remained unchanged at 3564 cm^{-1} (Figure 4.52). The reason might be i) ion-exchange adsorption of monomer **1b** on the HAP surface ii) formation of a surface complex iii) chemical reaction of monomer **1b** with the ions in HAP to form a new phase that precipitates out of solution [95].

On the other hand, in the monomer **2b** – HAP mixture, P=O (~ 1200 cm^{-1}) and P-O (~ 1000 and ~ 925 cm^{-1}) stretching vibrations showed a decrease in intensity which is an indication of an interaction between the phosphonic acid functional groups and the calcium ions of the HAP (Figure 4.53). A new band appeared at 1042 cm^{-1} which was assigned to the phosphonate salt indicating the interaction involves bonding of Ca ions with the $P\text{-}O^-$ ions of the monomer [96]. In addition, the vanishing of the 3570 cm^{-1} band in the monomer **2b** – HAP mixture allowed us to propose that monomer **2b** decalcify the HAP.

In dentistry, while some acids are used to demineralize HAP, some other acids are used to adhere or bind to human calcified tissues [71]. We can see that monomer **2b** is of the former class while monomer **1b** apparently has the highest chemical bonding efficacy.

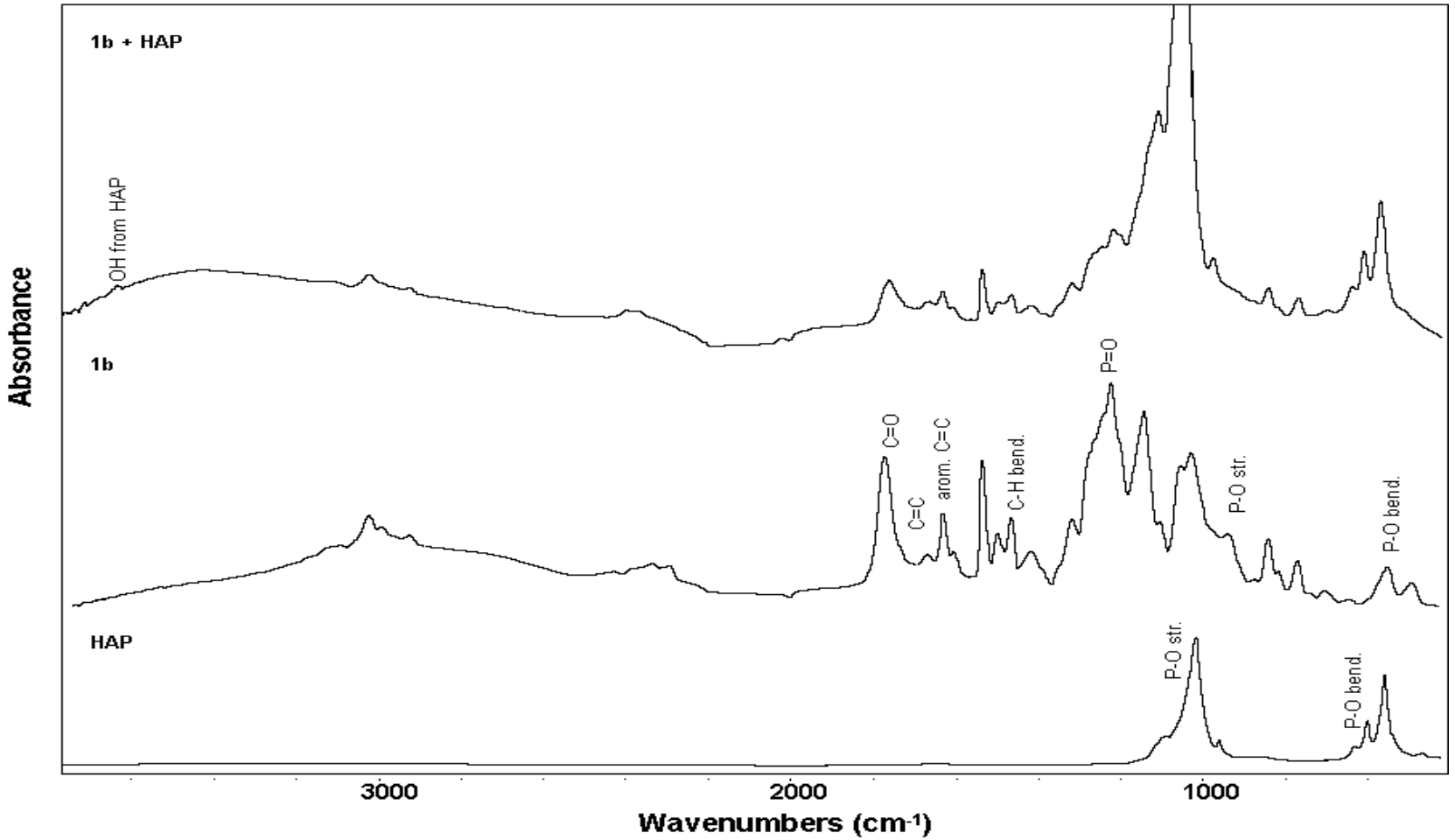

Figure 4.52. FTIR spectra of HAP, monomer **1b** without HAP and 10 mg HAP added monomer **1b**

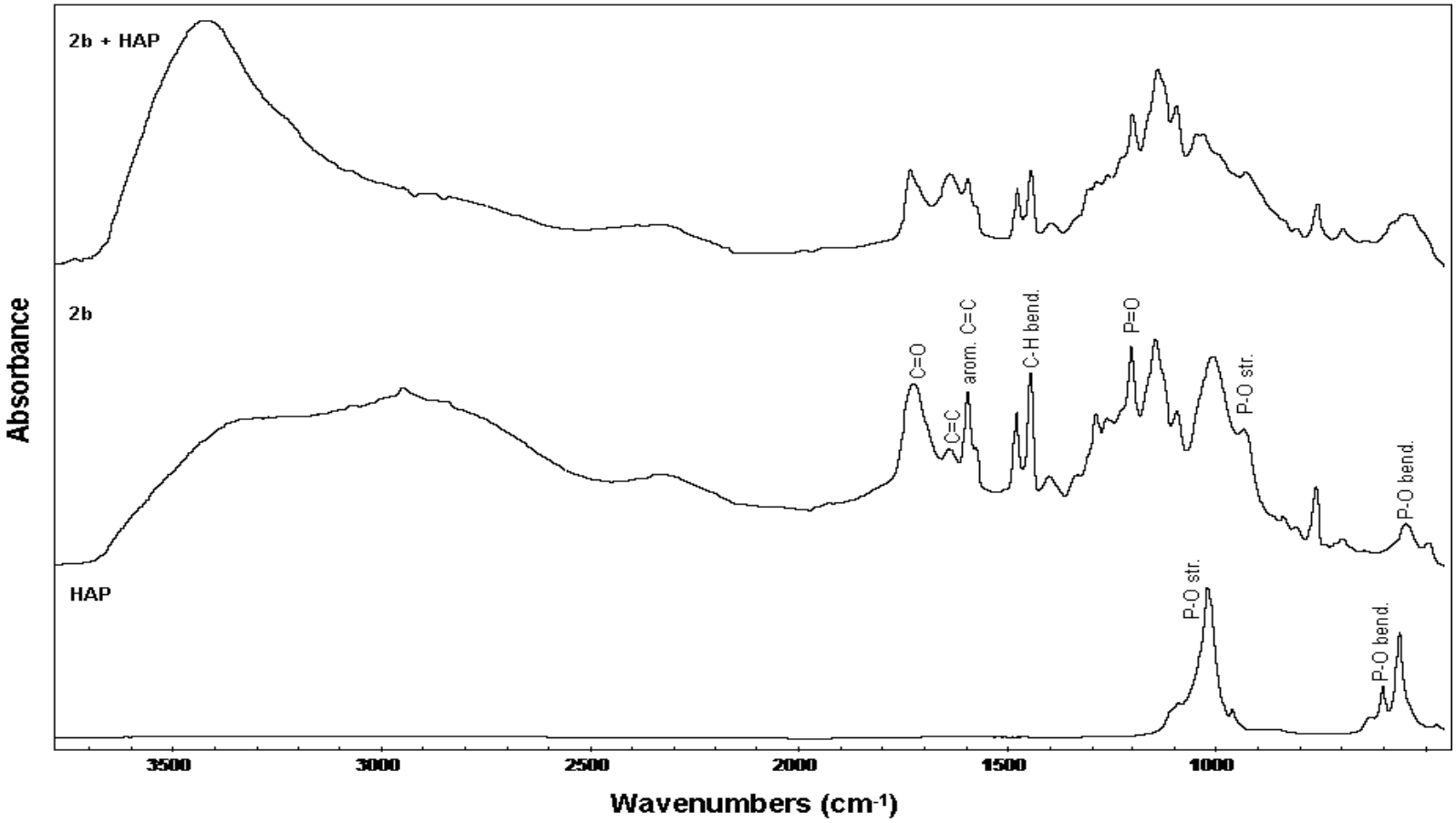

Figure 4.53. FTIR spectra of HAP, monomer **2b** without HAP and 10 mg HAP added monomer **2b**

4.2.3. Photopolymerization of Monomer 4a

The reactivity of monomer **4a** in photopolymerization was investigated using photodifferential scanning calorimeter (photo-DSC). All polymerizations were performed under identical conditions of initiator concentration (2.0 mol per cent), UV light intensity (20 mW/cm^2) and temperature (40 ^oC).

Figure 4.54 shows the photopolymerization rates of monomer **4a,** BisGMA, GDMA and HEMA. The rate of polymerization of monomer **4a** (0.026 s^{-1}) was very similar with HEMA (0.028 s^{-1}) but lower than GDMA (0.043 s^{-1}) and BisGMA (0.044 s^{-1}). This behavior can be due to the presence of bulky phenolic groups that are close to the double bond.

Conversion versus time graph of monomer **4a,** BisGMA, GDMA and HEMA is shown in Figure 4.55. Compared with commercial dental monomers, BisGMA (51.6 %) and GDMA (57.2 %) which contain two double bonds, monomer **4a** (69.9 %) has the highest conversion value.

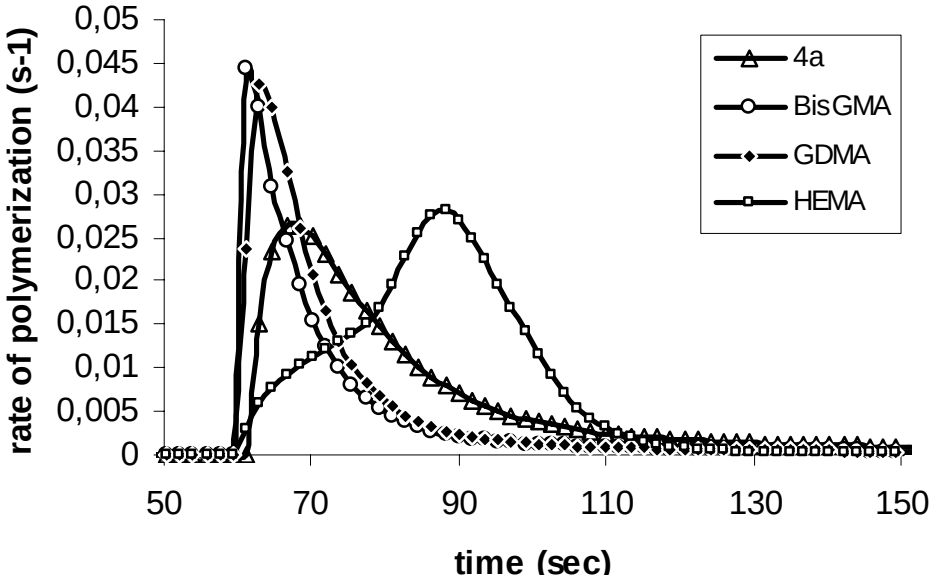

Figure 4.54. Rate of polymerization versus time graph of monomer **4a**, BisGMA, GDMA and HEMA

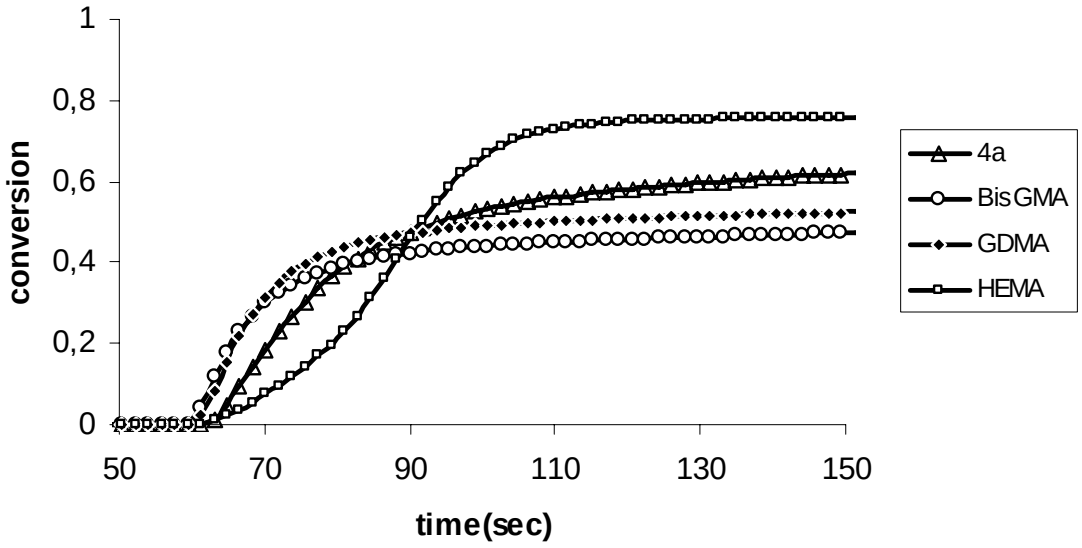

Figure 4.55. Conversion versus time graph of monomer **4a**, BisGMA, GDMA and HEMA

4.2.4. Polymerizations of Monomers 5a-6b

4.2.4.1. Photopolymerizations of Monomers **5a-6b**. The reactivities of the monomers **5a-6b** in photopolymerizations were investigated with photodifferential scanning calorimetry. All the polymerizations were performed under identical conditions; at temperature 40 ^{o}C with an initiator concentration of 2.0 mol per cent and UV light intensity of 20 mW/cm^2.

Monomer **5a** was homopolymerized just above its melting point (36 ^{o}C). The maximum rate and conversion were found to be 0.0004 s^{-1} and 7.2 %. The bulk polymerization of monomers **5b**, **6a** and **6b** was not possible because of their high melting points.

Copolymerization behaviors of synthesized monomers (of 10 mol %) with GDMA were investigated. Figures 4.56 and 4.57 show the rate of polymerization and conversion versus time graph for GDMA:monomer (90:10) mixtures.

Monomer **5a** gave clear solutions, whereas monomer **6a** formed homogeneous and milky solutions. The maximum rates of polymerizations for GDMA, GDMA:**5a**, GDMA:**5b**, GDMA:**6a** and GDMA:**6b** were found to be 0.046, 0.043, 0.033, 0.013 and 0.029 s^{-1}. The more rigid monomers **6a** and **6b** gave the lower conversions (52 % and 48.4 %). The reason is probably a combination of the lower flexibility of the monomers and their low mobilities due to their melting points being higher than the polymerization temperature.

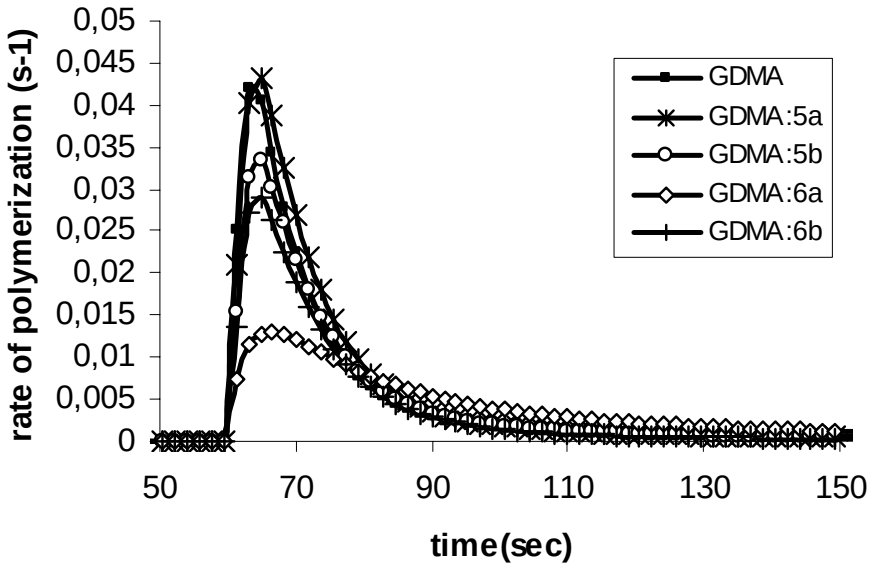

Figure 4.56. Rate of polymerization versus time graph for the mixtures of GDMA containing 10 mol % monomer (**5a-6b**)

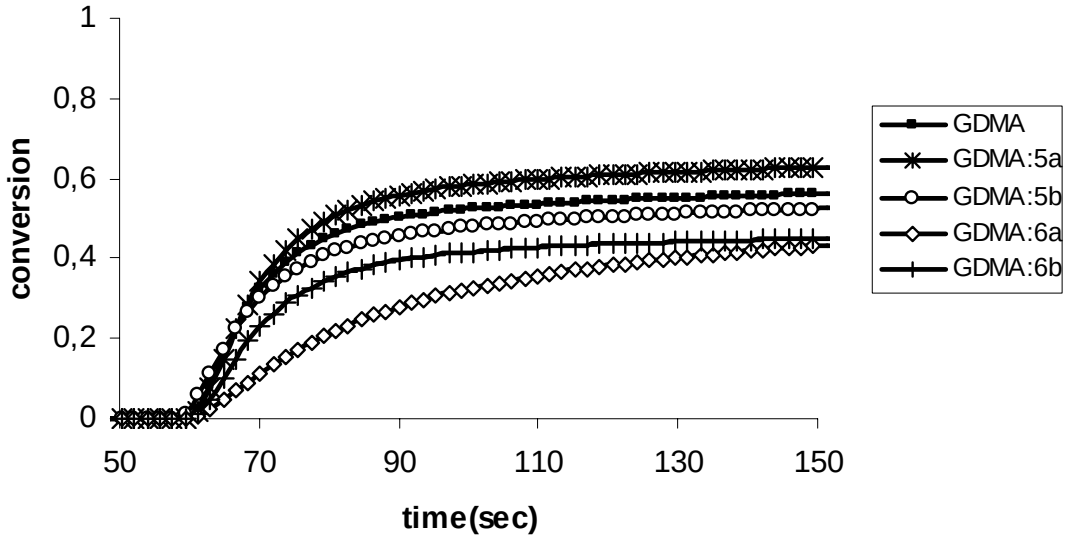

Figure 4.57. Conversion versus time graph for the mixtures of GDMA containing 10 mol % monomer (**5a-6b**)

4.2.4.2.Copolymerization of Monomers **5b** and **6b** with Acrylamide. In order to further investigate the copolymerizability of the synthesized monomers with commercial monomers, solution copolymerization of them with acrylamide was studied. Copolymerization of monomer **5b** with acrylamide (5:95 mol %) in the presence of V-50 as an initiator was carried out in water at 65 ºC (Table 4.2). The copolymer was soluble in water only and it was purified by precipitation into acetone to remove unreacted monomers. ^{1}H NMR spectra of the copolymer showed no residual double bonds (Figure 4.58). The copolymer composition was determined from the integrated ^{1}H NMR spectrum with the ratio of peak areas of backbone protons of the copolymer around 1.6-2.3 ppm to the peak areas of aromatic protons of monomer **5b** around 7.0-7.7 ppm. The fractions of monomer **5b** units in the copolymer were greater than in the feed composition, indicating the reactivity of monomer **5b** in the copolymerization (Table 4.2). The number average molecular weights (M_n) and the weight average molecular weights (M_w) were 481500 and 176300 for the homopolymer of AAm and 79500 and 38100 for the copolymer of AAm:monomer **5b** (95:5), as estimated by aqueous phase GPC.

Table 4.2. Copolymerization results of the monomers 5b-6b with AAm

Monomer	[M]	[I]	Time (min)	Yield (%)	M_w / Mn (g/mol)
AAm only	7.35	0.042	2	99.1	481500 / 176300
AAm:monomer **5b**	6.75	0.042	15	55.6	79500 / 38100
AAm:monomer **6b**	2.12	0.042	45	54.2	crosslinked

[a] V-50 in water. Temperature= 65 ºC

The copolymerization of the difunctional monomer **6b** with acrylamide (5:95 mol %) were run in water under the same conditions. Cross-linked polymer indicated the incorporation of the monomer **6b** in copolymer. To remove the residual monomers, the copolymer was swelled in water, excess water decanted, then treated with ethanol; this procedure being repeated until the pH of the aqueous part of the gel was not acidic.

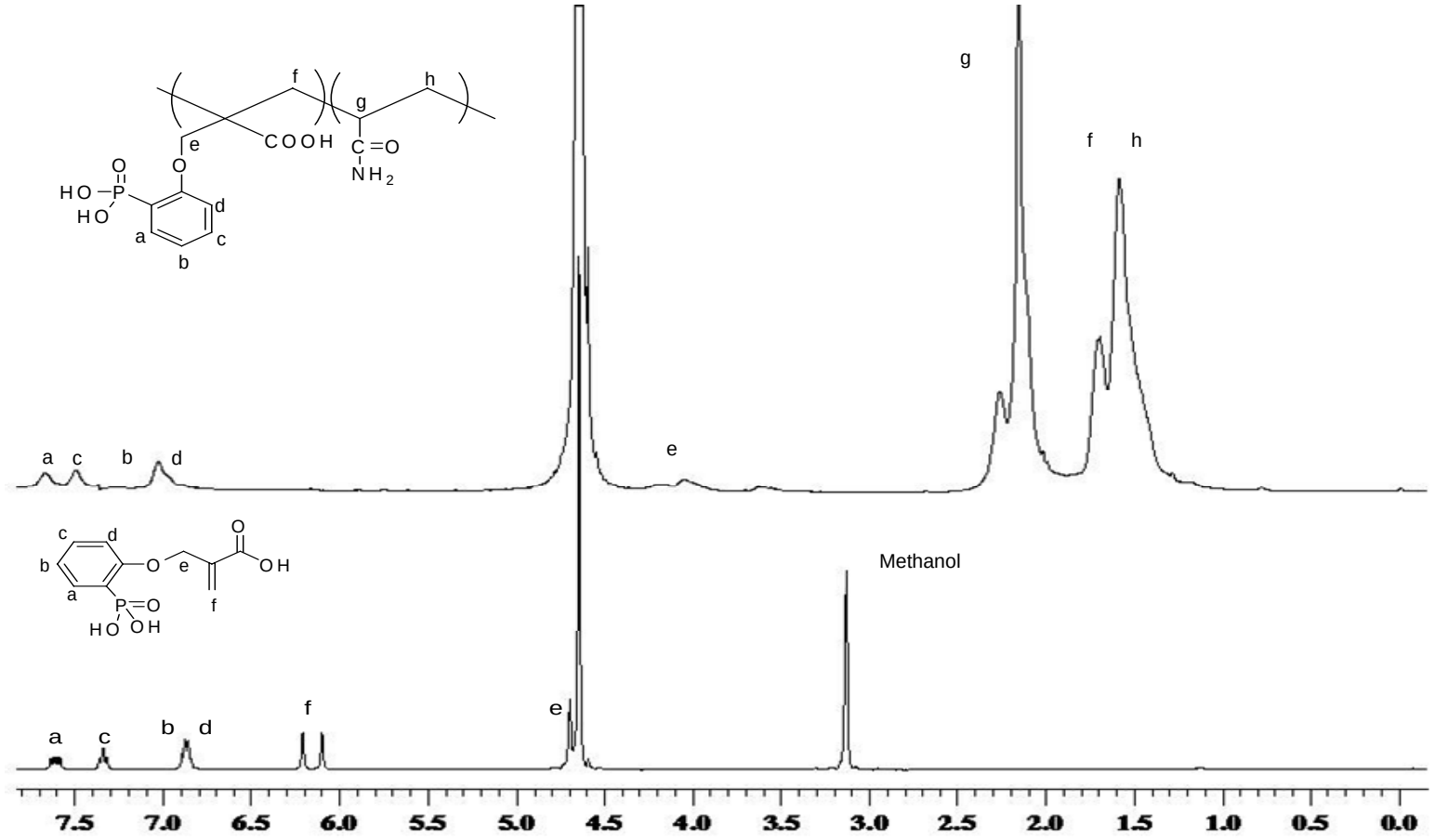

Figure 4.58. ^{1}H-NMR spectra of monomer 5b and copolymer of AAm:monomer 5b

Another proof of the incorporation of the monomers **5b**-**6b** into the copolymer matrix is provided by the FT-IR spectra (Figure 4.59). Pure polyacrylamide showed N-H stretching bands at 3333 and 3185 cm^{-1}. The peaks at 1648 and 1597 cm^{-1} are due to amide-I and amide-II modes. Amide-I mode is known to be dominated by the C=O stretching band whereas N-H bending contribution to the amide-II mode is the largest [97]. In the FTIR spectra of the copolymers, the presence of the bands due to P=O stretching around 1200 cm^{-1}, P-O stretching between 900 and 1030 cm^{-1} and P-O bending around 650-450 cm^{-1} indicated the incorporation of our monomers. Also, a decrease in the intensity of N-H stretching bands in the copolymer spectra relative to the pure polyacrylamide spectrum might be the result of hydrogen bond weakening between acrylamide groups with the incorporation of our monomers [98, 99].

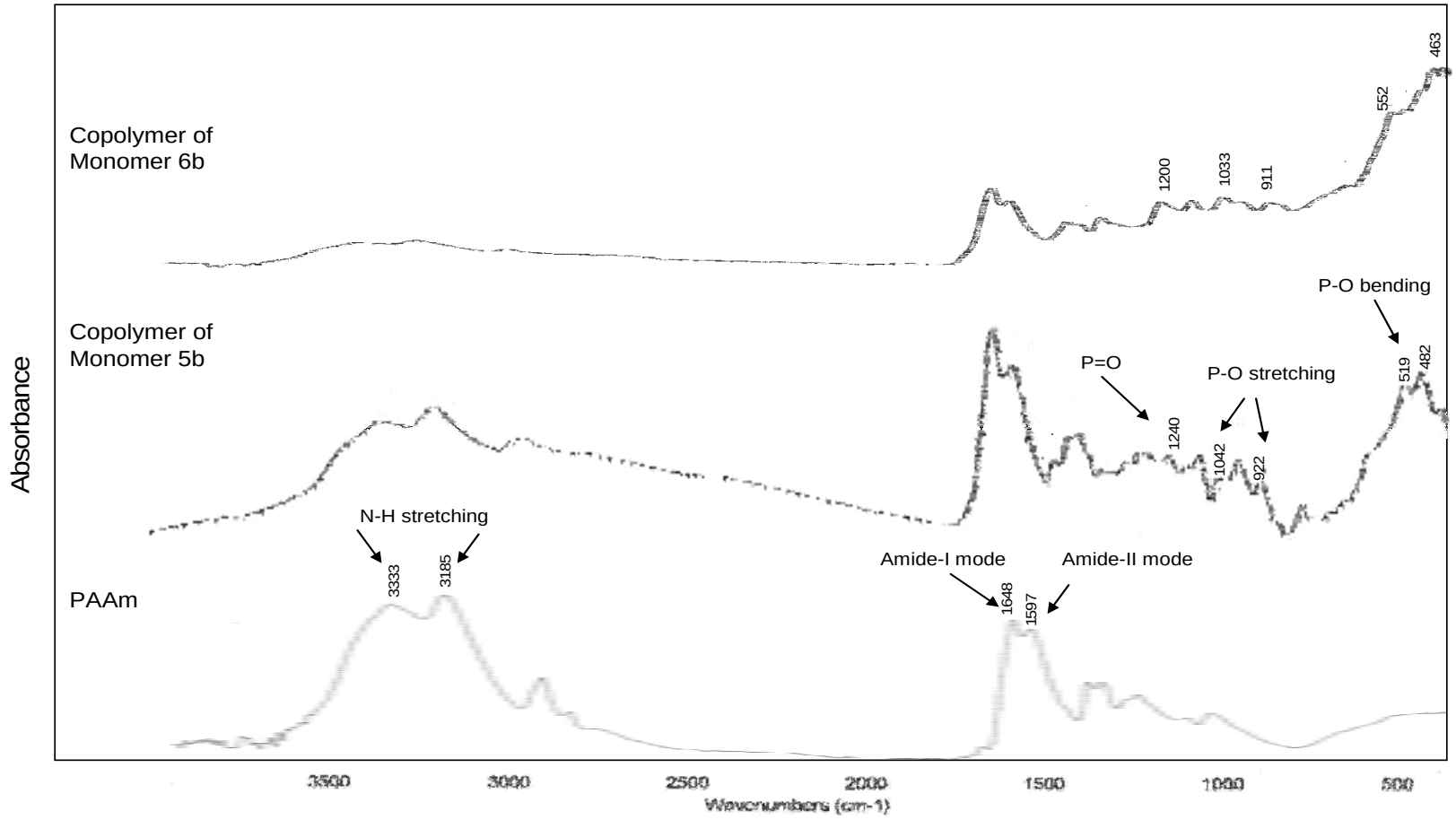

Figure 4.59. FT-IR spectra of poly(AAm) and copolymers of AAm:monomer **5b**-**6b**

The thermal stabilities and thermal degradation behaviour of the homopolymer of acrylamide and copolymers of monomers were investigated by TGA under nitrogen (Figure 4.60). Polyacrylamide has a three-step mechanism for the thermal degradation based on their TGA and DSC [100]. First thermal decomposition stage (50 - 120 ^{o}C) is due to water lose from polymer, secondary stage (120 - 330 ^{o}C) is probably decomposition due to imidization and third stage is the random scission of the polymer chain. At 550 ºC, polyacrylamide had a char residue of 18.1 %.

For copolymers **5b**-**6b**, the weight loss in the interval 50 - 140 ^{o}C may be attributed to the decomposition of carboxylate groups and water lose from copolymers. For copolymer of monomer **5b** with acrylamide degradation began at 220 ^{o}C whereas crosslinked copolymer of monomer **6b** began to decompose at 200 and 185 ^{o}C. Acidic groups on the copolymers resulted in an increase in the char yields such that copolymer **5b** with one carboxylic acid and one phosphonic acid group gave char residues of 32.9 % 550 ^{o}C. Copolymer **6b** which had two carboxylic acid and two phosphonic acid groups gave higher amount of residue 42.3 % and 40.3 % respectively at 550 ^{o}C as expected.

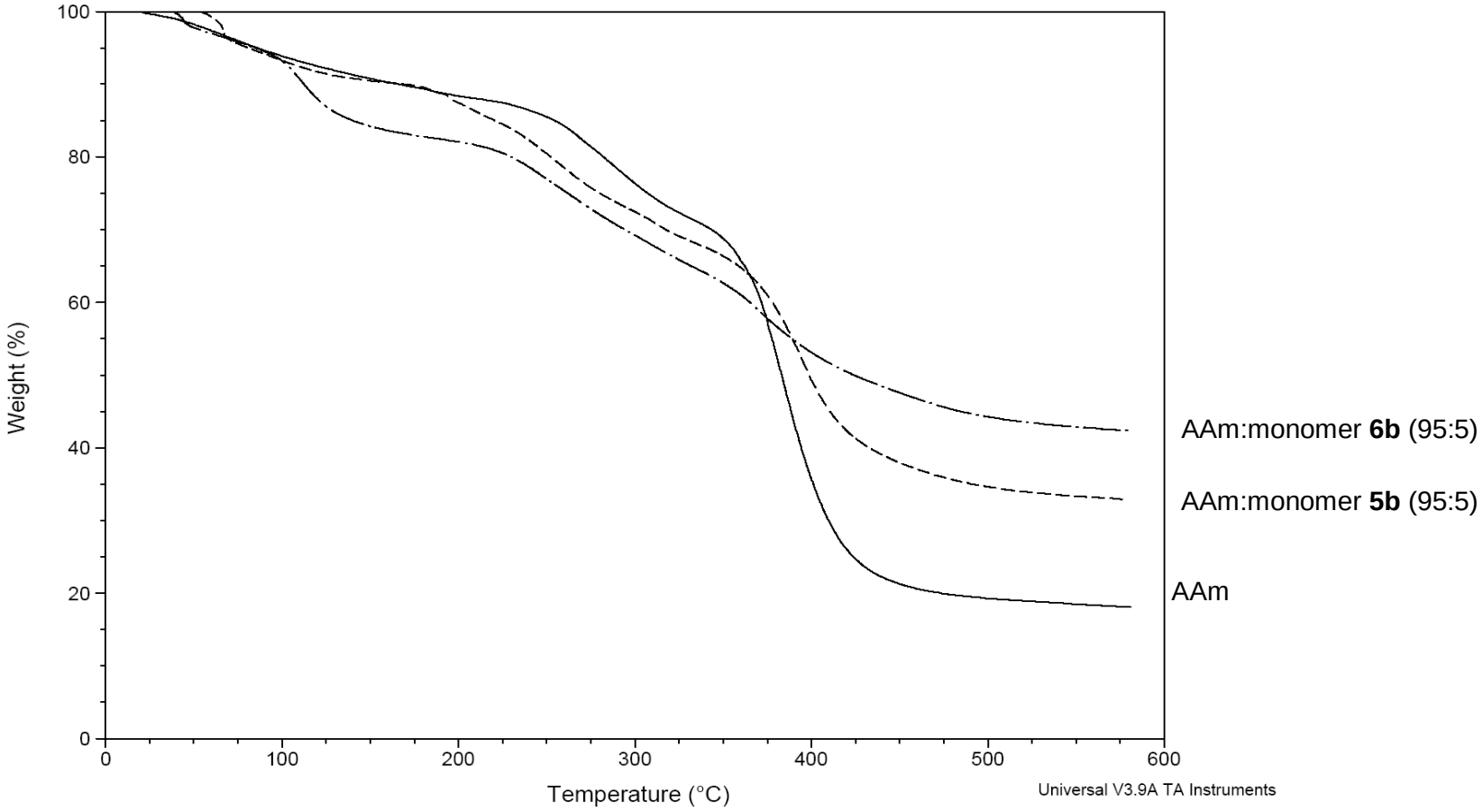

Figure 4.60. TGA curves of poly(AAm) and copolymers of AAm:monomers **5b-6b**

4.2.5. Acidity and Interactions of Monomers 5b and 6b with Hydroxyapatite

Monomer **5b** is a monomethacrylic acid containing one phosphonic acid group in the aromatic ring which is attached to the double bond through an ether linkage, whereas monomers **6b** is dimethacrylic acid monomer containing two phosphonic acid groups in the aromatic rings. Therefore, we expect these monomers to be hydrolytically stable.

Monomers **5b** and **6b** were soluble in ethanol and water which is very important property for dental applications. The aqueous solutions of monomers **5b** and **6b** (7 wt % in water) were acidic with pH values of 1.75 and 1.72, respectively. These values were higher than pH of 7 wt % aqueous phosphoric acid solution (pH=0.90) but in the range of acidity expected from a mild self-etching dental adhesive monomer (pH around 2 or more). The phosphonic acid groups of monomers can remove the smear layer, demineralize the dentin and enamel, and diffuses into collagen fibrils where the carboxylic acid groups of the monomers can form H-bonds with the hydroxyl and amino groups of the fibrils. This process forms a hybrid layer which facilitates binding of the composite resins.

4.2.5.1. ^{13}C-NMR Spectroscopy Technique. The interaction of monomers **5b** and **6b** with hydroxyapatite, as a model compound for dentin and enamel, was investigated using the ^{13}C-NMR [52]. Two different amounts of HAP (15 and 30 mg) were added to the aqueous solutions of the monomers (Figure 4.61). The addition of 15 mg of HAP to the solution of monomer **5b** resulted in an increase in the pH value from 1.75 to 3.25 and shifted the α-methylene carbon and carbonyl carbon peak to a lower field (Table 4.3). When the HAP amount is doubled, the chemical shift differences were 4.13 ppm for the α-methylene carbon and 1.60 ppm for the carbonyl carbon. These results clearly demonstrated that acid groups containing monomer **5b** demineralize the HAP.

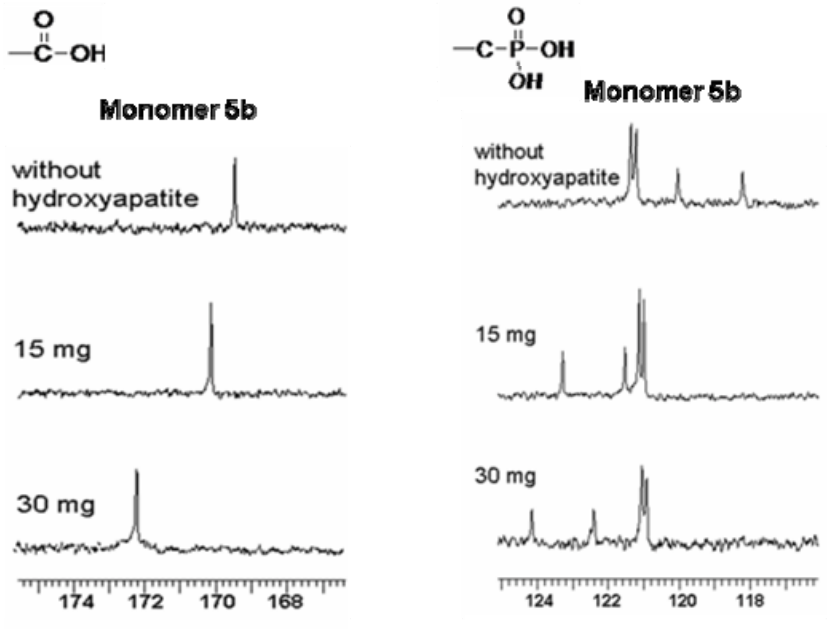

Figure 4.61. Expanded ^{13}C-NMR spectra of the carbonyl and methylene region of monomer **5b**

Table 4.3. Interaction of monomer **5b** with HAP

			In the presence of HAP		
Monomer	pH[a]	HAP[b] (mg)	pH[c]	-C-PO(OH)$_2$ S.D.[d]	-COOH S.D.[e]
5b	1.75	15	3.25	3.329	0.128
		30	3.45	4.134	1.600
6b	1.72	15	3.02	-	-
		30	-	-	-

[a)] pH of 7 wt % of monomer in water

[b)] Amount of HAP added to monomer solution

[c)] pH values of monomers after the addition of HAP

[d)] Chemical shift differences of the NMR peak for the α-methylene carbon next to phosphorus in monomer 5b after addition of HAP.

[e)] Chemical shift differences of the NMR peak for the carbonyl carbon of the carboxylic acid in monomer 5b after addition of HAP.

Interaction of monomer **6b** with HAP could not be determined using ^{13}C-NMR technique since no NMR peaks assigned to monomer **6b** were observed after addition of HAP. The reason of the missing signals might be i) ion-exchange adsorption of monomer **6b** on the HAP surface ii) formation of a surface complex iii) chemical reaction of monomer **6b** with the ions in HAP to form a new phase that precipitates out of solution [95]. It might be concluded that monomer **6b** with the lowest etching potential has the highest chemical bonding efficacy.

4.2.5.2. FT-IR Spectroscopy Technique. The interaction of monomers with HAP was also determined by FT-IR spectrometer (Figure 4.62). The monomer **5b** showed a very broad and strong OH peak of COOH at around 3500-2500 cm^{-1} whereas OH peak of POOH was moderate at around 2500–2000 cm^{-1}. The C=O and P=O stretching vibrations are at ~ 1700 and ~ 1260 cm^{-1}. The C-O stretching bands are at ~ 1290 whereas P-O stretching bands are at ~ 1000 and ~ 925 cm^{-1} respectively. The OH bending band of COOH appear at 1400 cm^{-1} and finally the peaks around 650-450 cm^{-1} are due to P-O bending modes of POOH. Similar spectrum was obtained for monomer **6b**, but presence of H-bonding among the molecules gave rise to shifting of the bands to a lower frequency region.

After mixing with HAP, P=O (~ 1260 cm^{-1}) and P-O (~ 925 cm^{-1}) stretching vibrations present in the pure monomers showed a sharp decrease in intensity which is an indication of an interaction between the phosphonic acid functional groups in the monomers and the calcium ions of the HAP. Analysis of the P-O stretching region around 1000 – 1100 cm^{-1} is complicated due to strong absorbance of the HAP matrix. Therefore, we could not assign a new band that was attributed to the phosphonate salt as an overlap between the PO_4^{-3} and the salt band was expected. Greish and Bowman assigned the band appeared at 1054 cm^{-1} to the polyphosphonate salt [96].

D'Andrea and Fadeev proposed that the reduction in the sharp peak at 3570 cm^{-1} (OH from the lattice of HAP) was due to changes in the crystalline structure and bulk modification of the HAP matrix [94]. The vanishing of the 3570 cm^{-1} band in the monomer **5b**-HAP mixture while the same band remained unchanged in the monomer **6b** – HAP mixture allowed to propose once more that monomer **5b** decalcify the HAP while

monomer **6b** was adsorbed on the HAP surface via probably formation of a surface complex or hydrogen bonding.

On the other hand, a decrease in the intensity of C=O (~ 1700 cm^{-1}) and C-O (~ 1290 cm^{-1}) stretching vibrations was observed which might be due to the neutralization of the COOH groups of monomer **5b** with HAP. However, stretching vibrations of the carboxylate salts were not visible in our spectra. Tomlinson et al. assigned the asymmetric stretching vibrations of $2(COO^{-})Ca^{++}$ as a slightly visible, a very weak broad shoulder at 1540-1560 cm^{-1} [95].

As NMR peaks of monomer **6b** disappeared after addition of HAP to a solution of monomer **6b**, the decrease in the intensities of both P=O and C=O stretches could be also explained due to H-bonding of the functional groups in monomer **6b** with HAP or due to a decrease in the extinction coefficient which is not uncommon in the spectroscopy of adsorbed species [101].

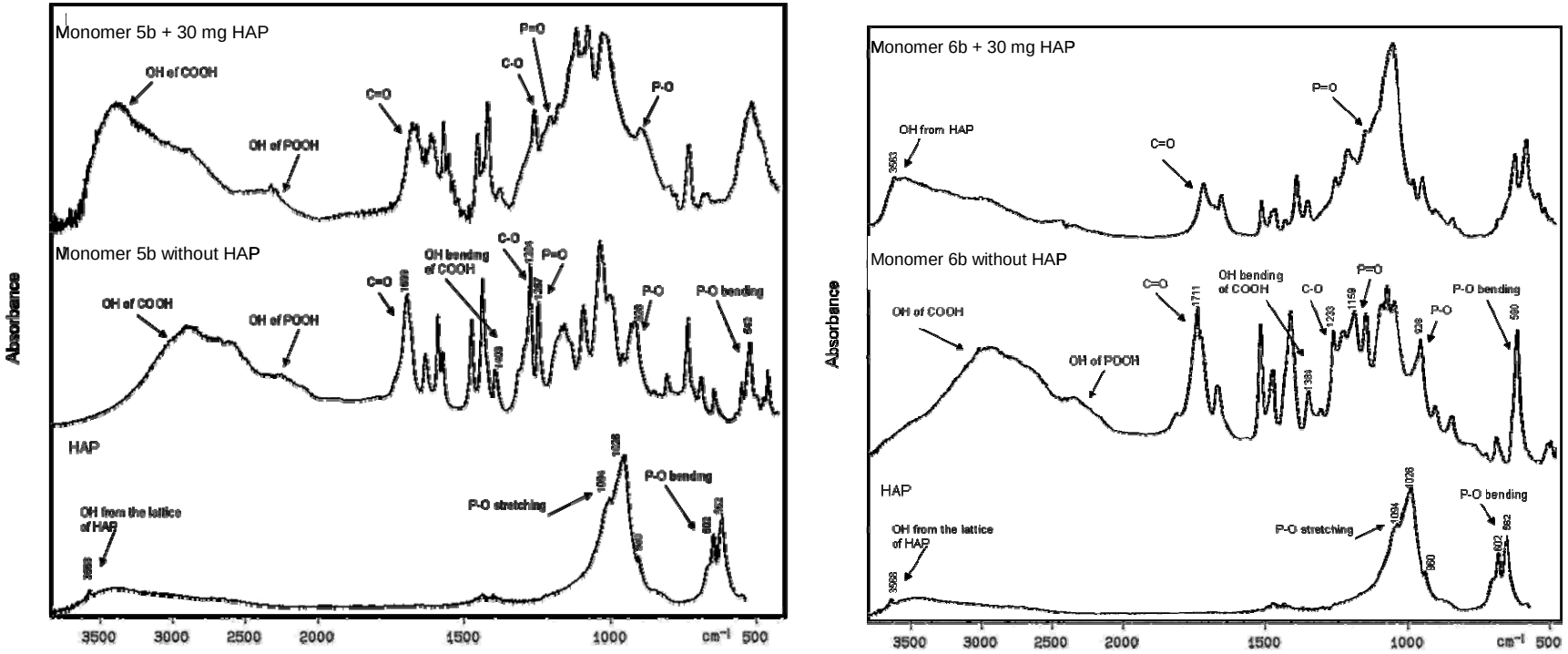

Figure 4.62. FTIR spectra of HAP, monomer **5b** – **6b** without HAP and 30 mg HAP added monomers as KBr pellet forms

4.2.6. Photopolymerization of Monomer 7a

The reactivity of monomer **7a** in photopolymerization was investigated using photodifferential scanning calorimeter (photo-DSC). All polymerizations were performed under identical conditions of initiator concentration (2.0 mol per cent), UV light intensity (20 mW/cm^2) and temperature (40 ^oC).

Figure 4.63 shows the photopolymerization rates of monomer **7a,** BisGMA, GDMA and HEMA. The rate of polymerization of monomer **7a** (0.0090 s^{-1}) was lower than HEMA (0.028 s^{-1}), GDMA (0.043 s^{-1}) and BisGMA (0.044 s^{-1}).

Conversion versus time graph of monomer **7a,** BisGMA, GDMA and HEMA is shown in Figure 4.55. Monomer **7a** (62.2 %) has higher conversion value than BisGMA (51.6 %) and GDMA (57.2 %).

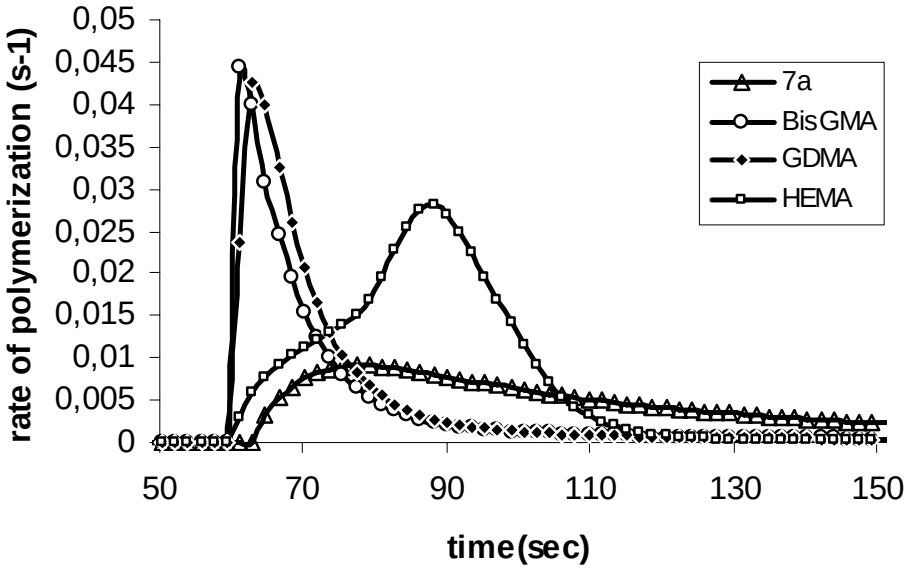

Figure 4.63. Rate of polymerization versus time graph of monomer **7a**, BisGMA, GDMA and HEMA

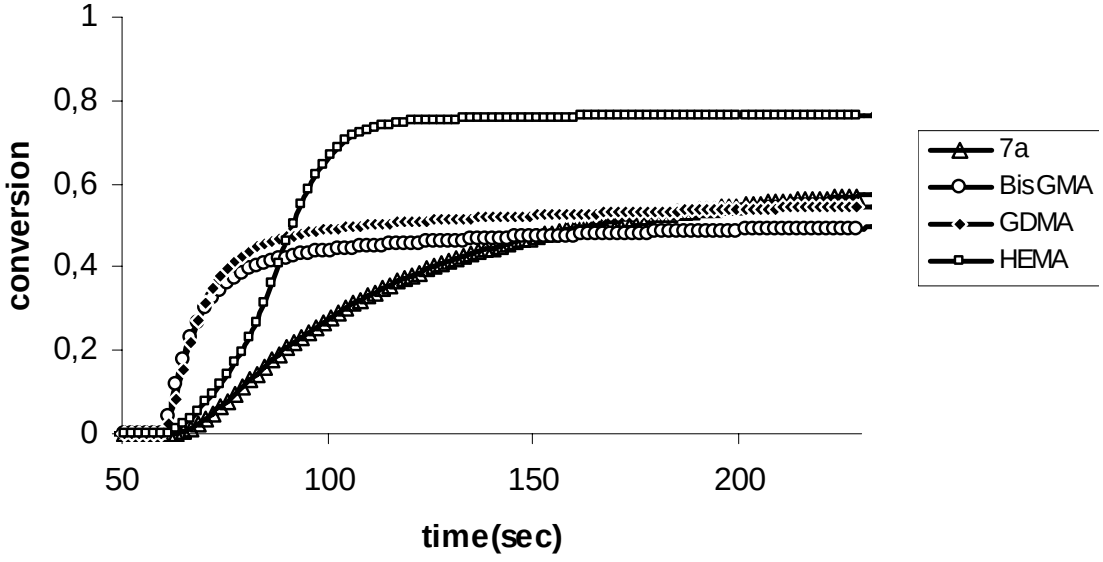

Figure 4.64. Conversion versus time graph of monomer **7a**, BisGMA, GDMA and HEMA

5. CONCLUSIONS

The use of reactions o-hydroxyaryl phosphonates with alkyl α-hydroxyl methacrylate derivatives and GMA was found to be an easy method to prepare new aromatic phosphonated mono- and dimethacrylate monomers.

Seven phosphonated mono- and dimethacrylate monomers were synthesized. Hydrolysis of phosphonate and t-butyl ester groups gave four new dental monomers with phosphonic and carboxylic acid adhesive groups to tooth tissue. In two of these monomers acid groups are attached to double bonds through ether linkages. Therefore we expect them to be hydrolytically stable. The other two monomers may be prone to cleavage due to ester linkages.

Acid monomers were soluble in water or ethanol which is required for dental adhesive monomers. pH value of them were in the range of mild-self etching dental adhesive monomers. It was shown that these monomers can interact with HAP by either demineralizing the calcium phosphate in the HAP or bind to HAP surface.

The novel mono-functional (meth)acrylate synthesized from GMA homo and copolymerize rapidly to give crosslinked polymers. This monomer can be used as reactive diluents for BisGMA and improve the cure efficiency, material properties and binding ability of dental composites. Unfortunately, hydrolysis of this monomer was not successful.

Photopolymerization rates and conversions of other phosphonated monomers were found to be low. This may be due to the presence of a bulky Bisphenol A and phenolic groups close to the double bond.

The phosphonic acid-containing monomers would be expected to improve adhesive properties without decreasing rate of polymerization and conversion of commercial dental monomers such as BisGMA and GDMA.

REFERENCES

1. *Tooth,* http://en.wikipedia.org/wiki/tooth*,* 2008

2. Ten Cate, A. R. *Oral Histology: Development, Structure, and Function.* 5th ed., Mosby-Year Book, 1998.

3. *Dental Materials*, http://www.azom.com/details.asp?articleid=527, 1996.

4. *Structure of a Normal Tooth*, http://www.mydr.com.au, 2003.

5. Ferracane, J. L., *Materials in Dentistry*, 2nd ed., Lippincott Williams & Wilkins, Baltimore, 2001.

6. *Fundemantals of Dental Materials*, http://www.free-ed.net/sweethaven/ medtech/dental/ dentmat/lessonmain.asp?inum=fra0103, 2005.

7. Moszner, N. and U. Salz, "New Developments of Polymeric Dental Composites", *Progress in Polymer Science*, Vol. 26, pp. 535-576, 2001.

8. *Oral Health Topics*, http://www.ada.org/public/topics/fillings.asp#types, 2005.

9. *Composite Resin,* http://www.affordabledentistryandorthodontics.com/Education/ treatmentsFillings.htm, 2004.

10. Espevik, S., "Dental Amalgam", *Annual Review of Materials Science*, Vol. 7, pp.55-72, 1977.

11. *Amalgam…Silver Fillings*, http://www.qualitydentistry.com/dental/amalgam/amalgam, 2004.

12. Anderson M. and R. B. Mccoy, "Dental Amalgam: The State Of The Art and Science", Dental Clinics of North America, Vol. 37, pp. 419-431, 1993.

13. Kent, B. E. and A. D. Wilson, "The Properties of a Glass-Ionomer Cement", *British Dental Journal*, Vol. 135, pp. 322-326, 1973.

14. *Dental Fillings*, http://www.goadentist.com/fillings.htm, 2008.

15. Nicholson, J. W., "Chemistry of Glass-Ionomer Cements: a Review", *Biomaterials*, Vol. 19, pp. 485-494, 1998.

16. Verbeeck R. M., E. A. Maeyer, A. M. Luc, R. J. De Moor, A. M. De Witte and L.M. Trimpeneers, "Fluoride Release Process of (resin-modified) Glass-Inomer Cements versus (polyacid-modified) Composite Resins", *Biomaterials*, Vol. 19, pp. 509-519, 1998.

17. Culbertson, B. M., "Glass Ionomer Dental Restoratives", *Progress in Polymer Science*, Vol. 26, pp. 577-604, 2001.

18. Mount G. J. *An Atlas of Glass-Ionomer Cements: a Clinician's Guide*. 2nd ed., Informa Healthcare, London, 1994.

19. *Amalgam Fillings - Various Types of Tooth Fillings*, http://www.colgate.com/app/Colgate/US/OC/Information/OralHealthBasics/CheckupsDentProc/Fillings/TypesOfFillings.cvsp, 2005.

20. Hatton, P. V., K. Hurrell-Gillingham and I. M. Brook, "Biocompatibility of Glass Ionomer Cements", *Journal of Dentistry*, Vol. 34, pp. 598-601, 2006.

21. Millar, B. J., F. Abiden and J. W. Nicholson, "In Vitro Caries Inhibition by Polyacid-Modified Composite Resins (Compomers)", *Journal of Dentistry*, Vol. 26, pp. 133-136, 1998.

22. Forsten, L., "Fluoride Release and Uptake by Glass-Ionomers and Related Materials and Its Clinical Effect", *Biomaterials*, Vol. 19, pp. 503-508, 1998.

23. Nicholson, J. W., "Adhesive Dental Materials and Their Durability", *International Journal of Adhesion & Adhesives*, Vol. 20, 11-16, 2000.

24. Davy, K. W. M., S. Kalachandra, M. S. Pandain and M. Braden, "Relationship between Composite Matrix Molecular Structure and Properties", *Biomaterials*, Vol. 19, pp. 2007-2014, 1998.

25. Ruyter I. E. and H. Oeysaed, "Composites for use in posterior teeth: Composition and conversion", *Journal of Biomedical Materials Research*, Vol. 21, pp. 11-23, 1987.

26. Peutzfeldt A. "Resin composites in dentistry: the monomer systems", *European Journal of Oral Sciences*, Vol. 105, pp. 97-116, 1997.

27. Hino, K., J. Yamauchi and K. Nishida, *Dental Compositions*, US Pat, 1994; 5 321 053, Kuraray Co.

28. Mccabe J. F. and A. Walls, *Applied Dental Materials*, 7th ed., Wiley-Blackwell, Oxford, 1992.

29. Sideridou I., V. Tserki, and G. Papanastasiou, "Effect of Chemical Structure on Degree of Conversion in Light-Cured Dimethacrylate-Based Dental Resins", *Biomaterials,* Vol. 23, pp. 1819–1829, 2002.

30. Nicholson J. W., "Polyacid-Modified Composite Resins ("Compomers") and Their Use in Clinical Dentistry", *Dental Materials*, Vol. 23, pp. 615–622, 2007.

31. Moszner, N. and S. Klapdohr, "New Inorganic Components for Dental Filling Composites", *Monatshefte für Chemi*e, Vol. 136, pp. 21-45, 2005.

32. Moszner, N. and U. Salz, "New Developments of Polymeric Dental Composites", *Progress in Polymer Science*, Vol. 26, pp. 535-576, 2001.

33. Moszner, N., U. K. Fischer, J. Angermann and V Rheinberger, “Bis-(acrylamide)s as New Crosslinkers for Resin-based Composite Restoratives”, *Dental Materials*, Vol. 22, pp. 1157-1162, 2006.

34. Andrzejewska E., L.-A. Linden and J. F. Rabek, “The Role of Oxygen in Camphorquinone-Initiated Photopolymerization”, *Macromolecular Chemistry and Physics,* Vol. 199, pp. 441-449, 1998.

35. Van Landuyta, K. L., J. Snauwaertb, J. De Muncka, M. Peumans, Y. Yoshidac, A. Poitevina, E. Coutinhoa, K. Suzuki, P. Lambrechtsa and B. Van Meerbeeka, “Systematic Review of The Chemical Composition of Contemporary Dental Adhesives”, *Biomaterials*, Vol. 28, pp. 3757–3785, 2007.

36. Imoto M. and S. Choe, “Vinyl Polymerization. V. Decomposition of Sym-Substituted Benzoyl Peroxides in Presence of Dimethylanilide”, *Journal of Polymer Science*, Vol. 15, pp. 485–501, 1955.

37. Martin R., S. J. Paul, H. Luthy and P. Scharer, “Dentin Bond Strength of Dyract Cem”, *American Journal of Dentistry*, Vol. 10, pp. 27–31, 1997.

38. Moodley D. and S. R. Grobler, “Compomers: Adhesion and Setting Reactions”, *South Africa Dental Journal*, Vol. 58, pp. 22-28, 2003.

39. Mou, L., G. Singh and J. W. Nicholson, “Synthesis of a Hydrophillic Phosphonic Acid Monomer for Dental Materials”, *Chemical Communications*, pp. 345-346, 2000.

40. Shaw A. J., T. Carrick and J. F. McCabe, “Fluoride Release from Glass-Ionomer and Compomer Restorative Materials: 6 Month Data”, *Journal of Dentistry*, Vol. 26, pp. 355-356, 1998.

41. Grobler S. R., R. J. Rossouw and K. A. VanWyk, “Comparison of Fluoride Release from Various Dental Materials”, *Journal of Dentistry*, Vol. 26, pp. 256–265, 1998.

42. Xu, X., L. Ling, X. Ding and J. O. Burgess, “Synthesis and Characterization of a Novel, Fluoride-Releasing Dimethacrylate Monomer and its Dental Composite” *Journal of Polymer Science: Part A: Polymer Chemistry*, Vol. 42, 985–998, 2004.

43. Ge, J., M. Trujillo and J. Stansbury, “Synthesis and Photopolymerization of Low Shrinkage Methacrylate Monomers Containing Bulky Substituent Groups”, *Dental Materials*, Vol. 21, pp. 1163–1169, 2006.

44. Stansbury, J.W. and J. M. Antonucci, “Dimethacrylate Monomers with Varied Fluorine Contents and Distribution”, *Dental Materials*, Vol. 15, pp. 166–173, 1999.

45. Sankarapandian, M., H. K. Shobha, S. Kalachandra, J. E. McGrath and D. F. Taylor, “Characterization of Some Aromatic Dimethacrylates for Dental Composite Applications”, *Journal of Materials Science: Materials in Medicine*, Vol. 8, pp. 465- 468, 1997.

46. Meyer J. M., M. A. Cattani-Lorente and V. Dupuis, “Compomers: Between Glass-Ionomer Cements and Composites”, *Biomaterials,* Vol. 19, pp. 529-539, 1998.

47. Nicholson, J. W. and M. Anstice, “The Development of Modified Glass-Ionomer Cements for Dentistry”, *TRIP*, Vol. 2, No. 8, pp. 272-276, 1994.

48. Rumphorst A., U. Salz, A. Gianasmidis, T. Volkel, N. Moszner and V. Rheinberger, *Radically Polymerizable Dental Material*, US Pat, 1999, 6281271, Ivaclor.

49. *The Various Categories of Adhesives*, https://decs.nhgl.med.navy.mil/1QTR04/QA/dm1.htm, 2004.

50. Itou, K., Y. Torii, Y. Nishitani, K. Ishikawa, K. Suzuki and K. Inoue, “Effect of Self-etching Primers Containing N-acryloyl Aspartic Acid on Dentin Adhesion”, *Journal of Biomedical Materials Research*, Vol. 51, pp. 569-574, 2000.

51. Schulze, K. A., S. A. Oliveira, R. S. Wilson, S. A. Gansky, G. W. Marshall and S. J. Marshall, "Effect of Hydration Variability on Hybrid Layer Properties of a Self-etching versus an Acid-etching system", *Biomaterials*, Vol. 26, pp. 1011-1018, 2005.

52. Nishiyama, N., K. Fujita, T. Ikemi, T. Maeda, K. Suzuki and K. Nemoto, "Efficacy of Varying the NMEP Concentrations in the NMGLY-NMEP Self-etching Primer on the Resin-Tooth Bonding", *Biomaterials*, Vol. 26, pp. 2653-2661, 2005.

53. Moszner, N., U. Salz and J. Zimmermann, "Chemical Aspects of Self-etching Enamel-Dentin Adhesives: A Systematic Review", *Dental Materials*, Vol. 21., pp. 895-910, 2005.

54. Moszner, N. and U. Salz, "Recent Developments of New Components for Dental Adhesives and Composites", *Macromoleuclar Materials and Engineering*, Vol. 292., pp. 245-271, 2007.

55. Moszner, N., F. Zeuner, S. Pfeiffer, I. Schurte, V. Rheinberger and M. Drache, "Monomers For Adhesive Polymers, 3", *Macromol. Materials and Engineering*, Vol. 286, pp. 225-231, 2001.

56. Omura, I., J. Yamauchi, Y. Nagase and F. Uemuro, *Adhesive Composition*, US Pat, 1987; 4 650 847, Kuraray Co.

57. Moszner, N., F. Zeuner, M. Drache, and V. Rheinberger, "Synthesis and Dental Aspects of Acrylic Phosphonic Acids", *Phosphorus, Sulphur and Silicon*, Vol. 177, pp. 2263, 2002.

58. Moszner, N., F. Zeuner, S. Pfeiffer, I. Schurte, V. Rheinberger, and M. Drache, "Monomers for Adhesive Polymers, 2", *Macromolecular Materials and Engineering*, Vol. 200, pp. 1062-1067, 1999.

59. Anbar, M. and E. P. Farley, "Potential Use of Organic Polyphosphonates as Adhesive in the Restoration of Teeth", *Journal of Dental Research*, Vol. 53, pp. 879-888, 1974.

60. Farley, E. P., R. L. Johnes and M. Anbar, "Improved Adhesion of Acrylic Restorative Materials to Dental Enamel by Pre-coating with Monomers Containing Phosphonate Groups", *Journal of Dental Research*, Vol. 56, pp. 943-952, 1977.

61. Erdmann, C., S. Ziegler, S. Neffgen, C. Bolln, W. Mühlbauer and R. Lück, *Dental Material Containing Phosphonic Acids*, US Pat, 2005; 6 902 608 B2, Ernst Muhlbauer GmbH & Co.

62. Beech, D. R., E. Rizzardo, W. D. Cook, and M. C. Smail, *Dental Restorative Material*, US Pat, 1988; 4 732 943, Commonwealth Scientific and Industrial Research Organization.

63. Nishiyama, N., K. Suzuki, H. Yoshida, H. Teshima and K. Nemoto, "Hydrolytic Stability of Methacrylamide in Acidic Aqueous Solution", *Biomaterials*, Vol. 25, pp. 965-969, 2004.

64. Nishiyama, N., K. Suzuki, K. Komatsu, S. Yasuda and K. Nemoto, "A ^{13}C-NMR Study on the Adsorption Characteristics of HEMA to Dentinal Collagen", *Journal of Dental Research,* Vol. 81, pp. 469-471, 2002.

65. Nishiyama, N., K. Suzuki, A. Nagatsuka, I. Yokota and K. Nemoto, "Dissociation States of Collagen Functional Groups and their Effects on the Priming Efficacy of HEMA Bonded to Collagen", *Journal of Dental Research*, Vol. 82, pp. 257-261, 2003.

66. Moszner, N., "New Monomers for Dental Application", *Macromolecular Symposia*, Vol. 217, pp. 63-75, 2004.

67. Tay, F. R., K. M. Moulding and D. H. Pashley, "Distribution of Nanofillers from a Simplified-Step Adhesive in Acid-Conditioned Dentin" *Journal of Adhesion Dentistry*, Vol. 1, pp. 103-117, 1999.

68. Matsunae, K. and A. Akahane, *Dental Adhesive Set*, US Pat, 2001; 6 217 644 B1, GC Corporation.

69. Atac, A. S., Z. C. Cehreli and B. Sener, "Antibacterial Activity of Fifth Generation Dentin Bonding Systems", *Journal of Endodontics*, Vol. 27, pp. 730-733, 2001.

70. Imazato, S., T. Imai, R. B. Russell, M. Torii and S. Ebisu, "Antibacterial Activity of Cured Dental Resin Incorporating the Antibacterial Monomer MDPB and an Adhesion Promoting Monomer", *Journal of Biomedical Research*, Vol. 39, pp. 511-515, 1998.

71. Yoshida, Y., B. V. Meerbeek, Y. Nakayama, M. Yoshioka, J. Snauwaery, Y. Abe, P. Lambrechts, G. Vanherle and M. Okazaki, "Adhesion to and Decalcification of Hydroxyapatite by Carboxylic Acids", *Journal of Dental Research*, Vol. 80, pp. 1565-1569, 2001.

72. Yoshida, Y., V. K. Nagakane, R. Fukuda, Y. Nakayama, M. Okazaki, H. Shintani, S. Inoue, Y. Tagawa, K. Suzuki, J. D. Munck and B. Meerbeek, "Comparative Study on Adhesive Performance of Functional Monomers", *Journal of Dental Research*, Vol. 83, pp. 454-458, 2004.

73. Albayrak, A. Z., *Synthesis of New Dental Adhesive Monomers and Polymers,* Ph.D. Thesis, Bogaziçi University, 2006.

74. Yoshida, H. and N. Nishiyama, "Development of Self-etching Primer Comprised of Methacrylamide, N-methacryloyl Glycine", *Biomaterials*, Vol. 24, pp. 5203-5207, 2003.

75. Nakabayashi, N., K. Kojima and E. Masuhara, "The Promotion of Adhesion by the Infiltration of Monomers into Tooth Substrates", *J. Biomed. Mater. Res*., Vol. 16, pp. 265-273, 1982.

76. Tay, F. R. and D. H. Pashley, "Aggressiveness of Contemporary Self-etching Systems. I: Depth of Penetration Beyond Dentin Smear Layers", *Dental Materials*, Vol. 17, pp. 296-308, 2001.

77. Nishiyama, N., K. Suzuki, T. Asakura, K. Komatsu and K. Nemato, "Adhesion of N-Methacryloyl-ω-Amino Acid Primers to Collagen Analyzed by ^{13}C-NMR", *Journal of Dental Research*, Vol. 80, pp. 855-859, 2001.

78. Decker, C., "Kinetic Study and New Applications of UV Radiation Curing", *Macromolacular Rapid Communication*, Vol. 23, pp. 1067-1093, 2002.

79. Andrajewska, E., "Photopolymerization Kinetics of Multifunctional Monomers", *Progressive Polymer Science*, Vol. 26, pp. 605-665, 2001.

80. Yagci, M. B., *Synthesis and Photopolymerizations of Novel Alkyl-α Hydroxymethyl Acrylate Based Dental Crosslinking Monomers*, M.S. Thesis, Bogaziçi University, 2006.

81. Jansen, J., A. A. Dias, M. Dorschu, and B. Coussens, "Fast Monomers: Factors Affecting the Inherent Reactivity of Acrylate Monomers in Photoinitiated Acrylate Polymerization", *Macromolecules*, Vol. 36, pp. 3861-3873, 2003.

82. Beckel, E. R., J. Nie, J. W. Stansbury, and C. N. Bowman, "Effect of Aryl Substituents on the Reactivity of Phenyl Carbamate Acrylate Monomers", *Macromolecules*, Vol. 37, pp. 4062-4069, 2004.

83. Niea, J. and C. N. Bowman, "Synthesis and Photopolymerization of N, NV-dimethyl,-N, NV-di(methacryloxy ethyl)-1,6-hexanediamine as a Polymerizable

Amine Coinitiator for Dental Restorations", *Biomaterials*, Vol. 23, pp. 1221– 1226, 2002.

84. Lee I. B., B. H. Cho, H. H. Son and C. M. Um, "A New Method to Measure The Polymerization Shrinkage Kinetics of Light Cured Composites", *Journal of Oral Rehabilitation*, Vol. 32, pp. 304–314, 2005.

85. Chandra, R. and R. K. Soni, "Recent Developments in Thermally Curable and Photocurable Systems", *Progressive Polymer Science*, Vol. 19, pp. 137-169, 1994.

86. *Restorative Dentistry: Dental Composite Depth of Cure with Halogen and Blue Led Technology*, http://www.nature.com/bdj/journal/v186/n8/full/4800120a.html, 2008.

87. Smith, T. J., B. J. Shemper, J. S. Nobles, A. M. Casanova, C. Ott, and L. J. Mathias, "Crosslinking Kinetics of Methyl and Ethyl (L-hydroxymethyl) acrylates: Effect of Crosslinker Type and Functionality", *Polymer*, Vol. 44, pp. 6211-6216, 2003.

88. Young, J. S., A. R. Kannurpatti, and C. N. Bowman, "Effect of Comonomer Concentration and Functionality on Photopolymerization Rates, Mechanical Properties and Heterogeneity of the Polymer", *Macromolecular Chemistry and Physics*, Vol. 199, pp. 1043-1049, 1998.

89. Dhawan, B. and D. Redmore, "o-Hydroxyaryl Diphosphonic Acids", *Journal of Organic Chemistry*, Vol. 49, pp. 4018-4021, 1984.

90. Melvin, L. S., "An Efficient Synthesis of 2-Hydroxyphenyl Phosphonates", *Tetrahedron Letters*, Vol. 22, pp. 3375-3376, 1981.

91. Yu, C., B. Liu, and L. Hu, "Efficient Baylis-Hillman Reaction Using Stoichiometric Base Catalyst and an Aqueous Medium", *Journal of Organic Chemistry*, Vol. 66, pp. 5413-5418, 2001.

92. Jariwala, C. P. and L. J. Mathias, "Synthesis, Polymerization, and Characterization of Novel Semifluorinated Methacrylates, Including Novel Liquid Crystalline Materials", *Macromolecules*, Vol. 26, pp. 5129-5136, 1993.

93. Pleshko, N., A. Boskey and R. Mendelsohn, "Novel infrared spectroscopic method for the determination of crystallinity of hydroxyapatite minerals", *Biophysical Journal*, Vol. 60, pp. 786-793, 1991.

94. D'Andrea, S. C. And A. Y. Fadeev, "Covalent Surface Modification of Calcium Hydroxyapatite Using *n*-Alkyl- and *n*-Fluoroalkylphosphonic Acids", *Langmuir,* Vol. 219, pp. 7904-7910, 2003.

95. Misra, D. N., "Adsorption from Solutions on Synthetic Hydroxyapatite: Nonaqueous vs. Aqueous Solvents", *Journal of Biomedical Materials Research Part B. Applied Biomaterials*, Vol. 48, pp. 848-855, 1999.

96. Greish, Y. E. And P. W. Brown "Chemically formed HAp-Ca poly(vinyl phosphonate) composites", *Biomaterials*, Vol. 22, pp. 807-816, 2001.

97. Dweik, H., W. Sultan, M. Sowwan and S. Makharza, "Analysis Characterization and Some Properties of Polyacrylamide Copper Complexes", *International Journal of Polymeric Materials*, Vol. 57, pp. 228-244, 2008.

98. Roberts, M. F. and S. A. Jenekhe, "Site-Specific Reversible Scission of Hydrogen Bonds in Polymers: An Investigation of Polyamides and Their Lewis Acid-Base Complexes by Infrared Spectroscopy", *Macromolecules,* Vol. 24, pp. 3142-3146, 1991.

99. Lemon, M. T., M. S. Jones and J.W. Stansbury, "Hydrogen bonding interactions in methacrylate monomers and polymers", *Journal of Biomedical Materials Research*, Vol. 83A, pp. 734-746, 2007.

100. Vilcu, R., I. I. Bujor, M. Olteanu and I. J. Demetrescu, “Thermal Stability of Copolymer Acrylamide-Maleic Anhydride”, *Applied Polymer Science*, Vol. 33, pp. 2431-2437, 1987.

101. Tomlinson, S. K., O. R. Ghita, R. M. Hooper and K. E. Evans, “Investigation of the Dual Setting Mechanism of a Novel Dental Cement Using Infrared Spectroscopy’, *Vibrational Spectroscopy*, Vol. 45, pp. 10-17, 2007.